New links for old pathways: Protein kinases that target PI4P 5-kinases with regulatory roles in polar tip growth in plants

Dissertation

zur Erlangung des
Doktorgrades der Naturwissenschaften
„doctor rerum naturalium“

der

Naturwissenschaftlichen Fakultät I
– Biowissenschaften –
der Martin-Luther-Universität Halle-Wittenberg,

vorgelegt von
Frau Franziska Hempel
geboren am 02. April 1985 in Göttingen

Gutachter Prof. Dr. Ingo Heilmann
Prof. Dr. Sacha Baginsky
Prof. Dr. Jörg Kudla

Tag der öffentlichen Verteidigung: 17. Juli 2015

1 Introduction 1
1.1 Polar tip growth and the endomembrane system 1
1.1.1 The mechanics of pollen tube elongation 2
1.2 Molecular mechanism of membrane fusion, endocytosis and exocytosis controlled by phosphoinositides (PIs) 6
1.2.1 PIs – synthesis and degradation 6
1.2.2 PtdIns(4,5)P_2 is synthetized by PI4P 5-kinases 7
1.2.3 Signaling molecules control polar tip growth 7
1.3 Three- dimensional structure of PI4P 5-kinases 9
1.4 Posttranslational regulation of PI4P 5-kinases 11
1.5 Protein kinases and protein phosphorylation 12
1.5.1 Mitogen-activated protein kinase (MAPK) signaling 13
1.5.2 Calcium sensing and protein kinase signaling 15
1.6 Hypothesis of phosphorylation dependent regulation of PI4P 5-kinases . 17
1.7 Aims and Objectives 17

2 Materials and Methods 18
2.1 Chemicals 18
2.2 Enzymes and molecular size markers 18
2.3 Kits..... 19
2.4 Equipment 19
2.5 Single-use materials 19
2.6 Software 19
2.7 Plant lines 20
2.8 Microorganisms 20
2.9 Plasmids 21
2.10 Contructs 21
2.11 cDNA-Modification and molecular biology techniques 22
2.11.1 Isolation of RNA from plant material 22
2.11.2 cDNA-Synthesis 23
2.11.3 Amplification of specific gene sequences by PCR 23
2.11.4 Assembly of DNA constructs 23
2.11.5 Site-directed mutagenesis 23
2.11.6 DNA sequencing 24
2.12 Cloning strategy 24

2.12.1 Heterologous protein expression in *E. coli* 24
2.12.2 cDNA-Constructs for split-ubiquitin membrane-based yeast two-hybrid analysis 25
2.12.3 cDNA-constructs for bifunctional fluorescence complementation 25
2.12.4 cDNA-constructs for transient overexpression in tobacco pollen 26
2.13 Protein expression and purification 26
2.13.1 Preparation of chemically-competent *E. coli* cells 26
2.13.2 Transformation of chemically-competent *E. coli* cells 26
2.13.3 Isolation of plasmid-DNA from *E. coli* 27
2.13.4 Heterologous protein expression in *E. coli* 27
2.13.5 Recombinant expression of MBP-AtPIP5K5 27
2.13.6 Recombinant expression of MBP-AtPIP5K1 and MBP-AtPIP5K6 28
2.13.7 Recombinant expression of MBP-NtPIP5K6 28
2.13.8 Recombinant expression of His_6-CPK11 and His_6-CPK11 D150A 28
2.13.9 Cell disruption by high pressure 28
2.13.10 Purification of proteins by affinity chromatography 29
2.13.11 Estimation of protein contents 29
2.13.12 Sodium dodecyl sulfate polyacrylamide gel electrophoresis (SDS-PAGE) 29
2.13.13 Immunodetection 30
2.13.14 *In vitro* test for PI4P 5-kinase activity 30
2.14 *In vitro* phosphorylation of PI4P 5-kinases by pollen extract 31
2.14.1 Preparation of *N. tabacum* pollen tube extract 31
2.14.2 *In vitro* phosphorylation assays with radiolabeled γ-[^{33}P]-ATP 32
2.15 Identification of protein kinases that phosphorylated AtPIP5K6 33
2.15.1 In-gel phosphorylation of purified recombinant AtPIP5K6 by complex extracts 33
2.15.2 In-gel digestion of proteins for mass spectrometric analysis 34
2.16 Mass spectrometry 35
2.16.1 Data-dependent acquisition of phosphopeptides by HR/AM LC-MS 35
2.16.2 Data-independent acquisition of peptides by Nano-LC-HD-MS^E 36
2.17 Analysis of protein-protein interactions 36
2.17.1 Interaction analysis by the split-ubiquitin membrane-based yeast two-hybrid system 36
2.17.1.1 Transformation of chemically competent yeast 38
2.17.1.2 Test for Interaction between PI4P 5-kinases and putative protein kinases 38

2.17.2 Interaction analysis by bimolecular fluorescence complementation 39
2.18 Transient expression of fluorescence-labelled proteins in tobacco pollen tubes 40
2.19 Microscopy 41

3 Results 42
3.1 Recombinant expression and purification of MBP-AtPIP5K6 42
3.2 *In vitro* phosphorylation of purified recombinant MBP-AtPIP5K6 by a protein extract prepared from tobacco pollen 45
3.2.1 Identification of phosphorylated AtPIP5K6 amino acid residues after incubation with pollen tube extract by mass spectrometry 46
3.3 An undirected approach to identify protein kinases that specifically phosphorylate AtPIP5K6 47
3.3.1 Identification of putative protein kinases that phosphorylate AtPIP5K6 by mass spectrometry 49
3.4 A new link between MAP-kinase signalling and PI4P 5-kinase function 51
3.4.1 Subcellular localization of MPK6 51
3.4.2 Protein-Protein interaction between MPK6 and AtPIP5K6 52
3.4.3 AtPIP5K6 and MPK6 interact at the apical PM in pollen tubes 53
3.4.4 MPK6 phosphorylates pollen-specific PIPKs *in vitro* 54
3.4.4.1 Database-aided identification of putative MPK6 phosphorylation sites 56
3.4.4.2 Identification of AtPIP5K6 amino acid residues phosphorylated by MPK6 57
3.4.5 Site-directed mutagenesis of the residues T590 and T597 of PIP5K6 58
3.4.5.1 *In vitro* phosphorylation of PIP5K6 variants 58
3.4.6 Effects of MPK6 on the catalytic activity of AtPIP5K6 *in vitro* 60
3.4.7 MPK6 does not affect AtPIP5K6 T590A T597A activity *in vitro* 61
3.4.8 Effects of MPK6 on the functionality of AtPIP5K6 *in vivo* 62
3.5 AtPIP5K6 and MPK6 have close homologs in *N. tabacum* 64
3.5.1 NtPIP5K6 is a close homolog of AtPIP5K6 64
3.5.2 *In vitro* phosphorylation of purified recombinant MBP-PIP5K6 by a protein extract prepared from tobacco pollen 65
3.5.3 NtSIPK is a close homolog of MPK6 65
3.5.4 Protein-protein interaction between salicylic acid-induced protein kinase (SIPK) and NtPIP5K6 66
3.5.5 MPK6 phosphorylates NtPIP5K6 *in vitro* 67
3.5.6 Co-expression of NtSIPK with NtPIP5K6 inhibits effects of NtPIP5K6 *in vivo* 68

3.5.7 Effects of NtPIP5K6 overexpression on the growth of pollen tubes of tobacco plants with reduced NtSIPK expression 69
3.6 A new link between CPK11 signaling and AtPIP5K6 function 71
3.6.1 Subcellular localisation of CPK11 71
3.6.2 Protein-protein interaction between CPK11 and AtPIP5K6 72
3.6.3 CPK11 and AtPIP5K6 interact at the apical PM of pollen tubes 73
3.6.4 CPK11 phosphorylates Arabidopsis PIPKs *in vitro* 74
3.6.5 Analysis of phosphorylation sites by phosphoproteomics 76
3.6.6 Effects of CPK11 on the catalytic activity of AtPIP5K6 *in vitro* 77
3.6.7 Effects of CPK11 on the functionality of AtPIP5K6 *in vivo* 79

4 Discussion 81
4.1 *In vitro* phosphorylation of AtPIP5K6 by pollen tube extract 81
4.2 Identification of putative upstream protein kinases of AtPIP5K6 82
4.3 Verification of MPK6 and AtPIP5K6 protein-protein interaction 84
4.4 Phosphorylation of AtPIP5K6 by MPK6 84
4.4.1 Phosphorylation of AtPIP5K6 by MPK6 controls activity 87
4.5 Functional connection of AtPIP5K6 and MPK6 *in vivo* 90
4.6 The interplay of MPK6 and AtPIP5K6 in pollen tube growth 91
4.7 Verification of CPK11 and AtPIP5K6 protein-protein interaction 93
4.8 Phosphorylation of AtPIP5K6 by CPK11 93
4.9 CPK11 negatively influences AtPIP5K6 activity *in vitro* 95
4.10 The interplay of CPK11 and AtPIP5K6 in pollen tube growth 96
4.11 Interconnection of the regulation of AtPIP5K6 by MPK6 and CPK11 97
5 Summary 99
6 Literature 101
7 Appendix 111
7.1 List of abbreviations 111
8 Publications 121
9 Acknowledgements – Danksagung 123

1 Introduction

Biochemical processes that underlie all functions of living cells are never static but are constantly modulated over developmental stages and adapt to biotic and abiotic factors. To permit these adaptations, there is a highly organized network of signaling mechanisms. Two conserved signaling mechanisms present in all eukaryotic organisms are phosphoinositide (PI) signaling and signals mediated by protein phosphorylation through mitogen-activated protein kinases (MAPKs) and calcium-dependent protein kinases (CDPKs). This thesis presents the first evidence for the phosphorylation of key enzymes of PI-signaling by protein kinases from these two families in the context of the control of polar tip growth in plant cells. The interconnection of PI-signaling and different protein kinases has important ramifications for our understanding of how polar tip growth and possibly other cellular processes are controlled.

1.1 Polar tip growth and the endomembrane system

Polar tip growth is an example for extreme polar cell elongation. In eukaryotic organisms it is a widespread means of cell morphogenesis, manifesting for example in the shape of fungal hyphae (Fischer *et al.* 2008), in the formation of root hairs and the directional growth of pollen tubes in plants (Franklin-Tong 1999; Hepler *et al.* 2001; Samaj *et al.* 2004) as well as for neuronal axons in animals (Rodriguez-Boulan and Powell 1992). The growth of these specialized cells is restricted to distinct areas of their surface - the apex - and results in the specialized cell shapes that are important for their function. In case of pollen tubes, elongation and delivery of the sperm cells is crucial for sexual reproduction of the plant (Fig 1.1). The pollen tube is a well-established model for the study of polarity and directional growth (Moscatelli and Idilli 2009). Additionally, it is easy to manipulate (Fu 2010). The two sperm cells and the vegetative nucleus are located distal in the shank. For delivery of the two sperm cells to the unfertilized female gametophyte, the pollen lands on the stigma, and generates a protrusion, the pollen tube, which enters the style. The directional growth is guided by cues from the maternal tissue (Kawashima and Berger 2011). Pollen tubes can obtain remarkable length to width ratios of >10 000 (Heilmann and Heilmann 2015).

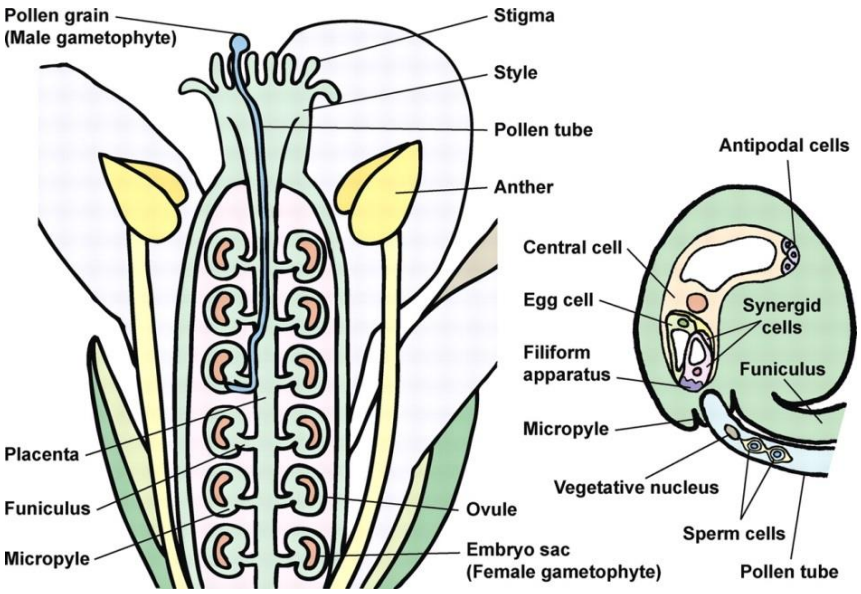

Figure 1.1: Overview of the sexual reproduction in *A. thaliana*. Left, overview of an Arabidopsis flower. Right, enlargement of the ovule. After the landing of the pollen grain on the stigma, the pollen tube emerges and grows through the style to the placenta. The ovule is connected by the funiculus to the placenta. To deliver the two sperm cells and fertilize the egg cell, the pollen tube finally enters the micropyle. Figure from Kawashima and Berger, 2011.

1.1.1 The mechanics of pollen tube elongation

Polar growth is strictly dependent on the fusion of vesicles containing plasma membrane (PM)- and cell wall material at the apical elongation region of the polar growing cell (Franklin-Tong 1999; Krichevsky *et al.* 2007). The apical fusion of vesicles in pollen tubes is restricted to a small region at the apical tip of the cell (Moscatelli *et al.* 2007; Ryan *et al.* 2001; Zonia and Munnik 2008), the so called clear zone. This zone does not refract light in bright field microscopy due to the absence of larger organelles and therefore appears “clear” (Feijo *et al.* 1999; Hepler and Winship 2015). The clear zone is, however, not empty, but contains mainly endomembrane compartments involved in secretion and the recycling of vesicles (Fig. 1.2). When the pollen tube elongates, cell wall and cytoplasm have to keep up the turgor to prevent collapsing of the tube. The composition of the cell wall components plays an important role in maintaining the balance between flexibility and rigidity. The cell wall of the shank contains cellulose and is rigid, compared to the apex of the pollen tube where there are more flexible zones enabling cell elongation. One of the major components of the expanding cell wall is pectin in its methoxy-esterified form (Bosch and Hepler 2005; Palin and Geitmann 2012; Parre and Geitmann 2005). To stabilize and stiffen the newly constructed cell wall at the apex, pectin undergoes demethoxylation and subsequent cross-linking with calcium ions (Bosch *et al.* 2005; Bosch and Hepler 2005; Palin and Geitmann 2012; Willats *et al.* 2001; Wolf and Greiner 2012). Pectin and membrane lipids for the expanding PM are transported to the

growing apex of the cell by vesicular trafficking. The transport of the vesicles occurs along actin filaments from the shank of the tube to the apical region. There are two types of actin to distinguish within the pollen tube. Actin filaments are spread along the pollen tube shank and reach until the sub apical region, contacting the clear zone (Fig. 1.2). At the apex the more massive actin filaments are substituted by a more intricate of cortical actin filaments, the "actin fringe". This actin fringe is highly dynamic and is implied in the maintenance of the apical polarity and the clear zone.

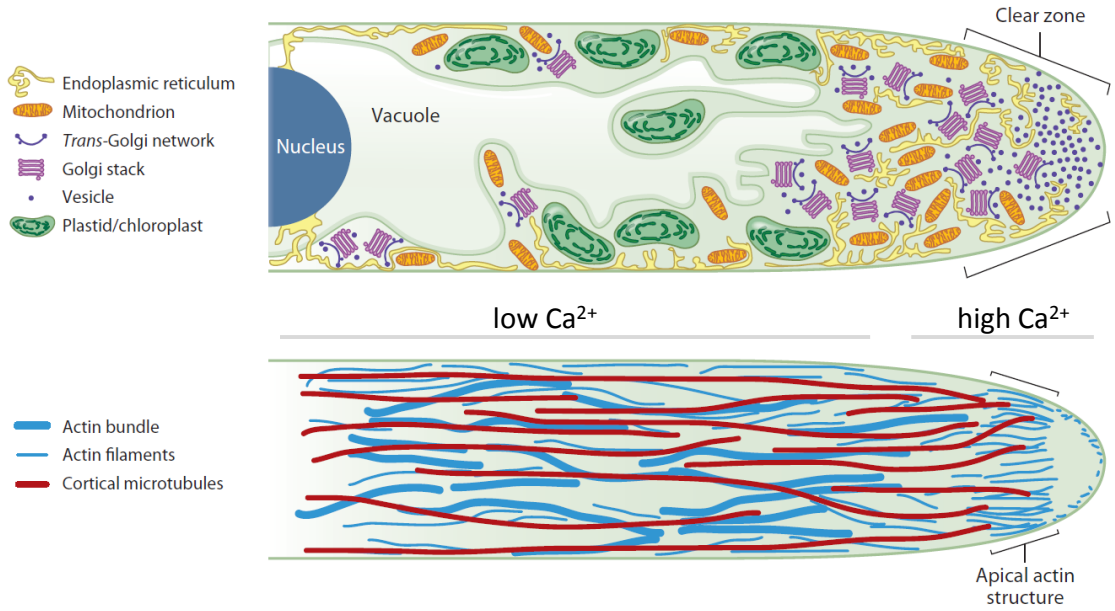

Figure 1.2: Cellular organization of polar growing cells. Pollen tubes consist of a single cell that elongates unidirectional by secretion of cell wall material to the apical pollen tube tip. Cell organelles are unevenly distributed along the pollen tube. The tip contains mainly structures necessary for secretion (vesicles, Golgi stacks and *trans*-Golgi network) and is referred to as clear zone. The shank region of the tube contains nucleus, vacuole, plastids and mitochondria. The differences between apex and shank are further manifested in the cytoskeletal organization: the apex contains circular actin filaments and the shank actin bundles and cortical microtubules constructed in the direction of tube elongation. Figure modified from Rounds and Bezanilla 2013.

Not only cell organelles are unevenly distributed along the pollen tube cell. One of the major characteristics of these cells is the tight maintenance of a calcium gradient with a maximum of 2-10 µM at the pollen tube apex and up to 0.2 µM in the shank of the pollen tube (Hepler *et al.* 2012; Holdaway-Clarke *et al.* 1997). Free calcium ions are severely toxic for the cell as they can form insoluble phosphate complexes, and therefore tight control of free calcium is crucial. The following sections first introduce important aspects of membrane structure and trafficking as well as general information about calcium-signaling in plants.

Eukaryotic membranes

Membranes are of outstanding importance for the structure of each cell and the basis of multicellular organisms (Horton *et al.* 2006). The principal components of all membranes are amphiphilic lipids; glycerophospholipids, glycolipids and sphingolipids. The polar head group of these lipids and the hydrophobic tail favor the formation of lipid bilayers in aqueous environments. In bilayers, the hydrophobic tails of the lipid molecules interact with each other, and form a hydrophobic barrier whilst the polar head groups are in contact with the aqueous surroundings of both sides of the bilayer (Fig 1.3). The PM (PM) surrounds the cell and is defined as a hydrophobic barrier. The PM separates the cytosol and the extracellular space and allows a controlled exchange of molecules between cells, compartments and the surrounding. The endomembranes allow the cell to compartmentalize into sub-structured organelles like nucleus, endoplasmic reticulum, Golgi, chloroplasts and mitochondria. To prevent non-selective diffusion of molecules, the exchange of energy, metabolites and information by the selective permeability of membranes is crucial (Horton *et al.* 2006). The hydrophilic surface of a membrane can attract various proteins that will associate via electrostatic interaction or flexible, acylated anchors that even penetrate the bilayer.

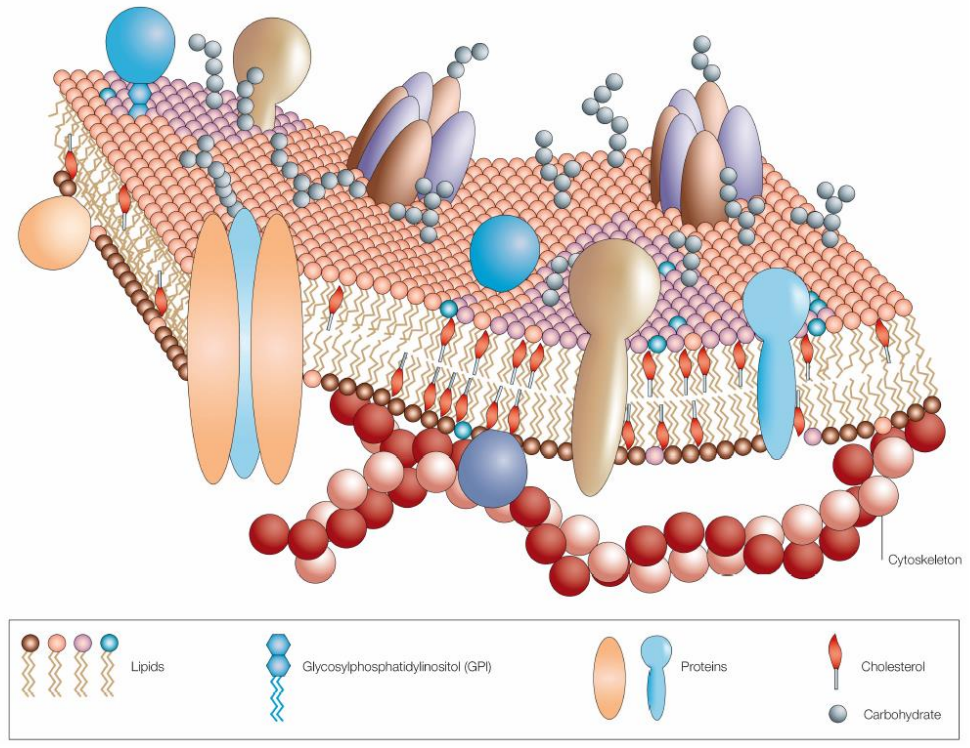

Figure 1.3: The eukaryotic PM. Fluid mosaic model according to (Singer and Nicholson 1972). The PM is composed of a lipid bilayer, containing proteins and lipids that link the membrane to intracellular and extracellular factors. Figure taken from Pietzsch 2004.

The cytoskeleton and membrane trafficking during polar tip growth in plants

Actin plays an important role during plant development, including cell division, organelle motility and polar growth. With a width of 7 nm, actin filaments (F-actin) are the thinnest elements of the cytoskeleton and consist of globular subunits (G-actin). Each of these subunits possesses a nucleotide binding site for ATP or ADP as ligands. F-actins is characterized by a polar structure, exhibiting a growing (+) - and a depolymerizing (-)-end. The association of the subunits takes place according to this polarity (head to tail). The external supplement of ATP leads to the polymerization of G-actin to F-actin *in vitro. In vivo*, these processes are tightly controlled by regulatory actin binding proteins (ABPs) (Chen *et al.* 2002; Yang and Pon 2002).

Calcium and membrane trafficking during polar tip growth in plants

The tip focused calcium gradient plays an important role in the apical tip growth of polar cells like pollen or root hair cells, as well as in fungal hyphae and mammalian neurons. Calcium is important for the fine tuning of pollen tube growth (Obermeyer and Weisenseel 1991; Picton and Steer 1983; Pierson *et al.* 1996). If calcium channels are blocked or ionophores are applied, pollen tube growth is inhibited (Obermeyer and Weisenseel 1991; Pierson *et al.* 1994). *In vivo*, the pistil of the flower supplies the growing pollen tube with external calcium that in turn promotes elongation (Franklin-Tong 1999). Growing pollen tubes possess a tip-focused calcium gradient that oscillates during growth. This oscillation is connected to growth, but is temporarily delayed (Cardenas *et al.* 2008). The molecular mechanisms that establish and regulate the calcium gradient are complex and require multiple transport systems (Hepler *et al.* 2012). Calcium is involved in the rigidification of pectin (see section 1.1.1), thereby controlling the elasticity of the apical tip (Bosch *et al.* 2005). Simultaneously high concentration of calcium can affect the de-polymerization of F-actin via ABPs (Samaj *et al.* 2006). Another important aspect of calcium signaling in pollen tubes contains the calcium sensor and response proteins (Schulz *et al.* 2013), which translate changes in cytosolic calcium concentration into signaling information (see section 1.5.2).

A study from Zhu and coworkers revealed that calcium modulates pollen development via annexin5-dependent membrane trafficking (Zhu *et al.* 2014). Annexins from plants and animals possess a conserved calcium and membrane-binding motif, and in plants are involved in controlling the cell cycle (Proust *et al.* 1999), in pollen germination (Zhu *et al.* 2014) and in primary root growth and root hair formation (Clark *et al.* 2005). To date, the underlying mechanisms that explain the correlation of pollen tube development and growth with actin cytoskeleton and PM and calcium remain unclear.

1.2 Molecular mechanism of membrane fusion, endocytosis and exocytosis controlled by phosphoinositides (PIs)

1.2.1 PIs – synthesis and degradation

PIs are glycerophospholipids with D-myo inositol as a polar head group, which can be phosphorylated at different positions (Balla 2006; Heilmann and Heilmann 2015; Stevenson *et al.* 2000; Thole and Nielsen 2008). All PIs derive from the phosphorylation of the membrane phospholipid phosphatidylinositol (PtdIns) by specific lipid kinases. A number of derivatives emerge from the phosphorylation of the hydroxyl groups at the position 3, 4 and 5 which are implied in specific regulatory functions in eukaryotic cells. Steric hindrance impedes the phosphorylation of position 2 and 6 of the lipid bound inositol ring. PIs resemble a family of structurally related lipids represented by phosphatidylinositol monophosphates (PtdIns3P, PtdIns4P, PtdIns5P), phosphatidylinositol bisphosphates (PtdIns(3,4)P_2, PtdIns(3,5)P_2, PtdIns(4,5)P_2) and phosphatidylinositol trisphosphates (PtdIns(3,4,5)P_3). It is still a matter of discussion whether PtdIns(3,4)P_2 and PtdIns(3,4,5)P_3 are present in plants (Fig. 1.4; Heilmann and Heilmann 2015). The lipid kinases that catalyze the phosphorylation of PI substrates are antagonized by lipid phosphatases. To date information about the role of these phosphatases is limited (Heilmann and Heilmann 2015).

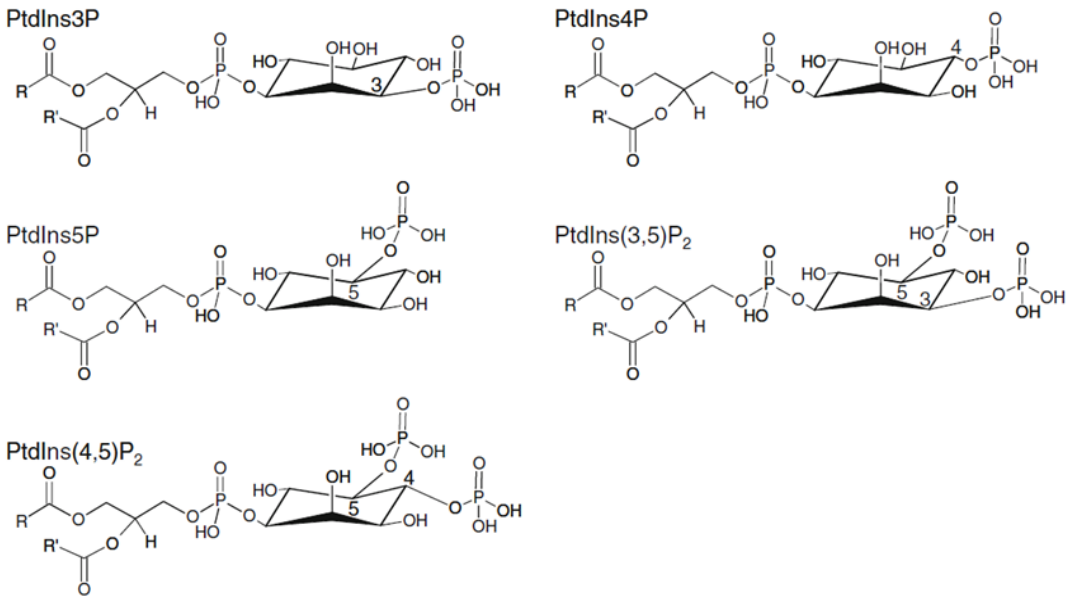

Figure 1.4: Structure of PIs present in plants. PIs are glycerophospholipids containing an inositol head group. The inositol ring can be phosphorylated at particular positions giving rise to six known PIs in plants: PtdIns3P, phosphatidylinositol-3-phosphate. PtdIns4P, phosphatidylinositol-4-phosphate. PtdIns5P, phosphatidylinositol-5-phosphate. PtdIns(3,5)P_2, phosphatidylinositol-3,5-bisphosphate. PtdIns(4,5)P_2, phosphatidylinositol-4,5-bisphosphate. Figure from Ischebeck *et al.* 2010a.

1.2.2 PtdIns(4,5)P_2 is synthetized by PI4P 5-kinases

In recent years, PtdIns(4,5)P_2 has emerged as a potent regulator of cellular processes in plants. The synthesis of the signaling lipid PtdIns(4,5)P_2 is the product of a sequential phosphorylation of the precursor molecule PtdIns. The first step is mediated by a PI 4-kinase, which transfers a phosphate to the position 4 of the inositol ring of PtdIns. In Arabidopsis four isoforms of PI 4-kinases could be identified in the Arabidopsis genome that can be subdivided in alpha and beta (Mueller-Roeber and Pical 2002). A third annotated γ-family appears not to harbor PI4-kinase activity (Galvao *et al.* 2008). PI 4-kinases are soluble enzymes and the alpha type possess a PH-binding domain that binds to PtdIns4P (Stevenson *et al.* 1998).

The second phosphorylation is introduced at position 5 of the inositol ring by a PI4P 5-kinase. The classification of phosphatidylinositol phosphate kinases results from their substrate specificity. The type I PIP-kinases favor the substrate PtdIns4P and add a second phosphoryl group to the inositol head group at position 5. All PIP-kinases investigated in this thesis belong to the type I PIP-kinases. Representative PIP-kinases belong to the type II, possess lipid kinase activity for PtdIns5P and phosphorylate the 4-position of the inositol ring in PtdIns. For this class of PIP-kinases no plant homolog could be identified to date. The Arabidopsis genome encodes for 11 isoforms of type I PIP-kinases (PI4P 5-kinases), which can be divided into two subclasses (Mueller-Roeber and Pical 2002). PI4P 5-kinases of subfamily A consist of a dimerization domain and the catalytic domain. PI4P 5-kinases of subfamily B possess additional N-terminal domains (Fig. 1.5).

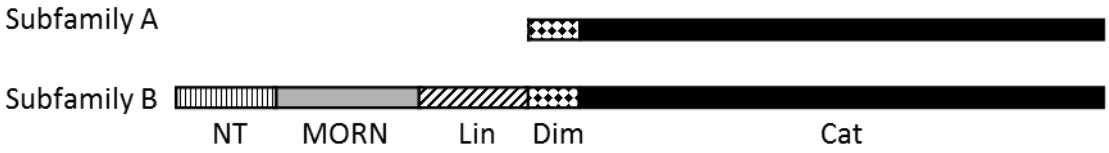

Figure 1.5: Domain structure of PI4P 5-kinases from Arabidopsis. In Arabidopsis PI4P 5-kinases are grouped into subfamilies A and B. PI4P 5-kinases of subfamily B are larger and contain additional N-terminal domains not present in the smaller enzymes of subfamily A. NT, N-terminal domain. MORN, membrane occupation and recognition nexus-domain. Lin, Linker domain. Dim, Dimerization domain. Cat, Catalytic domain. Figure from Ischebeck and Heilmann 2010.

1.2.3 Signaling molecules control polar tip growth

The elongation of a pollen tube cell is the result of a tight orchestration of numerous cellular processes and involves different signaling pathways. Endo- and exocytosis, crucial for growth, are dependent on the characteristics of the cell wall and the adjacent PM.

PI4P 5-kinases and PtdIns(4,5)P_2 control polar tip growth

In recent years, PIs have emerged as important regulators of vesicular trafficking in plants (Ischebeck *et al.* 2008; Ischebeck *et al.* 2010b; Ischebeck *et al.* 2013; Kusano *et al.* 2008; Sousa *et al.* 2008; Thole and Nielsen 2008; Zhao *et al.* 2010). Polar growing cells are a suitable system to investigate the influence of PIs on polarity. For instance, it was found that the synthesis of PtdIns(4,5)P_2 by the PI4P 5-kinase AtPIP5K3 is essential for the growth and polarity of root hairs (Kusano *et al.* 2008; Stenzel *et al.* 2008). Overexpression of the pollen specific PI4P 5-kinases AtPIP5K5 and AtPIP5K6 in tobacco (*Nicotiana tabacum*) pollen tubes leads to increased deposition of pectin at the apical PM (Fig. 1.6 C) (Ischebeck 2008; Ischebeck *et al.* 2010b; Stenzel *et al.* 2008; Stenzel *et al.* 2012; Zhao *et al.* 2010). During pollen tube growth, Arabidopsis PI4P 5-kinases, for instance AtPIP5K6, localize at the apical PM (Fig. 1.6 A). As a result of the enhanced secretion of pectin, pollen tubes undergo morphological changes dependent on the level of overexpression (Fig. 1.6 B and C) (Ischebeck 2008; Ischebeck *et al.* 2010b). The effects observed are initiated by the increased availability of PtdIns(4,5)P_2, not by the increasing amount of protein expressed (Ischebeck 2008; Ischebeck *et al.* 2010b), as it was verified by the expression of a catalytic inactive variant of AtPIP5K5.

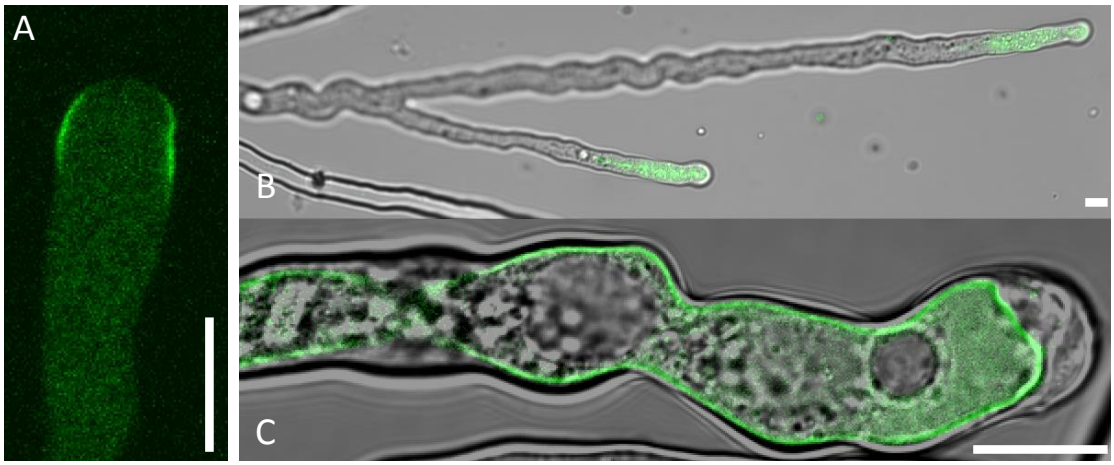

Figure 1.6: Overexpression of AtPIP5K6-EYFP in tobacco pollen tubes. A, AtPIP5K6 localizes to the apical PM B, intermediate overexpression of AtPIP5K6 causes branched phenotypes; merge of EYFP and bright field image. C, strong overexpression of AtPIP5K6 causes stunted pollen tubes with a trapped protoplast phenotype; merge of EYFP and bright field image. Bars = 10 µm.

So far, the exact molecular targets of PIs are not clear. Phosphoinositides, especially PtdIns(4,5)P_2, can be cleaved by PLC into membrane standing diacylglycerol (DAG) and the second messengers, such as inositol(1,4,5)P_3 (Ins(1,4,5)P_3; IP_3), which also influence cellular calcium concentration (Krinke *et al.* 2007; Pokotylo *et al.* 2014). Under physiological conditions, PtdIns(4,5)P_2 has been proposed to influence clathrin-mediated endocytosis (CME) (Ischebeck *et al.* 2013; König *et al.* 2008; Zhao *et al.* 2010). When AtPIP5K6 was down

regulated by RNA interference, CME was inhibited and pollen tube elongation was delayed (Zhao *et al.* 2010). The depletion of PtdIns(4,5)P_2 also influences the CME recycling of auxin efflux carriers PIN-FORMED (PIN) in the PM and disturbs the polar distribution of PIN1 and PIN2 in the cell (Ischebeck *et al.* 2013; Mei *et al.* 2012; Tejos *et al.* 2014).

Similarly, the effects of enhanced activity of PI-PLC indicate that synthesis and degradation of PtdIns(4,5)P_2 must be balanced to keep up normal pollen tube elongation (Klahre *et al.* 2006). Various studies indicate that an excess supply of PtdIns(4,5)P_2 perturbs the PI-system and induces abnormal pollen tube growth (Ischebeck *et al.* 2008). As the secretion of pectin is essential for the elasticity of the pollen tube under normal growth conditions (Krichevsky *et al.* 2007), the effects of perturbing PtdIns(4,5)P_2 formation on pollen tube growth can be explained by the effects on vesicle trafficking to the apical PM.

PIs influence the dynamics of the actin cytoskeleton. In animal cells, a high level of the regulatory phospholipid PtdIns(4,5)P_2 promotes actin polymerization, whereas low levels of PtdIns(4,5)P_2 lead to actin depolymerization (Yin and Janmey, 2003). Though actin itself is unable to bind PIs, certain ABPs have been found to be regulated by PtdIns(4,5)P_2 in plants (Braun *et al.* 1999). ABPs with destabilizing character from the family of actin depolymerizing factors (ADF)/cofilins selectively disassemble F-actin from the depolarizing-end in animals (Lassing and Lindberg 1985). In Arabidopsis, the ADF/cofilins are inhibited by PtdIns(4,5)P_2 (Gungabissoon *et al.* 1998), and it is possible that regions of the PM that are enriched in PtdIns(4,5)P_2 counteract the destabilization of actin filaments (Gungabissoon *et al.* 1998; Yin and Janmey 2003).

1.3 Three- dimensional structure of PI4P 5-kinases

To understand the roles of PtdIns(4,5)P_2 it is important to delineate modes of regulation of PI4P 5-kinases. Therefore a closer look has to be taken at the structural basics of PIP-kinases. The structural characteristics of PI4P 5-kinases were described for the first time in 1998 when Rao and coworkers succeeded in crystallizing the human PI5P 4-kinase II β (HsPIP4KIIβ, PDB 1BO1). It has been reported that the human PI5P 4-kinase is a homo dimer, joined by N-terminal dimerization domains of each monomer (Fig. 1.7 A) (Rao *et al.* 1998). It exhibits a large flattened membrane interaction domain with the active site located in the center (Fig. 1.7 B). Within the active site, ATP and PtdIns-monophosphate substrates are coordinated in a particular geometry favoring phosphorylation of the 4-position of inositol with magnesium within the active site. The flattened membrane interaction domain possesses several basic

patches that are proposed to facilitate interaction with the negative charged phospholipid bilayer by electrostatic interactions (Burden *et al.* 1999).

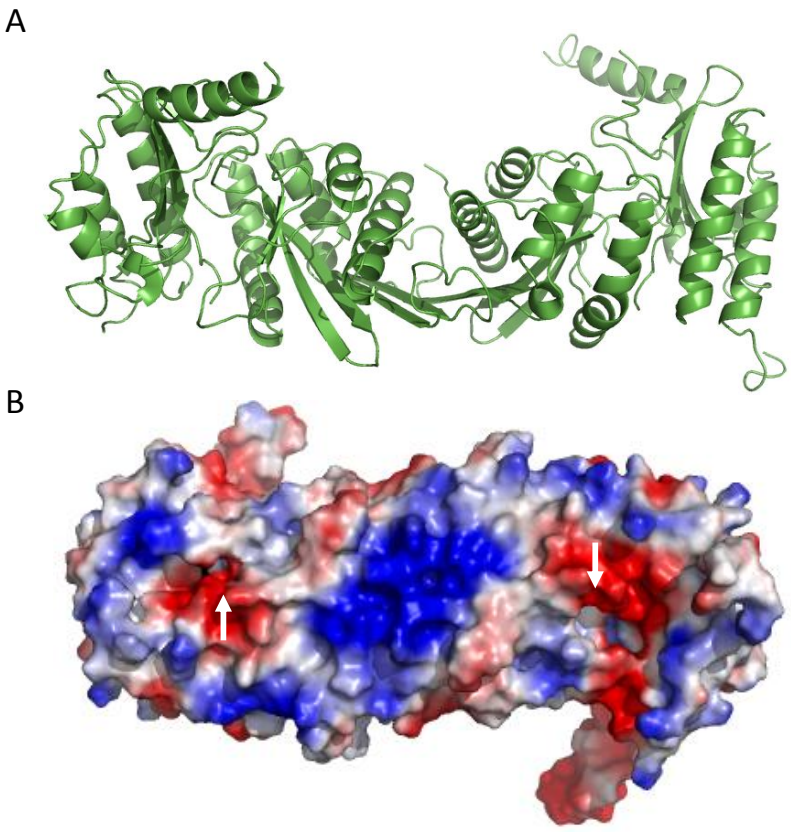

Figure 1.7: Crystal structure of human PIP4KIIβ (PDB 1BO1). A, homodimer in medial cartoon view. B, dimer in ventral view. The electrostatic potential is indicated in colors and was calculated with PyMol. Red, negative charge. Blue, positive charge. The active center with the binding sites for ATP and PtdIns-monophosphate are indicated by white arrows. Figure was generated with PyMol.

In contrast to other lipid modifying enzymes like phospholipase C (PLC), that penetrates the lipid bilayer with a membrane anchor by hydrophobic interactions of specific domains (Hurley and Grobler 1997), the concept of membrane association of PIP-kinases is different. The knowledge gained from the successful elucidation of the three-dimensional protein structure, provided information about the substrate conversion of PtdIns-monophosphates to PtdIns-bisphosphates. The closer examination of the membrane interface was carried out by the introduction of point mutations that changed local charges in the basic regions. When basic amino acid residues were changed to acidic amino acid residues, the affinity of the enzyme towards substrate vesicles, containing Ins4P, was strongly reduced (Burden *et al.* 1999; Fairn *et al.* 2009; Rao *et al.* 1998). Mutagenesis studies from the same group revealed that, indeed, the change of the charge within this basic membrane interaction domain has an effect on membrane affinity of the protein (Park *et al.* 2001).

In 2009, Fairn and coworkers took a closer look to the correlation of the surface potential of HsPIPKIα and its ability to associate to the PM of cells (Fairn *et al.* 2009). The authors observed that the introduction of a negative charge at the ventral site of the protein lowered enzyme activity *in vitro* and the ability of HsPIPKIα to associate to the PM of macrophage cells *in vivo*. This modulation can be hypothesized to function as an electrostatic switch to regulate PIP-kinase activity. Taken together, the findings presented in the section above indicates that the charge of the ventral membrane interaction domain is crucial for the association of the PIP-kinase with substrate lipids in the target membrane.

1.4 Posttranslational regulation of PI4P 5-kinases

Phosphorylation of PIP-kinases has been described for yeast, mammals and plants. In 1999 research from the group around Vancurova *et al.* revealed that a PM associated PI4P 5-kinase from *Schizosaccharomyces pombe* is phosphorylated by casein kinase I (CKI) (Vancurova *et al.* 1999). The results were confirmed for the yeast *Saccharomyces cerevisiae*. In *S. cerevisiae* the gene *MSS4* encodes for the single PI4P 5-kinase MSS4P. The enzyme is located at the PM and upon phosphorylation by CKI relocates to the nucleus (Audhya and Emr 2003). Studies from Park *et al.* from 2001 showed that human PI4P 5-kinase Type I (HsPIPKIα) is phosphorylated by protein kinase A (PKA), and upon phosphorylation the catalytic activity was reduced (Park *et al.* 2001). In turn, treatment with the protein phosphatase PP1 positively influenced HsPIPKIα activity. PKA belongs to the superfamily of AGC protein kinases (named after the protein kinases A, G and C). PKA is regulated by cyclic AMP and so far no homolog has been identified for Arabidopsis. Results published by Hinchliffe and Irvine in 2006 indicate phosphorylation of HsPIPKIIβ by protein kinase D (PKD) (Hinchliffe and Irvine 2006). The phosphorylation site was mapped to a conserved threonine residue within the activation loop, and the responsible protein kinase was identified as PKD. Upon site-directed mutagenesis, activity of the enzyme was reduced by 80 %, independent of the charge introduced (T to A or D; Hinchliffe and Irvine 2006). The authors concluded that the enzyme might not tolerate modification at this site of the protein and enzyme activity is regulated by protein turn over. The PKD belongs to the super family of calcium and calmodulin-dependent protein kinases (CAMK) and is activated by DAG and the lipid dependent AGC-kinase PKC (Rozengurt *et al.* 2005). Similar to PKA there is no homolog protein known for Arabidopsis.

Evidence for the phosphorylation of Arabidopsis PI4P 5-kinases, was published in 2001 by Westergren and coworkers. The experiments performed, lead to the hypothesis that AtPIP5K1 can be phosphorylated by PKA and a complex protein extract prepared from Arabidopsis

leaves. Furthermore the phosphorylation of PKA, as well as of leaf extract lowered catalytic activity *in vitro* (Westergren *et al.* 2001). The corresponding phosphorylation sites were not identified, raising the questions which amino acid residues are phosphorylated and, which kinases are involved in the phosphorylation of AtPIP5K1. During the last years, research undertaken in the group of Prof. Dr. Ingo Heilmann revealed, that several PI4P 5-kinases can be phosphorylated by plant extracts (Dr. Jennifer Lerche, Dissertation 2013, unpublished data). A non-targeted phosphoproteome analysis on Arabidopsis pollen and pollen tubes revealed the presence of phosphorylation sites in PI4P5-kinases including T590 and T597 in AtPIP5K6 (Mayank *et al.* 2012). The relevance of these sites and the protein kinases involved were not investigated.

Bases on the structural data (Fig. 1.7) and the notion that negatively charged residues at the PIP-kinase-membrane interface may interfere with PM-association of the enzyme; a model how phosphorylation may inhibit PI4P 5-kinase activity is proposed (Fig. 1.8).

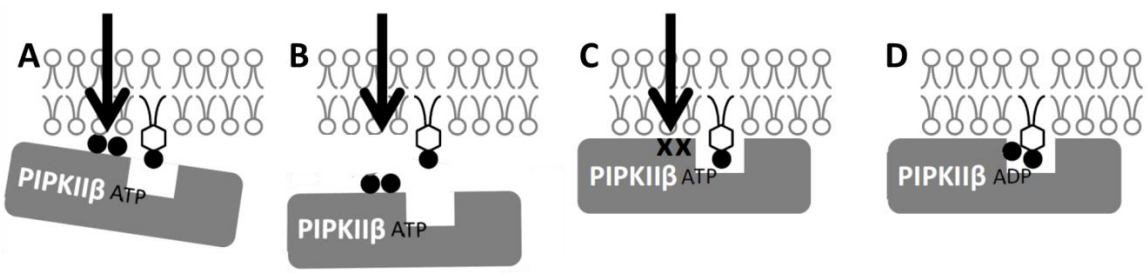

Figure 1.8: A model of phosphorylation regulating PI4P 5-kinase activity and/or membrane association. A, Phosphorylation at the membrane interface (circles, arrow) interferes with the electrostatic interaction of the basic ventral side of human PIP-kinase II beta with anionic phospholipids. B, PIP5KIIβ is removed from the membrane by phosphorylation at the membrane interface (circles, arrow). C, Dephosphorylation (crosses, arrow) enables interaction with the substrate lipids. C, Proper membrane binding leads to the formation of PtdIns(4,5)P_2.

1.5 Protein kinases and protein phosphorylation

Various organisms have evolved post-translational modifications of proteins as part of cellular signaling in response to stimuli or endogenous cues. Phosphorylation is a prominent example among these modifications. Besides the control of protein abundance by transcription and translation, activity, protein stability or subcellular localization can be modulated by phosphorylation (Olsen *et al.* 2006). The interaction with other biomolecules can also be affected by phosphorylation of one or both parties. The transient effect of a phosphorylation often induces a conformational change that influences the biophysical and biochemical properties of a protein (Johnson and Hunter 2005). This effect is reversible by phosphatases that remove the modification. Proteins can be phosphorylated by different protein kinases and

at multiple sites. Substrates for phosphorylation are amino acids with hydroxyl groups like serine, threonine and tyrosine. There is also evidence for histidine and glutamate phosphorylation though they are chemically less stable. The ratio of serine (S), threonine (T) and tyrosine (Y) phosphorylation has been estimated to ~86:12:2 (Hunter 1996; Olsen *et al.* 2006). The most abundant phosphorylated amino acids are serine and threonine. However, recent reports stress the importance of tyrosine phosphorylation (Lin *et al.* 2014; Nito *et al.* 2013; Oh *et al.* 2012). The protein S/T kinases and protein Y kinases specifically phosphorylate S/T and Y residues, respectively. Dual specificity kinases phosphorylate S/T as well as Y residues. For protein phosphatase, the specificity is similarly annotated: S/T phosphatases dephosphorylate phospho-S/T residues, phosphorylated S/T or Y residues are dephosphorylated by dual specificity phosphatases (reviewed by Pawson and Scott 2005).

Many protein kinases need to be activated before they can phosphorylate their substrates. This activation can either be conducted by autophosphorylation activity or through phosphorylation from required upstream protein kinases, as, for example, in the case of MAP-kinase cascades. Protein kinase activities can be regulated by molecules like cyclic AMP, proteins like calmodulin or cyclins, and ions like calcium.

1.5.1 Mitogen-activated protein kinase (MAPK) signaling

MAPKs have been termed “mitogen-activated protein kinases” because the first identified enzyme of MAPK signaling was involved in growth factor signaling in mammals. When these enzymes were identified for plants, it became clear that MAPK signaling is involved in diverse functions and specifically in signal amplification. Signal amplification occurs, because the MAPK family is represented by a three kinase cascade of protein kinases. The cascade is hierarchically organized as follows: a MAP kinase kinase kinase (MAP3K) is activated by a biotic or abiotic stimulus and in turn phosphorylates a MAP kinase kinase (MAP2K, also called MKK for MAPK kinase or MEK for mitogen/extracellular signal-regulated kinase). This phosphorylation activates the MAP2K, which subsequently phosphorylates a MAP kinase (MAPK or MPK). The MPKs will then phosphorylate their specific substrates and this represents the final step of the cascade. MAP3Ks phosphorylate MAP2Ks at a conserved S/T-$X_{3–5}$-S/T-motif (Chang and Karin 2001). The phosphorylation motif of MAP2Ks within MAPKs is composed of conserved T-X-Y-motif (Chang and Karin 2001). For yeast and mammals it is known that there are specific scaffolding proteins to connect MPKs and their substrates (Brown and Sacks 2009; Morrison and Davis 2003; Widmann *et al.* 1999). So far, for plants such proteins have not been identified. First evidences about MAPK kinase scaffolding proteins were reviewed by Suarez-Rodriguez and coworkers (Rodriguez *et al.* 2010), describing a putative scaffold function of the

Arabidopsis MAP3K MEKK1. A protein kinase-inactive variant of MEKK1 rescued the phenotype in a *mekk1* background, suggesting a kinase-activity independent function of MEKK1 (Suarez-Rodriguez *et al.* 2007). Furthermore, it is established for mammalian MAPK-signaling, that there are specific docking motifs within substrate proteins of the MAPK-pathway (Tanoue and Nishida 2003). So far, this concept of docking sites within MPK substrates was demonstrated only by one study (Schweighofer *et al.* 2007). Additionally, it was reported that MAPKs physically interact with substrate proteins (Doczi *et al.* 2012).

Not many MPK substrates are identified for plants to date. The phosphorylation motif of MAPKs is described as an S or T residue +1 amino acid in distance of a proline (P) (Biondi and Nebreda 2003). Examples of identified MAPK substrates are two proteins involved in ethylene signaling, ACS2/ACS6 (1-aminocyclopropan-1-carboxylic acid synthase, involved in ethylene biosynthesis; Liu and Zhang 2004) and ERF6 (ethylene response factor 6; Meng *et al.* 2013). Furthermore, two transcription factors were identified to be directly phosphorylated by MPK6: WRKY33 (camalexin biosynthesis; Mao *et al.* 2011) and BES1 (brassionosteroid insensitive 1-ethyl methanesulfonate-suppressor1, involved in plant immunity; Kang *et al.* 2015). Another relevant finding is the phosphorylation of MVQ proteins, which are involved in stress response (Pecher *et al.* 2014).

The protein kinases of the MAPK family play an important role in plant immunity and stress response (Pitzschke *et al.* 2009; Rodriguez *et al.* 2010; Tena *et al.* 2011). The initial stimulus that starts MAPK signaling is recognized by surface receptors like, for instance, the bacterial flagellin receptor FLAGELLIN SENSITIVE 2 (FLS2) that recognizes the elicitor peptide flg22 (Gomez-Gomez and Boller 2000), or the chitin receptor CHITIN ELICITOR RECEPTOR KINASE 1 (CERK1) (Miya *et al.* 2007). Interestingly, these receptors have jet not been reported for pollen tube signaling.

Recent findings revealed a connection between MAPK-signaling and cytoskeletal microtubule organization in Arabidopsis which was so far only described for animals (Komis *et al.* 2011). In two recent publications, *MPK6* was identified to be involved in the regulation of polar growth. MPK6 negatively regulates root hair formation and primary root elongation (Lopez-Bucio *et al.* 2014). Arabidopsis *mpk6* mutants showed increased number and length of root hairs compared to wild type, indicating a possible role in root hair development (Lopez-Bucio *et al.* 2014). Guan and coworkers investigated the role of *MPK6* in pollen tube growth in Arabidopsis in 2014. The authors observed that pollen of Arabidopsis *mpk3 mpk6* double mutants is disturbed in funicular guidance *in vivo*, leaving micropylar guidance unaffected (Guan *et al.* 2014). The findings indicate that MPK3 and MPK6 are involved in the activation of downstream

cues for funicular guidance and are possibly involved in the regulation of polar growth. The underlying mechanisms remain to be elucidated.

1.5.2 Calcium sensing and protein kinase signaling

Calcium is an important multifunctional signal in all living cells. Cytosolic concentrations are low (<1 µM), but can transiently elevate in recurring patterns characterized by frequency and amplitude up to 2-10 µM at the pollen tube apex (Feijo *et al.* 2001; Holdaway-Clarke *et al.* 2003). Calcium signals especially during polar growth are tightly controlled and underlie temporal and spatial changes. To decode the information of cytosolic calcium changes into a signaling event, calcium has to be perceived by specific calcium-sensor proteins such as calmodulin (CaM) or calcineurin B-like proteins (CBL) and calcium-dependent protein kinases (CDPKs; Fig.1.9) (Sanders *et al.* 2002; Steinhorst and Kudla 2013; 2014). The sensor proteins CaM and CBL do not possess protein kinase activity (Luan *et al.* 2002). Proteins that can sense calcium and transform this information, with protein kinase activity, into a posttranslational modification are classified as calcium sensor response proteins. There are CBL-interacting protein kinases (CIPKs) which form complexes with CBLs (Kolukisaoglu *et al.* 2004; Kudla *et al.* 1999; Shi *et al.* 1999). Within these complexes one protein is responsible for calcium sensing and the other for the response reaction.

A prominent example for proteins that can function as both sensor and response proteins are CDPKs, represented as a large group of proteins (Hrabak *et al.* 2003). Structural investigations revealed that their protein sequence contains a variable N-terminus, a protein kinase domain, an auto inhibitory domain, and a CaM-like domain (Harper and Harmon 2005). The protein kinase domain contains the ATP-binding site. The auto inhibitory domain inactivates the CDPK under calcium-free conditions. Calcium binding takes place via the CaM-like domain, containing four EF-hand motifs (Harper and Harmon 2005). Mutations at distinct amino acids within the protein kinase domain lead to the loss of activity. An amino acid exchange within the auto inhibitory domain leads to a constitutive activation of the enzyme (Rodriguez Milla *et al.* 2006). In the absence of calcium, the protein kinase activity is inhibited by the auto inhibitory domain. By the binding of four calcium ions to the corresponding EF-hand motifs, the inhibitory effect on the kinase domain is lifted and the enzyme is activated (Harper and Harmon 2005).

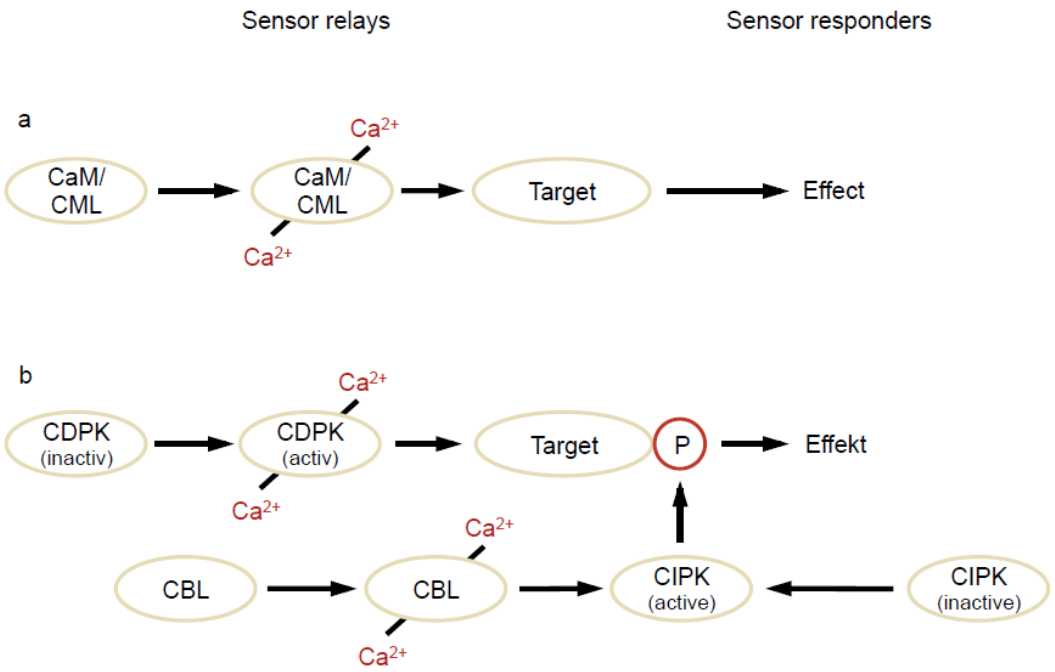

Figure 1.9: Calcium sensing and signaling. Calcium signaling can be subdivided into calcium sensor relays (a) and sensor responders (b). Figure taken from Heilmann 2015.

In the Arabidopsis genome 34 genes encoding for CDPKs were identified, that are expressed during the whole life cycle of the plant in various tissues. Out of 34, 28 bear a predicted N-terminal acylation sequence that is proposed to mediate PM association (Boudsocq and Sheen 2013; Myers *et al.* 2009). Nine CDPKs are exclusively expressed in pollen (Boudsocq and Sheen 2013). There is evidence that CDPKs also play a role in pollen tube elongation. For instance, the investigation of the role of CPK17 and CPK34 during polar growth of pollen tubes revealed, that pollen transmission efficiency is drastically reduced in a *cpk17 cpk34* double mutant (Myers *et al.* 2009). The authors conclude that CPK17 and CPK34 contribute to the fitness of pollen and the response to tropism cues. Additionally, results of the group around Prof. Dr. Tina Romeis showed that CPK2 and CPK20 regulate pollen tube growth by the mediation of the anion channel SLAH3 (Gutermuth *et al.* 2013). In 2013, Zhao and coworkers identified CPK11 and CPK24 as negative regulators of pollen tube growth. Furthermore in this study, a connection between the mentioned CPKs and the activation of the shaker pollen inward K^+-channel (SPIK) was outlined (Zhao *et al.* 2013). The molecular mechanisms of this connection remain unclear to date. CPK11 was shown to directly phosphorylate and interact with Di19, a product of a stress-induced gene (Rodriguez Milla *et al.* 2006), and CPK24 (Zhao *et al.* 2013).

In summary, the current literature suggests that several isoforms of the CDPK family seem to influence different ion channels indirectly, and that this regulation has relevance for pollen tube development.

1.6 Hypothesis of phosphorylation dependent regulation of PI4P 5-kinases

Overall, there is evidence that PI-signaling and protein phosphorylation events have important roles in the control of polar tip growth in plants. In this thesis, I confirmed the hypothesis that PI4P 5-kinases from plants are regulated by protein kinases. Evidence from the literature suggested phosphorylation as a conserved mechanism of PI4P 5-kinase activity regulation (Hinchliffe and Irvine 2006; Park *et al.* 2001) and possibly enzyme localization (Audhya and Emr 2003) in mammals and yeast (see section 1.4). The identification of a protein kinase, responsible for plant PI4P 5-kinase regulation, would integrate PI-signaling with other conserved signaling pathways, mainly protein phosphorylation cascades. So far, there has been no evidence in literature about the regulation and interconnection of PI-signaling with other signaling pathways.

1.7 Aims and Objectives

The aim of this work was the identification of protein kinases involved in the phosphorylation of Arabidopsis PI4P 5-kinases in pollen tubes. The specific objectives were as follows:

- Determine whether or not PI4P 5-kinases are phosphorylated by protein kinase activities from pollen tube extracts
- Identify protein kinases from tobacco pollen extract that phosphorylate AtPIP5K6
- Determine whether or not there are specific protein-protein interactions between PI4P 5-kinases and candidate protein kinases
- Determine the phosphorylation sites and establish a link between phosphorylation and PI4P 5-kinase function
- Characterize the effects of PI4P 5-kinase phosphorylation *in vitro* and *in vivo*

2 Materials and Methods

2.1 Chemicals

γ-[^{33}P]-ATP	Hartmann Analytics, Braunschweig, Germany
Agar	Invitrogen, Karlsruhe, Germany
Agarose	Duchefa Biochemie, Haarlem, The Netherlands
Carbenicillin	Duchefa Biochemie, Haarlem, The Netherlands
Desoxynucleotide triphosphate (dNTPs)	Roche Molecular Biochemicals, Mannheim, Germany
Isopropyl-β-D-thiogalactosylpyranoside (IPTG)	MBI Fermentas, St. Leon Rot, Germany
Kanamycin	Duchefa Biochemie, Haarlem, The Netherlands
Peptone	Invitrogen, Karlsruhe, Germany
PhosSTOP, Phosphatase Inhibitor Cocktail	Roche Diagnostics GmbH, Mannheim, Germany
Phospholipids	Avanti Polar Lipids Inc., Alabaster, AL, USA
Rifampicin	Duchefa Biochemie, Haarlem, The Netherlands

All other chemicals were supplied by the companies Karl Roth (Karlsruhe, Germany), Merck (Darmstadt, Germany), Fluka (Steinheim, Germany) or Sigma-Aldrich (Schnelldorf, Germany).

2.2 Enzymes and molecular size markers

GeneRulerTM 1kb DNA-Ladder	Thermo Fisher Scientific GmbH, Dreireich, Germany
Lysozyme	SERVA Electrophoresis GmbH, Heidelberg Germany
Protein phosphatase 1(PP1)	NEB, Ipswich, MA, USA
Phusion High Fidelity DNA-Polymerase	NEB, Ipswich, MA, USA
Protein kinase A (PKA) Catalytic subunit from bovine heart	Sigma-Aldrich, Schnelldorf, Germany
Prestained Protein Molecular Weight Marker	Thermo Fisher Scientific GmbH, Dreireich, Germany
Restriction endonucleases	Thermo Fisher Scientific GmbH, Dreireich, Germany
Trypsin from bovine pancreas	Sigma-Aldrich Schnelldorf, Germany
Unstained Protein Molecular Weight Marker	Thermo Fisher Scientific GmbH, Dreireich, Germany

2.3 Kits

GeneJET™ Gel Extraction Kit	Thermo Fisher Scientific GmbH, Dreireich, Germany
GeneJET™ Plasmid Miniprep Kit	Thermo Fisher Scientific GmbH, Dreireich, Germany
CompactPrep Plasmid Midi Core Kit	Qiagen, Hilden, Germany
Amylose Resin	NEB, Ipswich, MA, USA
MBP Trap HP, 5 ml	GE Healthcare Life Sciences, Stockholm, Sweden

2.4 Equipment

ÄKTA FPLC Protein Purification System	GE Healthcare Life Sciences, Stockholm, Sweden
Fluorescence Stereo Microscope AXIO IMAGER M1	Carl Zeiss, Jena, Germany
38 HE Filterset for EYFP	Carl Zeiss, Jena, Germany
43 HE Filterset for mCherry	Carl Zeiss, Jena, Germany
Laser Scanning Confocal Microscope LSM 780	Carl Zeiss, Jena, Germany
Helium driven particle delivery system PDS-1000	BioRad, Munich, Germany
SDS gel rigs, SE 250	Hoefer scientific instruments, Holliston, MA, USA
FRENCH^{TM}-PRESS	Gaulin, APV Homogeniser GmbH, Gatwick, UK
Fujifilm BAS-1500 phosphorimager	Fujifilm, Düsseldorf, Germany

2.5 Single-use materials

Cellulose Acetate Filter 0.2 µm	Sartorius, Göttingen, Germany
Micron Gold Microcarriers, Stopping Screens, Rupture Disks (1350 psi)	BioRad, Munich, Germany
Silica S60 thin layer chromatography plates 20 x 20 cm	Merck, Darmstadt, Germany

2.6 Software

Several software tools were used to process, image or sequence data as described in table 2.1.

Table 2.1: Software tools used in this thesis.

ImageJ (http://rsbweb.nih.gov/ij/)	Graphic tool for image analysis and processing
GIMP	Graphic tool for image analysis and processing

Photoshop 7.0 (Adobe Systems, Munich, Germany)	Graphic tool for image analysis and processing
TINA (Raytest, Straubenhardt, Germany)	Quantification of phosphor images
PhosPhAt 4.0 www.cbs.dtu.dk/services/NetPhos/ (Heazlewood *et al.* 2008)	Database for experimentally identified phosphorylation sites in *Arabidopsis* proteins
The PyMOL Molecular Graphics System, Schrödinger, LLC	3D-graphic software for the display of biomolecules

2.7 Plant lines

Table 2.2: Plant lines used during this thesis.

Name	Species	Transgenes	Obtained from
Arabidopsis wild type Col-0	*Arabidopsis thaliana* Ecotype *Columbia 0*	-	Department of Cellular Biochemistry MLU Halle-Wittenberg
Tobacco wild type	*Nicotiana tabacum* Ecotype Samsun N	-	Department of Cellular Biochemistry MLU Halle-Wittenberg
Tobacco pBE2113 empty vector pBE2113	*N. tabacum* Ecotype Samsun N	pBE2113	Seo *et al.*2007
WIPK/SIPKIR Line 2 and 3			

2.8 Microorganisms

Organism	Strain	Genotype	Reference
Escherichia coli	DH5α	fhuA2 Δ (argF-lacZ)U169 phoA glnV44 Φ80 Δ(lacZ)M15 gyrA96 recA1 relA1 endA1 thi-1 hsdR17	-
E. coli	Rosetta 2	F- ompT hsdSB (rB- mB-) gal dcm (DE3) pRARE2(Cam2)	-
Saccharomyces cerevisiae	*NMY51*	MATa his3Δ200 trp1-901 leu2-3,112 ade2 LYS2::(lexAop) 4-HIS3 ura3::(lexAop) 8-lacZ ade2::(lexAop) 8-ADE2 GAL4	(Hood *et al.* 1993)

2.9 Plasmids

Table 2.4: Plasmids used in this thesis.

Vector	Selection marker	Obtained from	Plasmid structure
pETM41	KanR	Dr. Achim Dickmanns, Göttingen, Germany	Plasmid contains an N-terminal MBP-tag for purification and a TEV cleavage site for removal of the MBP-tag
pMALc5g	AmpR	NEB, Ipswich, MA, USA	Plasmid contains an N-terminal MBP-tag for purification and a Genase cleavage site for removal of the MBP-tag
pLatGW	AmpR	Prof. Dr. Wolfgang Dröge-Laser, Würzburg, Germany	Plasmid contains a *Lat52* promotor used for pollen-specific expression in front of a Gateway cassette containing attR1 and attR2 sequences required for the Gateway®-System
pENTRY	AmpR	Dr. Mareike Heilmann, MLU Halle-Wittenberg	
pBT3C-OST4	KanR	Dr. Mareike Heilmann, MLU Halle-Wittenberg	
pPR3N	AmpR	(Hood *et al.* 1993)	

2.10 Contructs

Table 2.4: cDNA constructs used in this thesis

Construct	Promotor	Modifications	Obtained from
pETM41-*AtPIP5K1*	*T7*		Dr. Irene Stenzel, MLU Halle-Wittenberg
pMAL-*AtPIP5K5*	*T7*	c-terminal hexahis-tag	this thesis
pMAL-*AtPIP5K6*	*T7*	c-terminal hexahis-tag	this thesis
pMAL-*NtPIP5K6*	*T7*	c-terminal hexahis-tag	this thesis
pMAL-*AtPIP5K6 T590A*	*T7*		this thesis
pMAL-*AtPIP5K6 T590D*	*T7*		this thesis
pMAL-*AtPIP5K6 T597A*	*T7*		this thesis
pMAL-*AtPIP5K6 T597D*	*T7*		this thesis
pMAL-*AtPIP5K6 T590A T597A*	*T7*		this thesis
pMAL-*AtPIP5K6 T590D T597D*	*T7*		this thesis
pET24b-*CPK11*	*T7*		this thesis
pET24b-*CPK11 D150A*	*T7*		this thesis
pBT3C-*OST4-AtPIP5K5*	*CYC1*		Dr. Mareike Heilmann, MLU Halle-Wittenberg
pBT3C-*OST4-AtPIP5K6*	*CYC1*		this thesis
pBT3C-*OST4-NtPIP5K6*	*CYC1*		this thesis
pPR3N-*MPK6*	*CYC1*		this thesis
pPR3N-*CPK11*	*CYC1*		this thesis
pPR3N-*CPK12*	*CYC1*		this thesis
pPR3N-*NtSIPK*	CYC1		this thesis

pPR3N-*SNRK 2.5*	*CYC1*		this thesis
pLatGW-*AtPIP5K5*	*Lat52*	*EYFP*	Dr. Irene Stenzel, MLU Halle-Wittenberg
pLatGW-*AtPIP5K6*	*Lat52*	*EYFP*	Dr. Irene Stenzel, MLU Halle-Wittenberg
pLatGW-*NtPIP5K5*	*Lat52*	*EYFP*	Dr. Irene Stenzel, MLU Halle-Wittenberg
pENTRY-*AtPIP5K6 T590A T597A*	*Lat52*	*EYFP*	this thesis
pENTRY-*AtPIP5K6 T590D T597D*	*Lat52*	*EYFP*	this thesis
pENTRY-*MPK6*	*Lat52*	*mCherry*	this thesis
pENTRY-*CPK11*	*Lat52*	*mCherry*	this thesis
pENTRY-*CPK11 D150A*	*Lat52*	*mCherry*	this thesis
pENTRY-*NtSIPK*	*Lat52*	*mCherry*	this thesis
pENTRY-*AtPIP5K5*	*35S*	C-YFP^N	Dr. Mareike Heilmann, MLU Halle-Wittenberg
pENTRY-*AtPIP5K6*	*35S*	C-YFP^N	Dr. Mareike Heilmann, MLU Halle-Wittenberg
pENTRY-*NtPIP5K6*	*35S*	C-YFP^N	this thesis
pENTRY-*MPK6*	*35S*	C-YFP^C	this thesis
pENTRY-*NtSIPK*	*35S*	C-YFP^C	this thesis
pENTRY-*CPK11*	*35S*	C-YFP^C	this thesis

2.11 cDNA-Modification and molecular biology techniques

2.11.1 Isolation of RNA from plant material

Total RNA was isolated from Arabidopsis flowers using the TRIZOL-method (Chomczynski and Mackey 1995). Plant material was frozen with liquid nitrogen, homogenized with mortar and pestle and 1 ml TRIZOL containing 3.8 % (v/v) Roti-Phenol (Roth, Karlsruhe, Germany), 0.8 M guanidinium thiocyanate, 0.4 M ammonium thiocyanate, 133.6 mM sodium acetate pH 5.0, 5 % (v/v) glycerol. The suspension was transferred to a 2-ml plastic reaction tube and incubated at room temperature for 5 min. To remove cell debris the sample was sedimented at 20 000 x g at 4 °C for 10 min and the soluble fraction was transferred to a fresh tube. 200 µl chloroform were added and the sample was agitated for 15 s. After a short incubation step (2-3 min at room temperature) the samples were centrifuged for 15 min to facilitate phase separation. The aqueous phase was combined with 0.5 V 2-propanol and 0.5 V high salt precipitation buffer (0.8 M sodium citrate, 1.2 M NaCl), inverted and incubated at room temperature for 10 min. The samples were centrifuged at 20 000 x g at 4 °C for 10 min and the supernatant was discarded. The pellet, containing the RNA, was washed twice with 75 % (v/v) ethanol and centrifuged at 1100 x g at 4 °C for 5 min. The RNA was dried at room temperature and dissolved in 10-20 µl ddH_2O.

2.11.2 cDNA-Synthesis

To obtain the structural genes from an organism, the synthesis of complementary DNA (cDNA) of an RNA-template was necessary. The method of the reverse transcriptase-PCR developed by Mullis and Faloona in 1987, allows the amplification of sequence sections on the basis of the mRNA sequence. For the synthesis of cDNA the RevertAid^{TM} H Minus Reverse Transcriptase Kit (Fermentas, St. Leon, Germany) was used with RNA obtained from flowers of Arabidopsis or tobacco as a template in the presence of oligo(dT)-primers according to the manufacturer's recommendations.

2.11.3 Amplification of specific gene sequences by PCR

For DNA amplification from cDNA for application in cloning procedures Phusion High Fidelity Polymerase (NEB, Ipswich, MA, USA) was used according to the manufacturer's instructions. The following temperature gradient was used for polymerase chain reaction (PCR): 98 °C for 30s as initial denaturation step, 35 cycles at 98 °C for 20 s, annealing between 55-65 °C for 30s, and 72 °C for 1 min/kb for the elongation of the amplicon. The utilized primers are listed in Tab. 7.1 (see appendix).

2.11.4 Assembly of DNA constructs

For cloning of PCR amplicons into different vectors, plasmids and cDNA-fragments were restricted and ligated with the respective enzymes according to the manufacturer's recommendations. The constructs created in this thesis are listed in Tab. 2.4 (section 2.10).

2.11.5 Site-directed mutagenesis

The site-directed exchange of bases within a DNA-sequence was conducted by QuickChange technology (Stratagene, La Jolla, CA, USA). In this PCR-based approach primers containing the desired base exchange were used to amplify the DNA template. The PCR was performed with Phusion High Fidelity Polymerase (NEB, Ipswich, MA, USA) in a 50 µl reaction according to the manufacturer's instructions. The following thermal cycling steps were used for amplification: 98 °C for 30s as initial denaturation step, 18 cycles at 98 °C for 20 s, annealing between 55-65 °C for 30s and 72 °C for 1 min/kb for the elongation of the amplicon. The utilized primers are listed under section 7 (Tab. 7.1).

The mixture of template and amplicon was digested with 10 U of the methylation-dependent restriction enzyme DpnI, to degrade all DNA of bacterial origin. After digestion the non-

methylated amplicon DNA was transformed into chemically-competent *E. coli* as described in section 2.13.2.

2.11.6 DNA sequencing

To confirm successful cloning and to verify site-directed mutations in plasmids DNA was sequenced using the commercial service of GATC (Konstanz, Germany) according to the company's requirements.

2.12 Cloning strategy

2.12.1 Heterologous protein expression in *E. coli*

AtPIPK6 and *NtPIP5K6*

The expression of recombinant *AtPIP5K6* and *NtPIP5K6* was performed in *E. coli*. The utilized vector pMALc5g (NEB, Ipswich, MA, USA) contains an N-terminal maltose binding protein that favors translation and enhances solubility of heterologous proteins in *E. coli*. To obtain an amplicon that is in reading frame with the N-terminal tag, *AtPIP5K6* was amplified with the restriction endonucleases NdeI (5'-direction) and SalI (3'-direction). One exception is the cloning of the variant *AtPIP5K6 T590D T597D*, in this case the restriction endonuclease NotI was used in 3'-direction. The tobacco homolog *NtPIP5K6* was amplified and cloned with the restriction endonucleases NotI (5'-direction) and SalI (3'-direction). With the use of the restriction endonucleases described above no additional bases had to be included during primer design to avoid possible frameshifts. Constructs are listed in table 2.4 (section 2.10).

CPK11

CPK11 is a small and globular protein and it has been shown that no solubility tag is necessary for its expression. *CPK11* cDNA was cloned with the restriction endonucleases SalI (5'-direction) and NotI (3'-direction) in reading frame with a C-terminal hexa histindine(his^6)-tag of the pET24-b vector (Novagene). Constructs are listed in table 2.4 (section 2.10). The cDNA of *CPK11 D150A*, a catalytic inactive variant of *CPK11* published by Rodriguez Milla *et al.* 2005, was cloned as described above for *CPK11*.

2.12.2 cDNA-Constructs for split-ubiquitin membrane-based yeast two-hybrid analysis

For the protein-protein interaction studies in yeast (see section 2.17.1), the interaction partners were cloned into the corresponding yeast split-ubiquitin vectors. The bait vector pBT3C-OST4 was obtained from Dr. Mareike Heilmann (MLU Halle-Wittenberg) and contains the ER-membrane anchor protein OST4. To obtain a PCR-product that is in reading frame with the OST4 protein, the 5' amplification primer had to contain an additional base between the restriction site and the start codon. The amplicon (*AtPIP5K6* or *NtPIP5K6*) was cloned via two directional SfiI-sites into the target vector. SfiI recognizes the restriction site GGCCNNNNNNGGCC, where N describes any base, cutting between the fourth and the fifth unspecified base. The unspecified region contained at the 5'-cloning site the bases ATTAC, while the 3'-cloning site contained the bases GAGGC, favoring directional ligation. For the construction of the prey vectors, the following genes were amplified and cloned via two directional SfiI-sites into the target vector pPR3N-*MPK6*, pPR3N-*NtSIPK* and pPR3N-*CPK11*. The recombinant plasmids were transformed into *E. coli* DH5α (see section 2.13.2), selected, propagated and finally transformed into the yeast strain *NMY51* (see section 2.17.1.1). Constructs are listed in table 2.4 (section 2.10).

2.12.3 cDNA-constructs for bifunctional fluorescence complementation

The vectors used for the bifunctional fluorescence complementation (see section 2.17.2) were obtained from Dr. Mareike Heilmann (MLU Halle-Wittenberg). In principle two pENTRY vectors under the control of the *35S* promoter were used. One encodes the N-terminal part of *YFP* (YFP^N) and the other the C-terminal (YFP^C) part respectively. *AtPIP5K6* and *NtPIP5K6* were amplified and cloned with the restriction endonucleases SgsI (5'-direction) and XhoI (3'-direction) in reading frame with a C-terminal YFP^N leading to *35S::AtPIP5K6-*YFP^N. The cloning of *NtPIP5K6* was approached alike.

The interaction partners *MPK6*, *NtSIPK* and *CPK11* were cloned as follows: The *MPK6* sequence contains an XhoI site and was therefore amplified and cloned with the alternative restriction endonucleases SalI (5'-direction) and XbaI (3'-direction) in reading frame with a C-terminal YFP^C. The cDNAs for *SIPK* and *CPK11* were amplified and cloned as described above with the restriction endonucleases SgsI (5'-direction) and XhoI (3'-direction) in reading frame with a C-terminal YFP^C. The YFP part is located at the C-terminus of the fusion protein in all cases. Constructs are listed in table 2.4 (section 2.10).

2.12.4 cDNA-constructs for transient overexpression in tobacco pollen

All genes cloned into a pENTRY vector containing *lat52::mCherry* in this work were amplified with the restriction endonucleases SgsI (5'-direction) and XhoI (3'-direction) in reading frame with the C-terminal fluorophore. The single exception is *MPK6*, which contains an XhoI recognition sequence. To obtain a vector with a functional multiple cloning site (MCS) and the cDNA for a C-terminal *mCherry*, part of the MCS and the *mCherry* of an existing vector was removed with the restriction endonucleases SgsI (5'-direction) and BamHI (3'-direction) and replaced by the cDNA encoding *mCherry*, amplified and cloned with primers containing the latter endonucleases sites. To ensure *MPK6* can be cloned in reading frame to the *mCherry*, the 5'-primer contained one additional base.

2.13 Protein expression and purification

Recombinant proteins used for biochemical characterization were produced in transgenic *E. coli* culture.

2.13.1 Preparation of chemically-competent *E. coli* cells

A starter culture of DH5α cells was inoculated with a single colony and grown over night with continuous shaking at 37 °C in LB-media (1 % (w/v) peptone, 0.5 % (w/v) yeast extract, 1 % (w/v) NaCl). The following day, 250 ml main culture was inoculated with the starter culture to an OD_{600} of 0.2 and grown to an optical density OD_{600} of 0.6-0.8. The cells were chilled for 10 min on ice and subsequently sedimented for 10 min at 4 °C and 1000 x g. The pellet was resuspended in 80 ml TFB-buffer (10 mM PIPES, pH 6.7, 15 mM $CaCl_2$, 250 mM KCl, 55 mM $MnCl_2$) and chilled on ice for 10 min, followed by a centrifugation step. The pellet was resuspended in 20 ml of TFB-buffer containing DMSO with a final concentration of 7 % (w/v) DMSO. After a final incubation step on ice for 10 min, cells were aliquoted to 100 µl and immediately frozen in liquid nitrogen. Cells were stored until use at -80 °C.

2.13.2 Transformation of chemically-competent *E. coli* cells

Transformation of chemically-competent *E. coli* was carried out according to Inoue at al., 1990. For that purpose an aliquot of competent cells (see section 2.13.1) was thawed on ice. For each transformation 100 µl of cells were combined with 1-10 µl of plasmid DNA. This mixture was incubated on ice for 30 min and heat-shocked at 42 °C for 45 s. Subsequently, the cells were chilled on ice for 5 min and 500 µl of LB-media was added. For regeneration, cells were

grown at 37 °C for 45-90 min and plated on solid LB-plates (media as described above, containing 1.5 % (w/v) agar).

2.13.3 Isolation of plasmid-DNA from *E. coli*

Plasmid-DNA was isolated from 2 ml of liquid culture using the GeneJET™ Plasmid Miniprep Kit (Thermo Fisher Scientific GmbH, Dreireich, Germany) according to the manufacturer's instructions. To isolate larger amounts of plasmid-DNA a 'midi'-preparation was performed from 25 ml of liquid culture. This isolation was carried out with the CompactPrep Plasmid Midi Core Kit (Qiagen, Hilden, Germany) following the manufacturer's specifications.

2.13.4 Heterologous protein expression in *E. coli*

Recombinant proteins for the biochemical characterisation were expressed as soluble proteins in *E. coli* liquid cultures. To overcome codon-usage difficulties, *E. coli* Rosetta 2 cells were used. These are based on the BL21-strain but contain a pRARE-plasmid encoding tRNAs for seven rare codons (Merck, Darmstadt, Germany). The cells were transformed as described under 2.10.2. All constructs were freshly transformed into Rosetta 2 cells before expression and not stored. Transformed cells were picked from plate and cultured in a starter culture over night with continuous shaking at 30 °C in 2YT-medium (1.6 % (w/v) peptone, 1 % (w/v) yeast extract, 0.5 % (w/v) NaCl) with appropriate antibiotic selection. The starter culture was taken to inoculate the main culture in a baffled flask filled with a maximum of 30 % of its volume. Cells were grown until an OD600 of 06.-0.8 and expression was induced with 0.1 mM IPTG, unless stated otherwise. Expression temperature and time of expression were tested and optimised individually for each protein.

2.13.5 Recombinant expression of MBP-AtPIP5K5

The expressed fusion protein MBP-AtPIP5K5 accumulated as an aggregate in *E. coli* when expressed over longer periods independent of the temperature. Optimal expression conditions were defined at 37 °C for 1 h. To gain enough material for protein purification, 3 L of culture were harvested. Cells were harvested by centrifugation for 20 min at 4000 x g and the bacterial pellet was immediately frozen in liquid nitrogen and stored until use at -20 °C.

2.13.6 Recombinant expression of MBP-AtPIP5K1 and MBP-AtPIP5K6

The fusion protein MBP-AtPIP5K1 and pMAL-AtPIP5K6 were best expressed with 0.1 mM IPTG at 22 °C for 4 h. For purification 1 L of culture was sufficient. Cells were harvested by centrifugation for 20 min at 4000 x g and the bacterial pellet was immediately frozen in liquid nitrogen and stored until use at -20 °C.

2.13.7 Recombinant expression of MBP-NtPIP5K6

Previous expression studies of MBP-NtPIP5K6 (bachelor thesis Sarah Bönisch, data not shown) revealed that under the conditions described, the fusion protein is predominantly accumulated in the pellet. The best expression conditions were found at 37 °C for 30 min. Cells were harvested by centrifugation for 20 min at 4000 x g and the bacterial pellet was immediately frozen in liquid nitrogen and stored until use at -20 °C. For purification 3 L of culture was used.

2.13.8 Recombinant expression of His_6-CPK11 and His_6-CPK11 D150A

The CPK11 protein was expressed at 22 °C for 8 h, expression was induced with 0.5 mM IPTG as was previously described (Zhao *et al.* 2013). Cell pellets corresponding to an OD_{600} of 10 were aliquoted, frozen in liquid nitrogen and stored at -20 °C.

2.13.9 Cell disruption by high pressure

Cell disruption was initiated with the addition of lysozyme (Serva, Heidelberg, Germany) to digest the bacterial cell wall. Ultrasound was used for the disruption of small volumes, while larger volumes were homogenized by a high pressure cell disruption French™-Press system (Gaulin, APV Homogeniser GmbH, Gatwick, UK) at 1200 bar. After both treatments, crude lysate was centrifuged at 20 000 x g for 20 min at 4 °C to sediment intact cells and debris. Crude lysate was kept on ice until further use and neither frozen nor stored.

Cell disruption by ultrasound

The cell suspension with a volume of 1 ml was kept in a 1.5 ml plastic reaction tube and chilled in ice-water. The sample was treated with ultrasound for 1 s pulse and 3 s pauses for 5 min (Bioblock Scientific 72442, Vibra Cell, Sonics and Materials Inc., CT, USA) at 60 % power.

French-Press homogenisation

The bacterial pellet was suspended in 40 ml extraction buffer (50 mM TRIS, 300 mM NaCl, 1 mM EDTA; for AtPIP5K5 at pH 7.5, for AtPIP5K6 at pH 8, for NtPIP5K6 at pH 7.5) supplemented with proteinase inhibitor (Sigma, Schnelldorf, Germany) and 1 mM phenylmethylsulfonyl fluoride (PMSF) on ice. Lysozyme was added and incubated stirring for 1 h.

2.13.10 Purification of proteins by affinity chromatography

Purification of the full-length fusion proteins was performed by affinity chromatography using an MBPTrap column (GE Lifesciences, Uppsala, Sweden). The MBP fusion proteins bind to amylose, an artificial sugar, which is immobilised in the column matrix and are eluted with the disaccharide maltose.

2.13.11 Estimation of protein contents

Estimation of protein content was performed with the Bradford assay (Bradford 1976). The Bradford reagent consists of 0.1 % (w/v) Coomassie Brilliant Blue G250, 5 % (v/v) ethanol and 8.5 % (v/v) o-phosphoric acid. The Coomassie dye forms complexes with cationic and nonpolar side chains of polypeptides and becomes stabilized. The absorption of this complex can be measured in a spectro photometer at 595 nm. Protein concentrations were calibrated with BSA. Protein purity was tested by SDS-PAGE.

2.13.12 Sodium dodecyl sulfate polyacrylamide gel electrophoresis (SDS-PAGE)

Proteins were electrophoretically separated by SDS-PAGE and stained with Coomassie, according to Laemli, 1970. The SDS gel is divided into the stacking and the resolving gel. The acrylamide concentration of all gels used in this thesis was 10 % (v/v). The stacking gel was composed of 0.66 ml acrylamide/bisacrylamide (30 %/ 0.8 % (w/v)), 0.8 ml 0.6 M TRIS-HCl pH 6.8, 2.5 ml H_2O, 40 µl 10 % SDS and 2.5 µl tetramethylethylenediamine (TEMED). The resolving gels consisted of 2 ml acrylamide/bisacrylamide (30 %/ 0.8 % (w/v)), 2.2 ml 1.8 M TRIS-HCl pH 8.8, 2.75 ml H_2O, 60 µl 10 % SDS and 6 µl TEMED. The polymerization reaction was started by the addition of 0.5 % (w/v) ammonium persulfate (APS). For casting of SDS-gels a multiple gel caster (SE 200 series, Hoefer, Holliston, MA, USA) was used. The samples were denatured with SDS sample buffer (5 x, 225 mM TRIS HCl pH 6.8, 5 % (w/v) glycerol, 5 % SDS (w/v), 0.05 % (w/v) Coomassie Brilliant Blue G250, 250 mM dithiothreitol (DTT). Gels

were run with 25 mA for 1 h in SE 250 gel chambers (Hoefer, Holliston, MA, USA) filled with SDS-PAGE running buffer (25 mM TRIS, 200 mM glycine and 0.3 mM SDS). SDS-gels were subsequently stained with Coomassie staining solution (40 % (v/v) methanol, 10 % (v/v) acetic acid and 0.25 % (w/v) Coomassie Brilliant Blue G250 or subjected to immunodetection (2.13.13).

2.13.13 Immunodetection

The specific detection of MBP-tagged recombinant proteins was performed by immunodetection (western blotting). Proteins were separated by a denaturing SDS-PAGE and then transferred to a nitrocellulose membrane (Optitran BA-S 85, 0.45 µm; Whatman, Maidstone, UK) via a wet blot cell (Mini Trans-Blot© cell; Bio-Rad, Hercules, CA, USA). The transfer was conducted in transfer buffer (0.6 % (w/v) TRIS, 0.3 % (w/v) glycine, 0.4 % (w/v) SDS and 20 % (v/v) methanol) at 60 V for 1 h. After the transfer the nitrocellulose membrane was washed with TBS buffer (20 mM TRIS HCl pH7.5, 50 mM NaCl) to remove residual SDS. The membrane was incubated with the primary antibody (rabbit anti MBP, Sigma, Schnelldorf, Germany; diluted 1:10 000 in TBS) and 1 % of BSA in TBS for 2 h at 4 °C, following three washing steps with TBS for 10 min. The secondary antibody (anti rabbit, Sigma, Schnelldorf, Germany; dilution 1:30 000 in TBS) was conjugated to an alkaline phosphatase, that catalyzes the color reaction of 5-bromo-4-chloro-3-indolyl phosphate (BCIP) and nitro blue tetrazolium chloride (NBT). After incubation of the secondary antibody the washing steps were repeated and the membrane was equilibrated in AP buffer (100 mM TRIS HCl pH 9.5, 100 mM NaCl, 5 mM $MgCl_2$). For the staining reaction 10 ml AP buffer, containing 35 µl BCIP (50 mg/ml in dimethylformamide (DMF) and 45 µl NBT (75 mg/ml in 70 % DMF), were added to the membrane and incubated in the dark initially for 5 min. The reaction was terminated by washing the membrane with ddH_2O to dilute the components of the color reaction. The blot was scanned for documentation of the staining.

2.13.14 *In vitro* test for PI4P 5-kinase activity

The catalytic activity of recombinant PI4P 5-kinases was determined by their ability to phosphorylate PtdIns4P in the presence of γ-[^{33}P]-ATP according to Cho and Boss, 1995. Each reaction contained 6.4 fM PtdIns4P (Avanti Polar Lipids Inc., Alabaster, AL, USA). The lipid substrate, solved in chloroform, was dried in an air stream, solubilised in detergent (2 % (v/v) Triton X-100) and evenly suspended in a water bath sonicator for 15 min. The lipid kinase activity was assayed with 15-30 µg recombinant protein in a reaction mix containing 15 mM

$MgCl_2$, 1 mM Na_2MoO_4, 1 mM ATP, 5 µCi γ-[^{33}P]-ATP (10 mCi/ml; Hartmann, Braunschweig, Germany), 1mM TRIS pH 7.2 and the lipid substrate in a total volume of 50 µl. Samples were incubated at 22 °C for 1 h and the lipid products were isolated by acidic lipid extraction (1.5 ml chloroform:methanol (1:2 (v/v)), 45 µM EDTA, 0.44 M HCl, 500 µl chloroform) (Cho *et al.* 1992). The organic phase was collected and the mixture was re-extracted with 500 µl chloroform. The organic phases were combined and washed with 1 ml HCl in methanol:H_2O (1:1 (v/v)). The washed organic phase was transferred to a fresh tube and lipids were dried under air stream. To separate the dried lipid products, samples were dissolved in 20 µl chloroform and applied to thin layer chromatography onto silica S60 plates (Merck, Darmstadt, Germany) and chloroform:methanol:ammoniumhydroxide:H_2O (45:45:4:11 (v/v/v/v)) as mobile phase (Perera *et al.* 2005). The extent of ^{33}P-incorporation was quantified with a phosphorimager (BAS-MP 2040s, Fujifilm, Düsseldorf, Germany) and sensitive imager screens (BAS-1500, Fujifilm, Düsseldorf, Germany).

2.14 *In vitro* phosphorylation of PI4P 5-kinases by pollen extract

The phosphorylation of recombinant PI4P 5-kinase protein used in this work was assayed in the presence of extracts prepared from *N. tabacum* pollen tubes or selected recombinantly expressed protein kinases from Arabidopsis.

2.14.1 Preparation of *N. tabacum* pollen tube extract

N. tabacum pollen tube extract was used as a source of protein kinase activity. Ripe pollen from tobacco flowers was harvested, solubilised and germinated in pollen growth media. After the germinated pollen was separated from the growth media, the pollen tube material was frozen in liquid nitrogen and stored at -80 °C until use.

Table 2.6: List of phosphatase and protease inhibitors

Inhibitor	Inhibition of	Final concentration
PhosSTOP (Roche, Penzberg, Germany)	acid and alkaline phosphatases, serine/threonine/tyrosine phosphatases	According to manufacturer's instructions
Na_3VO_4	tyrosin and alkaline phosphatases	1 mM
NaF	serine/threonine phosphatases	2.5 mM
Protease inhibitor cocktail (Sigma Aldrich, Schnelldorf,	serine, cysteine, aspartic and metalloproteases, aminopeptidases	According to manufacturer's

Germany)	instructions

For the protein extraction, ice cold protein extraction buffer containing 10 mM TRIS HCl pH 7.5, 10 mM $MgCl_2$, 50 mM NaCl, 2.5 mM NaF, 1 mM Na_3VO_4, 0.1 mM EDTA, 0.1 mM DTT, PhosSTOP (Roche, Penzberg, Germany) and protease inhibitor cocktail (Sigma, Schnelldorf, Germany) was added to the material and the cells were broken with a mini pestle. The addition of phosphatase inhibitors (see Tab. 2.6) is crucial to prevent the inactivation of phosphorylated protein kinases by dephosphorylation. To remove particles from the extract, the suspension was centrifuged at 20000 x g and 4 °C for 20 min. The protein concentration was measured using the Bradford-assay (section 2.13.11) and the extract was kept on ice to prevent protein degradation and protein kinases inactivation.

2.14.2 *In vitro* phosphorylation assays with radiolabeled γ-[^{33}P]-ATP

Transphosphorylation can be detected by monitoring the incorporation of radiolabelled γ-phosphate of γ-[^{33}P]-ATP into the protein.

Recombinant expressed PI4P 5-kinase (5-10 µg) were incubated with 15 µg of freshly prepared pollen extract in the presence of 50 µm ATP containing 10 µCi γ-[^{33}P]-ATP (10 mCi/ml; Hartmann, Braunschweig, Germany) in 1 x kinase buffer (10 mM TRIS HCl pH 7.5, 10 mM $MgCl_2$, 50 mM NaCl, 0.1 mM EDTA, 0.1 mM DTT and PhosSTOP) in a volume of 50 µl for 30 min. Variations to the experiments performed with recombinant protein kinases are described below.

For kinase assays performed with recombinant, activated MPK6, the sample volume was 20 µl. For each reaction 0.2 µg of MPK6 was used. MPK6 was obtained from Pascal Pecher, IPB Halle, Germany.

For the kinase assay performed with CPK11, CPK11 was prepared as a crude extract and 5 µg were added to 25 µl reaction volume. Additionally, 0.55 mM $CaCl_2$ was added to ensure activity of the protein kinase.

During incubation time the samples were gently agitated. The reaction was stopped with SDS sample buffer and the sample was applied to SDS-PAGE. The gel was stained with Coomassie and dried over night by clamping the gel between two cellophane sheets soaked with 3 % (v/v) glycerol, 30 % (v/v) methanol and 10 % (v/v) acetic acid. Radiolabeled bands were visualized using a radiosensitive imager screen (BAS MP 2040s, Fujifilm, Düsseldorf, Germany) and the extent of ^{33}P-incorporation was quantified with phosphor imager technology (BAS 1500,

Fujifilm, Düsseldorf, Germany). The gel was scanned to document the sample loading. A prestained protein ladder was used to estimate sizes of phosphorylated proteins.

2.15 Identification of protein kinases that phosphorylated AtPIP5K6

2.15.1 In-gel phosphorylation of purified recombinant AtPIP5K6 by complex extracts

To identify proteins from biological extracts that phosphorylate a protein of interest, in-gel kinase-assays can be used. The in gel kinase assay was performed as previously described (Zhang and Klessig 1997). Pollen tube extracts were prepared as described in section 2.14.1 and 80 µg were loaded on a 10 % SDS-gel. As a substrate for the protein kinases from the extract, 0.25 mg/ml of MBP-AtPIP5K6 were co-polymerized into the resolving gel. A control with no protein embedded in the gel was used as an autophosphorylation control. The catalytic subunit of protein kinase A (PKA) from bovine heart (1 U, Sigma, Schnelldorf, Germany) was used as a positive control. After electrophoresis, the gel was washed three times for 30 min with washing buffer (25 mM Tris pH 7.5, 0.5 mM DTT, 0.1 mM Na_3V0_4, 5 mM NaF, 0.5 mg/ml (w/v) BSA, 0.1 % (v/v) Triton X-100) at room temperature with gentle agitation to remove SDS. To renature protein kinases, the gel was incubated in renaturing buffer (25 mM Tris pH 7.5, 0.5 mM DTT, 0.1 mM Na_3V0_4, 5 mM NaF) over night at 4 °C with three changes of buffer. Subsequently, the gel was equilibrated in the kinase reaction mix (25 mM Tris pH 7.5, 2 mM EGTA,12 mM $MgCl_2$, 10 mM $CaCl_2$, 1 mM DTT, 0.1 mM Na_3V0_4) and the kinase reaction (30 ml) was started by the addition of 200 nM ATP containing 50 µCi γ-[^{33}P]-ATP (10 mCi/ml; Hartmann, Braunschweig, Germany). The gel was incubated for 60 min with gentle agitation. The reaction was stopped by the addition of 5 % (w/v) trichloroacetic acid (TCA) and 1 % (w/v) sodium pyrophosphate to fixate proteins in the gel and remove unbound γ- [^{33}P]-ATP for 6 h with at least five changes of buffer. The control gel was stained with Coomassie. A prestained protein ladder was used to estimate sizes of phosphorylated proteins. After washing, the gels were dried over night by clamping the gel between two cellophane sheets soaked with 3 % (v/v) glycerol, 30 % (v/v) methanol and 10 % acetic acid. Radiolabeled bands were visualized using a radiosensitive imager screen (BAS MP 2040s, Fujifilm, Düsseldorf, Germany) and the extent of ^{33}P-incorporation was quantified with phosphor imaging (BAS 1500, Fujifilm, Düsseldorf, Germany).

2.15.2 In-gel digestion of proteins for mass spectrometric analysis

To identify proteins from of a certain protein size, corresponding bands were excised from an SDS-PAGE and digested with trypsin according to Shevchenko and coworkers (Shevchenko *et al.* 1996). The endopeptidase trypsin cleaves at the C-terminal position after the basic amino acids arginine and lysine. Gel slices were cut into smaller pieces and soaked in 100 µl of ddH_2O to remove Coomassie. The sample was agitated for 10 min at room temperature and the washing step was repeated. Next, the gel pieces were washed with destaining solution (30 % (v/v) acetonitrile (ACN) in 100 mM NH_4HCO_3) and incubated at room temperature for 15 min with agitation. The supernatant was discarded and the procedure was repeated four times. The samples were dried by a centrifugal evaporator linked to a refrigerated cool trap (RC10 and Juan RCT 60, MedServ GmbH, Leipzig, Germany). To break secondary structures and reduce cysteine residues, the dried gel slices were incubated with 40 µl of 10 mM DTT in 100 mM NH_4HCO_3 pH 8.5, for 5 min at room temperature and 30 min at 50 °C. The supernatant was discarded and the samples were washed with 100 µl ACN. The addition of 40 µl 54 mM iodoacetamide in 100 mM NH_4HCO_3 pH 8.5 started an alkylation reaction of free thiol groups for 15 min in the dark. The supernatant was discarded and the samples were washed twice with 100 µl destaining solution. Subsequently the gel slices were dried by vacuum. For digestion the dried gel fragments were covered with trypsin solution (3 ng/µl trypsin (Sigma, Schnelldorf, Germany), 50 mM NH_4HCO_3 pH 8.5, 5 % (v/v) ACN) and incubated over night at room temperature. The peptides were extracted with 50 % (v/v) ACN and 0.1 % (v/v) trifluoroacetic acid (TFA) (in the same volume as the trypsin solution with agitation for 40 min. The supernatant was transferred to a new tube and the extraction was repeated for 15 min. Both supernatants were pooled and the peptides were dried. For storage, peptides were solved by sonication in 20 µl 0.1 % (v/v) TFA for 5 min and kept at -20 °C until further analysis.

In-gel tryptic digestion for phosphopeptide analysis

To identify proteins that emitted a phosphorylation signal, proteins were phosphorylated in a kinase assay without radiolabeled ATP (see section 2.14.2), separated by SDS-PAGE and stained with Coomassie. The protein band of interest was excised and digested with trypsin as described above. The in-gel digest of samples subjected to phosphopeptide identification was performed by Petra Majovsky in the laboratory of Dr. Wolfgang Hoehenwarter (Proteome Analytics, IPB, Halle (Saale)).

Desalting of peptide solutions for mass spectrometry analysis

To minimize the abundance of ions like sodium or phosphate salts which increase the noise background during the measurement, samples were desalted as previously described (Majovsky *et al.* 2014), using Empore C18 silca packed STAGE-tips (3M, St. Paul, MN, USA). STAGE-tips were equilibrated with 80 % (v/v) ACN, 0.1 % (v/v) formic acid (FA) and washed in 0.1 % (v/v) FA, both in H_2O. The peptides were loaded onto the equilibrated tips and washed with 0.1 % (v/v) FA. Peptides were eluted with 80 % (v/v) ACN and dried to completion in a vacuum incubator. Finally, the dried and desalted peptides were dissolved in 5 % (v/v) ACN, containing 0.1 % (v/v) TFA. The desalting of samples subjected to phosphopeptide identification was performed by Petra Majovsky in the lab of Dr. Wolfgang Hoehenwarter (Proteome Analytics, IPB, Halle (Saale)).

2.16 Mass spectrometry

Mass spectrometry (MS) is an analytical technique that transforms molecules into ions, to measure the characteristics of the individual molecule. The analysis of complex protein mixtures is performed by the coupling of liquid chromatography (LC) and MS, to enhance mass resolving.

2.16.1 Data-dependent acquisition of phosphopeptides by HR/AM LC-MS

Site specific phosphorylation of AtPIP5K6 by MPK6 was studied using *in vitro* kinase assay followed by liquid chromatography on-line with high resolution accurate MS (HR/AM LC-MS) using an Orbitrap Velos Pro System (Thermo Scientific, Dreireich, Germany). The proteins from the kinase assay were separated by SDS-PAGE. Following in-gel protein digestion with trypsin (see section 2.15.2), peptides were measured with a data dependent acquisition (DDA) scan strategy with inclusion list to specifically select and isolate AtPIP5K6 phosphorylated peptides for MS/MS peptide sequencing. The use of an inclusion list aimed for the identification of low abundant species in the survey scan (targeted DDA). Multi stage activation (MSA) was applied to further fragment ion peaks resulting from neutral loss of the phosphate moiety by dissociation of the high energy phosphate bond to generate b- and y- fragment ion series rich in peptide sequence information. MS/MS spectra were used to search the TAIR10 database (ftp://ftp.arabidopsis.org) amended with mutant AtPIP5K6 sequences (AtPIP5K6 T590A, AtPIP5K6 T597A and AtPIP5K6 T590A T597A) with the Mascot software v.2.5 integrated in Proteome Discoverer v.1.4. The phosphoRS module was used to localize the phosphorylation site within the primary structure of the peptide. The measurement and data analysis was performed by Dr. Wolfgang Hoehenwarter (Proteome Analytics, IPB, Halle (Saale).

2.16.2 Data-independent acquisition of peptides by Nano-LC-HD-MS^E

The identification of protein kinase candidates from the IGKA (see section 2.15.1) was performed by liquid chromatography high definition multi-parallel collision-induced dissociation MS (Nano-LC-HD-MS^E) using an ACQUITY UPLC System and a coupled Synapt G2-S (Waters, Eschborn, Germany) in resolution mode with positive ionization (Helm *et al.* 2014). The peptides were measured in data independent acquisition (DIA) mode. In contrast to DDA, during DIA no pre-selection of precursor ions occurs and all ions are fragmented, avoiding loss of information (Helm *et al.* 2014). Glu-Fib (Glu-1-Fibrinopeptide B) was used as lock mass (m/z = 785.8426, z = 2) and mass correction was applied to the spectra during data processing in ProteinLynx Global Server (PLGS 3.0, Apex3D algorithm v. 2.128.5.0, 64 bit, Waters, Eschborn, Germany). The processing parameters were set as described (Helm *et al.* 2014). The intensity of precursor ions was ≥180 counts and for fragment ions ≥15 counts to be distinguished from noise. The designation of fragment ions to precursor ions was achieved by by PLGS 3.0 and is manly based on comparison of peak form, retention time, isotope cluster and m/z value as well as ion mobility. Further data analysis was also carried out by PLGS 3.0. MS^E data were searched against the modified *A. thaliana* database (TAIR10, ftp://ftp.arabidopsis.org) containing common contaminants such as keratin (ftp://ftp.thegpm.org/fasta/cRAP/crap.fasta). Protein identification required the detection of two fragment ions per peptide, a minimum of five fragment ions and two peptide matches. Primary digest reagent was trypsin with one missed cleavage allowed, as previously described (Helm *et al.* 2014). The measurements and data analysis were performed by Stefan Helm from the group of Prof. Dr. Sacha Baginsky (Department of Plant Biochemistry, MLU Halle-Wittenberg).

2.17 Analysis of protein-protein interactions

The interaction studies performed in this thesis are based on the reconstitution of a reporter protein. Interaction of two proteins, each fused to a part of the reporter protein, results in a signal that originates from the reconstitution of the reporter. Using a suitable readout this signal can be detected and quantified.

2.17.1 Interaction analysis by the split-ubiquitin membrane-based yeast two-hybrid system

The split-ubiquitin (Ub) membrane-based yeast two-hybrid system (SUS) Dualmembrane Kit 3 (Dualsystems Biotech, Zürich, Switzerland) is designed for the analysis of extra-nuclear

proteins, including membrane-associated and integral membrane proteins. Johnsson and Varshavsky described the SUS in 1994 (Johnsson and Varshavsky 1994). In this work, a split-Ub was identified as a protein-protein interaction sensor *in vitro* to monitor interaction at the natural sites of protein localization in the cell. In comparison to the classic yeast two hybrid system, which is limited to soluble and nuclear localized proteins, the SUS can overcome these restrictions (Stagljar *et al.* 1998). The system uses the conserved mechanism that reconstituted Ub fusion proteins are subsequently cleaved by Ub specific proteases at the last amino acid position of Ub. Only correctly folded Ub proteins are recognized by these proteases. This selectivity is employed in the SUS. Both the N-terminal half of the ubiquitin (Nub, residues 1-38) and the C-terminal part of the ubiquitin (Cub, 34-76) fused to the transcription factor LexA-VP16 are necessary for efficient cleavage. Bait and prey constructs encoding for *AtPIP5K6*, *NtPIP5K6*, *MPK6*, *NtSIPK* and *CPK11* were assembled as described in detail in section 2.12.2. Both constructs were co-transformed in the yeast strain *NMY51* (Dualsystems Biotech, Zürich, Switzerland) and upon positive interaction and the reconstitution of Ub, the transcription factor is released by proteolytic cleavage. The transcription factor LexA-VP16 induces the expression of different reporter genes. These genes code for *HIS3* (Imidazoleglycerolphosphate dehydratase), which is crucial for histidine biosynthesis and *ADE2* (Phosphoribosylaminoimidazole carboxylase) involved in the *de novo* synthesis of purine nucleosides. The lack of the latter also causes the accumulation of phosphoribosyl-aminoimidazol, a red intermediate of adenosine biosynthesis in deprived cells. An additional reporter gene is LacZ, which codes for ß-galactosidase. Reconstitution of the Ub moieties can be modulated by mutations within the N-terminal half of Ub. A mutation of isoleucine 3 to glycine (NubG) lowers the ability of NubG to Cub. Both Ub moieties, each fused to a protein interaction partner, will only reconstitute upon close proximity. Only correctly folded Ub proteins will be recognised by proteases as a substrate and transcription factor release takes place.

The bait protein was co-transformed with a positive and a negative control. The selection on SD-media, lacking leucine and tryptophan (SD-LW), ensured that only yeast survived that contain both bait and prey respectively control plasmid. The positive control consisted of a native Ub-half (NubI) fused to the Alg5 protein. NubG fused to the ER-localized protein Alg5 served as a negative control. The positive control served as a control for the expression level of the bait protein. To monitor an interaction, single yeast clones were grown on SD-media lacking leucine, tryptophan and histidine (SD-LWH). For the interpretation of an interaction, it is most relevant to check for significantly increased growth compared to the negative control.

2.17.1.1 Transformation of chemically competent yeast

The transformation of yeast with external plasmid DNA is accomplished with the aid of chemicals like lithium acetate (LiOAc) and polyethylene glycol (PEG) (Ito *et al.* 1983) which render the membrane porous so that DNA can be taken up. A heat shock at 42 °C facilitates the entry of the charged DNA into the cell.

A starter culture of *NMY51* was grown over night at 30 °C with continuous shaking at 200 rpm. The following day the main culture was inoculated to an OD_{600} of 0.15 and cultivated at 200 rpm and 30 °C until an OD_{600} of 0.4-0.6. Cells were harvested at 2500 x g for 5 min and the sediment suspended in 20 ml 1 x TE-buffer containing 10 mM TRIS pH 7.5, 10 mM EDTA. The cell pellet was washed and centrifuged in 1 ml LiOAc master mix (0.1 mM LiOAc in TE-buffer) and finally suspended in 600 µl LiOAc master mix. For each transformation reaction 100 µl aliquots were combined with 2-4 µg of plasmid DNA per construct and 700 µl PEG transformation master mix, containing 560 µl 50 % PEG-4000 (w/v), 70 µl 1 M LiOAc and 70 µl 10 x TE-buffer pH 7.5. The reactions were incubated for 30 min at 30 °C shaking at 200 rpm. Subsequently after incubation, 10 % DMSO (v/v) were added and cells were heat-shocked for 15 min. The cells were centrifuged at 700 x g for 5 min and the supernatant was discarded. The cells were washed and centrifuged twice with 500 µl 1 x TE-buffer at 700 x g for 3 min to remove residual LiOAc and PEG. Finally, cells were suspended in 500 µl 0.9 % (w/v) NaCl and 200 µl were plated on agar plates containing SD-medium lacking L and T. The plates were incubated at 30 °C and colonies formed after 2-3 days.

2.17.1.2 Test for Interaction between PI4P 5-kinases and putative protein kinases

Qualitative growth assay

To test for protein-protein interactions drop tests were performed. Therefore the bait construct was transformed together with the positive control pPR3N-*AI-Alg5* and the negative control pPR3N-*DL-Alg5* as well as with the putative interaction partners (see cloning strategies for details on constructs) as described above. Cells from a fresh master plate were suspended in 1 x TE buffer to determine the OD_{600}. Dilutions from an optical density of 1 to 0.0001 were prepared in dilution stages of 10-fold, unless stated otherwise. The dilutions were dropped onto selection plates (SD-LT SD-LTH), the yeast was cultivated at 30 °C and growth was monitored for three to five days.

Quantitative β-galactosidase activity assay

Protein-protein interaction of bait and prey protein in the SUS does not only lead to the expression of auxotrophy genes, but also leads to the activation of a *LacZ* reporter gene, coding for β-galactosidase. The strength of the interaction can thus be quantified by measuring the β-galactosidase activity. For this a colorimetric test is used where *ortho*-nitrophenyl-β-D-galactopyranoside (ONPG) is supplied as a substrate. β-galactosidase hydrolyses ONPG to galactose and o-nitrophenol. o-Nitrophenol is yellow and its absorption can be quantified at 420 nm. For the quantification cells from a fresh master plate were suspended in 1x TE buffer to determine the OD_{600}. A defined volume of cells was sedimented by centrifugation with 20 000 x g for 1 min and suspended in 500 µl Z-buffer (40 mM Na_2HPO_4, 60 mM NaH_2PO_4, 10 mM KCl, 1 mM $MgSO_4$). By adding 50 µl chloroform and vigorous agitation for 15 s the cells become lysed. The colorimetric reaction was started by the addition of 100 µl OPNG (4 mg/ml in Z-buffer). The samples were incubated for 15 min at 37 °C and the reaction was stopped with 500 ml Na_2CO_3. To remove the cell debris from the soluble fraction the samples were centrifuged briefly and the absorption of supernatant was measured at 420 nm.

The β-galactosidase activity was calculated according to the following equation:

$$\text{Miller Units} = (100 * A_{420})/(V(ml) * t(min) * OD_{600})$$

2.17.2 Interaction analysis by bimolecular fluorescence complementation

Bimolecular fluorescence complementation (BiFC) is a method to validate protein-protein interactions. In this work the proteins tested were pollen specific and therefore the BiFC was performed in a physiological relevant tissue, *N. tabacum* pollen.

The underlying principle of the BiFC experiment is similar to the SUS test. The coding sequences of interest are fused to the N-terminal and C-terminal halves of *YFP*, respectively. Only upon close physical interaction, the two YFP fragments can reconstitute to a functional YFP protein and emit fluorescence. For details on the constructs see section 2.12.3. The constructs were transiently transformed into tobacco pollen and the cells were grown for 14-18 h until microscopic evaluation. A mCherry fluorophore under the control of a *lat52*-promotor was co-transformed to identify transformed cells. The reconstitution of the fluorescence indicates protein-protein interaction and also provides information about the subcellular localization of the interaction.

2.18 Transient expression of fluorescence-labelled proteins in tobacco pollen tubes

For transient transformation of plant tissue by biolistic particle bombardment (Klein *et al.* 1988; Klein *et al.* 1989) DNA coated gold particles penetrate the cell forced by a helium-driven particle gun. Entering the plant cell, the particles strip of the DNA and the expression of the recombinant DNA is initiated when the DNA enters the nucleus or plastids. A disadvantage of particle bombardment is the damage of the cell wall. Using pollen grains for transformation this is not an issue, because the cell wall of the pollen tube develops as the pollen germinates.

DNA-precipitation on gold particles

For the preparation 50 mg of gold particles (1 µm, Bio-Rad,) were surface sterilised by 1 ml 96 % (v/v) ethanol and mixed for 5 min. The suspension was centrifuged briefly to sediment of the particles. The supernatant was discarded and the particles were washed three times with 1 ml of ddH_2O. The gold particle suspension was split in aliquots of 2.5 mg and stored at -20 °C. For the precipitation of the DNA to the particles 6 µg of plasmid DNA were added to a gold aliquot and mixed for 1 min. Subsequently 50 µl 2.5 M $CaCl_2$ was added and the suspension mixed for 1 min. The precipitation of the DNA to the gold particles was supported by the addition of 20 µl 0.1 M spermidine. After a brief centrifugation step the supernatant was discarded and the particles were washed three times with 180 µl 96 % ethanol. Finally, DNA-coated particles were stored in 60 µl 96 % (v/v) ethanol at -20 °C.

Preparation of *N. tabacum* pollen

Ripe pollen of *N. tabacum* flowers (four flowers per transformation) was harvested, and resuspended in pollen medium (5 % (w/v) saccharose, 12.5 % (w/v) PEG-6000, 0.03 % (w/v) casein hydrolysate, 15 mM MES-KOH pH 5.8, 1 mM $CaCl_2$, 1 mM KCl, 0.8 mM H_3BO_3, 3 µM $CuSO_4$ and 10 µg/ml rifampicin). The pollen was transferred to a cellulose acetate filter (0.2 µm, Sartorius, Göttingen, Germany) by filtration and kept on a filter paper soaked with pollen medium until transformation.

Particle bombardment of *N. tabacum* pollen

After harvesting, the pollen material was immediately bombarded by a helium-driven particle gun (PDS-100/He, Bio-Rad) using 1350 psi rupture discs and a vacuum of 28 inches of mercury according to the manufacturer's recommendations. After bombardment, pollen was suspended in growth media and evenly distributed in a thin layer on microscope slides. For the

analysis of protein localization and phenotype observations, pollen was grown 6-8 h. Visualisation of protein-protein interaction with split-YFP was analysed after 14-18 h.

2.19 Microscopy

All proteins used in this thesis were either fused to the enhanced yellow fluorescent protein (EYFP) or the red fluorophore mCherry.

For the microscopy of pollen phenotypes and the observation of BiFC experiments the AXIO IMAGER M1 microscope (Carl Zeiss, Jena, Germany) equipped with the camera AxioCam MRm was used. The observation of phenotypes was performed with a 20x magnification objective lens using the filter set 38 high efficiency (HE) for EYFP detection and the filter set 43 HE for mCherry detetction (all filters were obtained by Carl Zeiss, Jena, Germany). EYFP was excited at 514 nm and imaged using a FT 495 nm beam splitter and a 470/40 nm band pass filter; mCherry was excited at 561 nm and imaged using a FT 570 nm beam splitter and a 550/25 nm band pass filter. Images were taken with the corresponding software program (Axio Vision, Carl Zeiss, Jena, Germany).

For the distinct localization of proteins the confocal laser scanning microscope LSM780 (Carl Zeiss, Jena, Germany) was used with a 40x magnifying objective. EYFP was excited with an Ar-laser and a wavelength of 488 nm and detected between 493-598 nm; mCherry was excited with a DPSS-laser and a wavelength of 561 nm and detected between 578-696 nm. Images were taken with the corresponding software program (Zen Software, Carl Zeiss, Jena, Germany).

3 Results

PtdIns(4,5)P_2 mediates various important functions in all eukaryotic cells, and thus the synthesis of this signaling lipid needs to be tightly controlled. In previous studies, it was shown that PIPKs from different organisms are phosphorylated and that their catalytic activity is regulated upon this posttranslational modification. It was the aim of this work to identify protein kinases that are involved in the regulation of the pollen-expressed AtPIP5K6 from Arabidopsis and thereby link PtdIns(4,5)P_2-production to conserved upstream signaling-pathways. AtPIP5K6 was chosen from a number of PI4P 5-kinases tested, because it expressed best and provided sufficient amount of protein for the *in vitro* tests, in particular for the in-gel kinase-assay (section 3.3).

3.1 Recombinant expression and purification of MBP-AtPIP5K6

The characterization of phosphorylation of recombinant purified AtPIP5K6 was an important aspect of this study. To enable phosphorylation experiments, an expression and purification protocol was established. The use of a recombinant expression system is an important tool to study proteins. In comparison to eukaryotic expression systems, prokaryotic expression systems lack phosphoinositide signaling. Thus, the overexpression of AtPIP5K6 in *E. coli* does not interfere with endogenous signaling. This gives the opportunity to investigate crude extracts which omit endogenous PIP-kinase activity. Furthermore, recombinant proteins produced in prokaryotic expression are likely not posttranslational modified. Alternative expression systems like eukaryotic cell culture or yeast were considered not favourable for this study, because the investigation of posttranslational modifications is a central aspect of this work. Previous experiments (personal communication Dr. Irene Stenzel, MLU Halle-Wittenberg) showed that AtPIP5K6 can be expressed in *E. coli* in an insoluble form and accumulates in inclusion bodies. For this reason the solubility tag maltose binding protein (MBP) was used to enhance solubility of AtPIP5K6.

Purification of the full length fusion protein was performed by affinity chromatography using an MBPTrap column (GE Life Sciences, Uppsala, Sweden). To evaluate the purification, samples were taken from each step and monitored by SDS-PAGE (Fig. 3.1 A). After cell disruption with high-pressure cell disruption, there is a strong band at the size of 120 kDa which resembles the

full-length MBP-AtPIP5K6 fusion-protein in the crude lysate. After centrifugation, crude lysate was divided into pellet and crude extract fractions. Approximately one third of the total protein was removed by the centrifugation (Tab 3.1). MBP-AtPIP5K6 was still enriched in the pellet, for further experiments sufficient residual amount of soluble fusion-protein remained in the crude extract fraction. After the crude extract was applied to the chromatography column, full-length fusion protein was still present in the flow-through (Fig 3.1), the amount of total protein was not drastically reduced (Tab. 3.1). In the wash fraction unbound protein was removed and a band for MBP-AtPIP5K6 at 120 kDa was also visible (Fig. 3.1). The overall protein content in the wash fraction was low (Tab. 1.3). The elution fraction contained a main band at 120 kDa and some additional bands between 40 and 60 kDa. Proteins eluted with amylose from the column represented only 4 % of the initial total protein. During purification the number of Coomassie-stained bands decreased and the band for the full length AtPIP5K6 intensified compared to the bands of minor size. The identity of the 120 kDa protein band in the elution fraction was confirmed by immunoblotting using an antibody that specifically recognizes the MBP-tag of the fusion protein. For the immune detection (Fig. 3.1 B) the elution fraction of the purification was tested. Nearly all bands in that fraction stained by Coomassie were thus identified as MBP-fusions. The presence of those proteins can be explained with premature translational breakdown (compare bachelor thesis Sarah Bönisch).

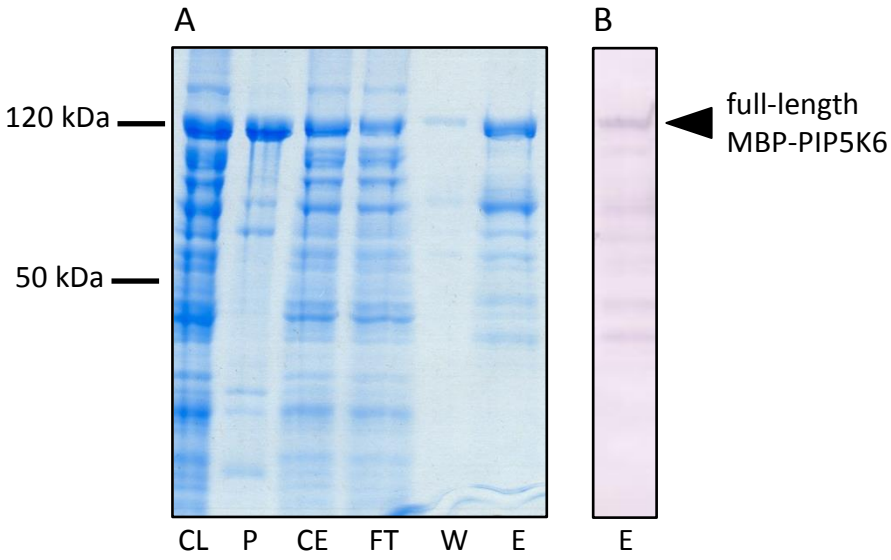

Figure 3.1.: Enrichment of MBP-PIP5K6 by affinity chromatography. Purification of recombinant expressed MBP-ATAtPIP5K6 was performed with an MPBTrap column. The single steps of purification were documented by a Coomassie-stained SDS-PAGE (A) and the eluate was verified by immune detection using an antibody against MBP (B). CL, crude lysate; P, pellet; CE, crude extract; FT, flow-through; W, wash; E, eluate. The size of the full-length MBP-AtPIP5K6 fusion protein is indicated by a black arrowhead, protein sizes according to a commercially available protein marker are indicated and apply for A and B. The purification was performed multiple times with comparable results; a representative SDS-PAGE and Western Blot are shown.

Table 3.1.: Purification of MBP-AtPIP5K6 by affinity chromatography. The data show the course of enrichment, comparing the activity of crude lysate, crude extract and the eluted fraction. The results are the outcome of duplicates.

Step	Total protein (mg)	Total activity (fmol/min)	Specific activity fmol/min/mg	Factor of enrichment
Crude lysate	180	101439	563	1
Crude extract	126,5	77679	614	1
Pooled peak	6,3	1059823	168226	298

With a lipid kinase activity test (Cho *et al.* 1992) the activity of PI4P 5-kinase against PtdIns4P was measured. The specific activities of crude lysate, crude extract and the elution fraction were compared to the total protein amounts of each fraction (Table 3.1). During purification the protein content from crude lysate to crude extract decreased by one third. The subsequent centrifugation step removes cell debris and protein aggregates, which had only minor contribution to the specific activity of MBP-AtPIP5K6. In comparison, the protein content in the elution fraction was further depleted to 4 % of the initial protein amount. Based on the amount of protein and the enzyme activities, a purification factor of ~300 was achieved.

Impurities remaining after affinity chromatography impede the calculation of specific activities, because absolute protein concentrations cannot be determined. In experiments where activities of enriched proteins were measured or compared, the protein used always originated from the same preparation. This takes into account, that MBP-AtPIP5K6 fragments of non-uniform activity might have diluted the measurements.

It was attempted to separate full length MBP-AtPIP5K6 from minor sized proteins using preparative gel filtration. The MBP-AtPIP5K6 full length protein eluted with the void volume of around 600 kDa of the S200 column and could not be separated from the MBP-PIPK6 fragment visible at 70 kDa (data not shown). It is published for human PI5P 4-kinases that they form homo dimers (Rao *et al.* 1998). An assumed size for a MBP-AtPIP5K6 dimer of 240 kDa is still below the exclusion volume of the column used and should have been detectable. It is possible that upon *E. coli* expression, MBP-AtPIP5K6 forms larger aggregates that exceed the size of the expected dimers.

The advantage that *E. coli* does not possess endogenous PI4P5-kinase activity rules out that any endogenous co-enriched protein would dilute the results of measurements performed. The purified recombinant MBP-AtPIP5K6 fusion protein was used for further experiments. The expression and purification of AtPIP5K1, AtPIP5K5 and NtPIP5K6 (data not shown) were performed according to the procedure described above. Variations are described in detail in section 2.13.

3.2 *In vitro* phosphorylation of purified recombinant MBP-AtPIP5K6 by a protein extract prepared from tobacco pollen

To investigate whether phosphorylation is involved in the regulation of AtPIP5K6, purified recombinant MBP-AtPIP5K6 was incubated with an extract prepared from tobacco pollen tubes germinated for 4 h. After incubation for periods of 1-40 min, the proteins were separated by SDS-PAGE and the incorporation of ^{33}P was visualized by phosphor imaging.

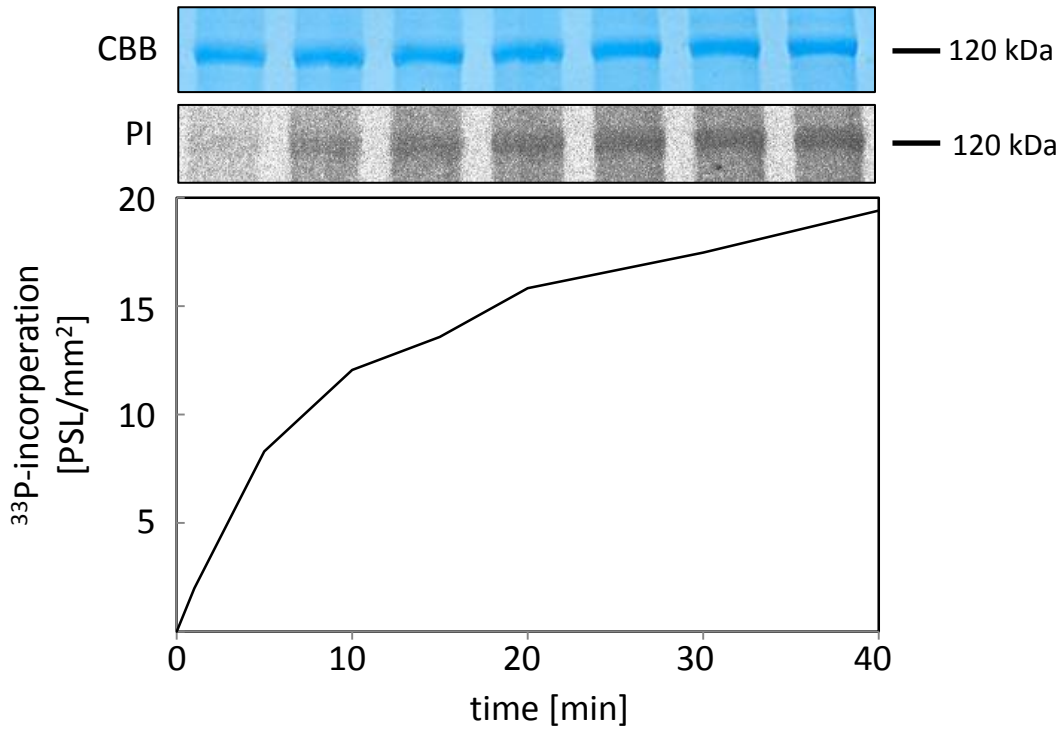

Figure 3.2: Recombinant MBP-AtPIP5K6 is phosphorylated by an extract prepared from tobacco pollen. Recombinant MPB-AtPIP5K6 was incubated with pollen extract, γ-[^{33}P]-ATP and pollen extract. Proteins were separated by SDS-PAGE. Phosphorylated bands were visualised by a phosphorimager. The Coomassie-stained SDS-PAGE (CBB) shows equal loading of MPB-AtPIP5K6. The incorporation of [^{33}P] is documented by a phosphor image (PI). Incorporation of [^{33}P] is quantified over time and protein content in the graph. The gel was dried and exposed for 2 d to a phosphor imager screen.. The experiment was performed twice in this setup to monitor a dynamic phosphorylation over time.

The MBP-AtPIP5K6 full-length protein was phosphorylated by pollen extract in a time-dependent manner. The highest increase in signal intensity occurred between one and five min and achieved around 50 % of the total ^{33}P-incorporation. In the remaining 35 min phosphorylation further increased, displaying saturation after >40 min. The data imply that phosphorylation of MBP-AtPIP5K6 is a dynamic process, and that the pollen tube extract contains relevant protein kinase activities.

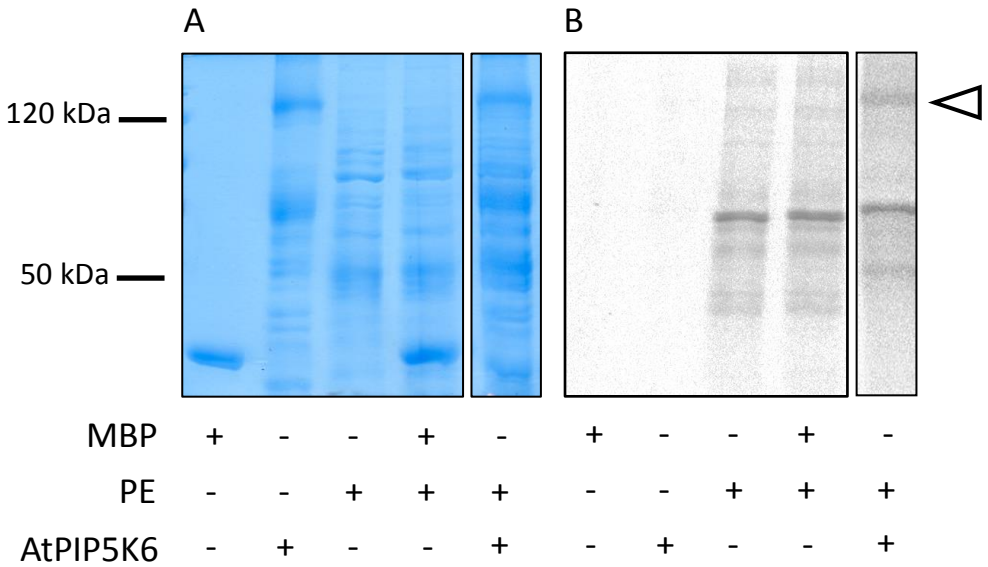

Figure 3.3: Recombinant MBP-AtPIP5K6 is phosphorylated by an extract prepared from tobacco pollen tubes. Recombinant MPB-AtPIP5K6 was incubated with (+) or without (-) pollen tube extract (PE) for 30 min at 22 °C. Proteins were incubated with γ-[^{33}P]-ATP and separated by SDS-PAGE (A). Phosphorylated bands were visualised by a phosphorimager (B). The black arrowhead indicates the size of the MBP-AtPIP5K6 fusion protein. The gels were dried and exposed for 2 d to a phosphor imager screen. The experiment was performed three times with comparable results.

In Figure 3.3 (lanes 1-3), MBP, MBP-AtPIP5K6 and the pollen protein extract were tested for autophosphorylation. Neither the solubility-tag MBP, nor the MBP-AtPIP5K6 shows autophosphorylation. In comparison to that, there were several phosphorylated bands from tobacco pollen tube extract. These bands are most likely due to autophosphorylated proteins and kinases as well as a number of endogenous substrate proteins. No additional band appeared when pollen extract was incubated together with MBP alone (Fig. 3.3, lane 4).

The data shown in Figures 3.2 and 3.3 indicate that AtPIP5K6 is phosphorylated by protein kinase activities present in tobacco pollen tube extract.

3.2.1 Identification of phosphorylated AtPIP5K6 amino acid residues after incubation with pollen tube extract by mass spectrometry

The protein extract that was used for the experiments shown in Figures 3.2 and 3.3 was heterogeneous and likely contained a multitude of protein kinases. Also, the protein sequences of AtPIP5K6 and NtPIP5K6 contain putative recognition motifs for a variety of protein kinases. These motifs include R-X-S/T (R, basic amino acid; X, any amino acid) for AGC-kinases and calcium-dependent protein-kinases and more infrequent motifs, like MAP-kinase recognition motifs (S/T-P). A global analysis of the pollen phosphoproteome (Mayank *et al.* 2012) revealed two phosphorylation sites within AtPIP5K6, namely T590 and T597. These motifs are putative MAPK-motifs. To investigate if tobacco pollen tube also contains MAPK-kinase activity, recombinant MBP-AtPIP5K6 was phosphorylated by pollen extract in the

presence of 1 mM ATP. Proteins were separated by SDS-PAGE and the band of the full-length MBP-AtPIP5K6 excised. The samples were digested with trypsin and analysed for MAPK-specific phosphorylation sites using HR/AM LC-MS with an Orbitrap Velos Pro System (Thermo Scientific, Dreireich, Germany) (see detailed information under 2.16) in cooperation with Dr. Wolfgang Hoehenwarter (Proteome Analytics, IPB, Halle (Saale)). The outcome of this analysis is summarized in Table 3.2.

Table 3.2: Summary of experimentally verified phosphorylation sites for AtPIP5K6. The amino acid positions listed in this table are potential phosphorylation sites and were determined by MS analysis. Cat, catalytic domain.

Amino acid	Domain	Identified with	Protein kinase motif
S588	Cat	Mass spectrometry	R-X-S
		this thesis	various kinases
T590	Cat	Mass spectrometry	T-P
		this thesis, PhosPhAT4.0	putative MAP-kinase motif

Two phosphorylation sites were identified by MS analysis, S588 and T580 (Tab. 3.2), which both resided in the catalytic domain of AtPIP5K6. The site S588 is located within an R-X-S motif where the basic amino acid R is resembled by lysine. This motif serves as a recognition signal for a variety of kinases, as mentioned already above, and a direct assignment to a certain protein kinase family is not possible. The second site identified is T590. This phosphorylated threonine is located adjacent to a proline residue. This sequence is accepted as a MAPK recognition motif. Taken together, the preliminary analysis of phosphorylation events after incubation of recombinant AtPIP5K6 with pollen tube extract indicates the presence of several phosphorylated amino acid residues, which can be partially attributed to MAPK phosphorylation.

3.3 An undirected approach to identify protein kinases that specifically phosphorylate AtPIP5K6

To clarify the identity of the protein kinase(s) from pollen tube extract involved in the phosphorylation of MBP-AtPIP5K6, an undirected experimental approach was chosen. The in-gel kinase-assay (IGKA) is commonly used to identify kinase substrate proteins, but it also offers the possibility to identify relevant protein kinases. Proteins from pollen tube extract are separated according to their size in a SDS-PAGE that contains recombinant purified AtPIP5K6 protein copolymerized in the gel. After electrophoresis, the proteins are renatured and incubated with γ-[^{33}P]-ATP to enable phosphorylation of the AtPIP5K6 substrate by protein

kinases from the extract. Phospho signals can be assigned to protein kinases by subsequent MS analysis (see Fig. 3.4 and section 2.15). MBP-AtPIP5K6 was co-polymerised in the separating gel of an SDS-PAGE. Two protein extracts, prepared from tobacco pollen germinated for 1h and 4h respectively, were loaded on the gel. As a positive control the catalytic subunit of protein kinase A (PKA) from bovine heart (Sigma, Schnelldorf, Germany) was used, which is known to phosphorylate PI4P 5-kinases *in vitro* (Rao *et al.* 1998; Westergren *et al.* 2001). After electrophoretic separation, the proteins in the gel were reconstituted and incubated with γ-[^{33}P]-ATP. The in-gel phosphorylation of the AtPIP5K6 substrate by radiolabelled ATP was monitored by phosphor imaging. To distinguish between autophosphorylation of kinases from the extract, a control gel, cast without AtPIP5K6 substrate in the resolving gel, was performed.

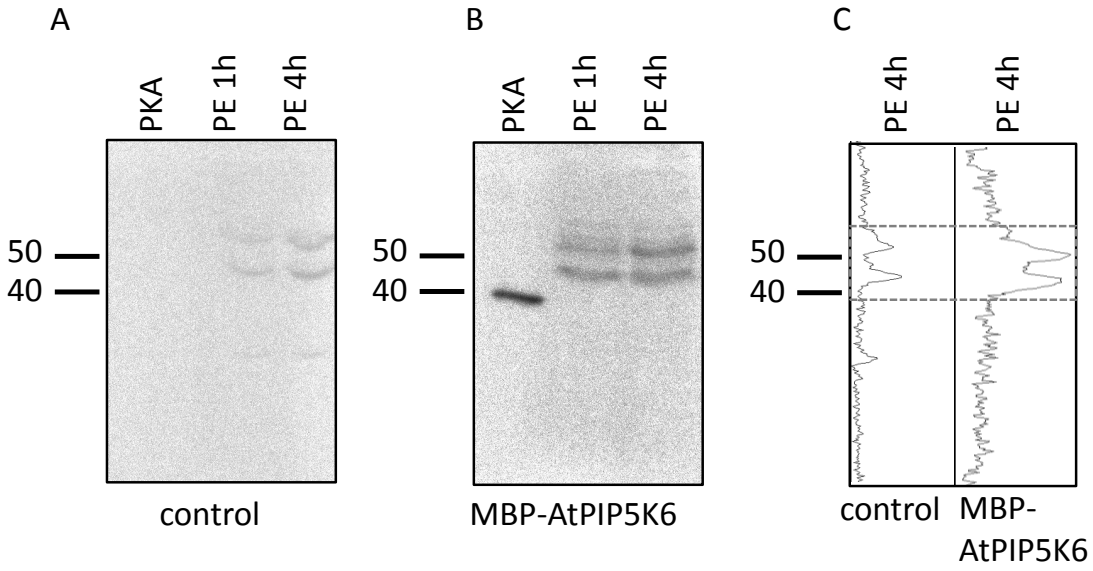

Figure 3.4: An in-gel kinase-assay reveals protein kinase candidates. Samples were prepared from tobacco pollen, grown for 1 and 4h respectively. Protein kinase A (PKA) was used as a positive control. A, SDS-PAGE gel for the control was prepared as usual. B, MBP-AtPIP5K6 was copolymerised in the SDS-PAGE gel during casting of the separating gel. After reconstitution of the proteins overnight, the kinase reaction was performed with 200 nM cold ATP and 50 µCi γ-[^{33}P] for 1h. The experiment was performed twice with comparable results.

The control showed no signal for PKA, but several phosphorylated bands between 45 and 55 kDa (Fig 3.4 A) as well as a faint band around 30 kDa for the pollen tube protein preparation. These bands are not due to phosphorylation of the AtPIP5K6 substrate protein. In contrast, the IGKA (Fig. 3.4 B, C) showed a strong signal for PKA at 40 kDa, the size of the catalytic subunit of PKA. Between 45 and 55 kDa are several phosphor bands from the pollen tube protein preparation that have intensified compared to the control. In order to identify the protein kinases from pollen tube extract which are responsible for the in-gel phosphorylation of the AtPIP5K6 substrate, pollen tube extract from the identical preparation was separated by SDS-PAGE, the in-gel phosphorylation performed without radiolabel, and the bands at a size of

45 kDa and 55 kDa were excised, digested with trypsin and subjected to Nano-LC-HD-MS^E using an ACQUITY UPLC System (Waters, Eschborn, Germany; in cooperation with Prof. Dr. Sacha Baginsky, MLU Halle-Wittenberg). The method (Helm *et al.* 2014) is described in more detail in section 2.16.

3.3.1 Identification of putative protein kinases that phosphorylate AtPIP5K6 by mass spectrometry

The MS-analysis of the excised proteins by Nano-LC-HD-MS^E using an ACQUITY UPLC System (Waters, Eschborn, Germany) identified a total of 260 proteins, with only seven of these being protein kinases (Tab. 3.3). The MS-MS-data gained from proteins of the tobacco pollen tube extract were used to search the Arabidopsis TAIR10 database (ftp://ftp.arabidopsis.org). The use of a data independent method increased the sensitivity compared to measurements performed with DDA (see for comparison section 2.16) and does not allow quantification. The designation of peptides to the corresponding proteins was achieved according to previously-established criteria (Helm *et al.* 2014), as described in more detail in section 2.16.1. This heterologous comparison introduces a degree of uncertainty and requires targeted verification of the candidates identified. The protein kinases identified by this approach belong to two different protein kinase families: the mitogen-activated protein kinase family and the CDPK-SnRK superfamily of protein kinases.

Table 3.3: Candidate protein kinases revealed by MS analysis. The table shows the annotated genes that were identified by MS analysis. Based on the similarity of proteins tobacco pollen tube extract, best matches were assigned by the TAIR10 database. Sample measurement and data analysis were performed by Stefan Helm (Prof. Dr. Sacha Baginsky, Plant Biochemistry, MLU Halle-Wittenberg). R, root; M, mesophyll; P, pollen.

Accession-No.	Gene annotation	Expressed tissue
AT2G43790	Mitogen-activated protein kinase 6, MPK6	R , M , P
AT2G18170	Mitogen-activated protein kinase 7, MPK7	R, M
AT2G42880	Mitogen-activated protein kinase 20, MPK20	R, M, P
AT3G18040	Mitogen-activated protein kinase 9, MPK9	R, M, P
AT1G35670	Calcium dependent protein kinase 11, CPK11	R, M, P
AT5G23580	Calcium dependent protein kinase 12, CPK12	R , M, P
AT5G63650	SNF1-related protein kinase 2.5, SnRK 2.5	R, M

Members of these protein kinase families are all S/T protein kinases have been already previously shown to be able to renature and subsequently display activity in IGKAs (Vidal *et al.* 2007; Zhang and Klessig 1997).

Phosphorylation assays as well as the IGKA revealed that there is transphosphorylation activity between the substrate protein MBP-AtPIP5K6 and tobacco protein kinases. The identified protein kinases may be conserved interaction partners in the homolog Arabidopsis system. The approach to map back Arabidopsis proteins from original tobacco peptides may discriminate a variety of enzymes, but Arabidopsis is the favoured model system.

The identified candidate protein kinases that may be involved in the phosphorylation of AtPIP5K6 have been further characterized (see the following sections). Expression levels of the identified protein kinases were evaluated according to their representation in mature pollen grains and growing pollen tubes as well as mesophyll and root cells (Tab.3.3) to exclude false positive hits (eFP Browser, Winter *et al.* 2007). Additionally, candidate protein kinases were subjected to SUS tests for interaction with AtPIP5K6 (see appendix, Fig. 7.1). Two candidates, MPK6 and CPK11, were chosen for further analysis in the present work. The MAP-kinase MPK6 was chosen because i) it is a MAP-kinase mainly expressed in pollen (Tab. 3.4) and ii) previous findings propose a role in polar growth (Guan *et al.* 2014; Lopez-Bucio *et al.* 2014). The calcium sensor response protein CPK11 was chosen because i) it is highly expressed in pollen and pollen tubes and ii) it was shown to be a negative regulator of pollen tube growth (Zhao *et al.* 2013).

In order to test whether the candidates MPK6 and CPK11 are truly involved in the phosphorylation of AtPIP5K6 and whether this phosphorylation has relevant functional consequences for pollen tube growth, further experiments were performed. These experiments were designed to answer the following questions:

- Do MPK6/CPK11 and AtPIP5K6 localize to the same subcellular units of pollen tubes?
- Do MPK6/CPK11 and AtPIP5K6 physically interact?
- Do recombinant MPK6/CPK11 and atPIP5K6 phosphorylate AtPIP5K6 *in vitro*?
- What are the respective phosphorylation sites?
- Does the phosphorylation have an effect on AtPIP5K6 activity?
- What are the functional effects of the phosphorylation *in vivo*?

The links between PIP5K6 isoforms from Arabidopsis and tobacco and MPK6 and CPK11 are described in the following chapters.

3.4 A new link between MAP-kinase signalling and PI4P 5-kinase function

The non-targeted analysis of protein kinases from pollen tube extracts that phosphorylate AtPIP5K6 identified MPK6 as one candidate for further analysis. Information about the role of MPK6 in polar growth was first reported in 2014 by two individual groups. Guan *et al.* reported that MPK6 is involved in the funicular guidance of pollen tubes (Guan *et al.* 2014). Another group (Lopez-Bucio *et al.* 2014) elaborated on the involvement of MPK6 in polar growth of root hair cells. Various reports have proven the important role of PtdIns(4,5)P_2 and PI4P 5-kinases during polar growth of pollen and root hairs. The first test for a possible link between MPK6 and AtPIP5K6 was for their subcellular localization.

3.4.1 Subcellular localization of MPK6

Proteins are unevenly distributed within a cell and protein localization can be visualized by the tagging of proteins with fluorescent fusion proteins. The localization of proteins with fluorescent fusions enables the assingnment to cellular substructures. To study the subcellular localization of MPK6 in pollen tubes, MPK6 fused to mCherry fluorescent protein was expressed under the control of pollen specific promoter.

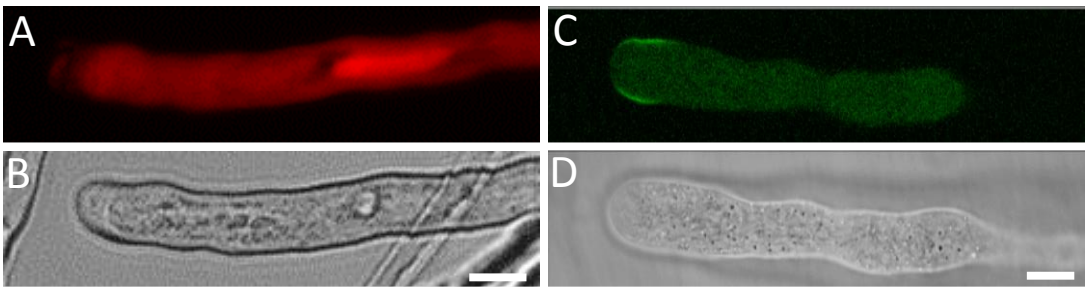

Figure 3.5: Subcellular localization of MPK6 and AtPIP5K6 fusion protein. Transient transformation of tobacco with *lat52:MPK6-mCherry* and *lat52:AtPIP5K6-EYFP*. A, Subcellular localization of MPK6-mCherry in a pollen tube expressing AtPIP5K6-EYFP. B, bright field image. C, Subcellular localization of AtPIP5K6-EYFP. D, Bright field image. A, epifluorescence image. C, confocal image. The Bar = 10 µm.

MPK6-mCherry localized in the cytoplasm and accumulated in the vegetative nucleus of pollen (Fig. 3.5, A). This pattern has also been described by Guan and co-workers (Guan *et al.* 2014). In contrast to that, AtPIP5K6-EYFP showed distinct tip-focused PM localization (Fig 3.5 C), which has been reported before for other PI4P 5-kinases (Ischebeck *et al.* 2008; Kost *et al.* 1999; Sousa *et al.* 2008; Stenzel *et al.* 2012; Zhao *et al.* 2010). AtPIP5K6-EYFP fluorescence was also observed in the cytosol. The pollen tube showed an AtPIP5K6-overexpression phenotype (trapped protoplast, Ischebeck *et al.* 2008; Stenzel *et al.* 2012). The localization tests showed

that MPK6 and AtPIP5K6 displayed distinct localization in the cell and overlap in their cytoplasmic localization.

3.4.2 Protein-Protein interaction between MPK6 and AtPIP5K6

Another important test to verify a possible link between MPK6 and AtPIP5K6 is to determine whether these proteins physically interact. To test whether AtPIP5K6 interacts with the candidate protein kinase MPK6, SUS experiments were performed with the Dualmembrane Kit 3 (Dualsystems Biotech, Zürich, Switzerland). In comparison to the conventional, nuclear-localized yeast two-hybrid system, the SUS is designed for membrane-associated or integral membrane proteins that do not reside in the nucleus. Reconstitution of the single Ub subunits takes place outside the nucleus.

AtPIP5K6 was cloned into the bait vector encoding an AtPIP5K6-OST4-Cub-transcription factor fusion residing at the ER (detailed description in section 2.12). The prey construct was cloned with the cDNA of *MPK6* to encode a NubG fusion. The positive control consists of a native Ub-half (NubI) fused to the Alg5 protein. NubG fused to the ER-localized protein Alg5 served as a negative control. For the interpretation of an interaction, it is most relevant to check for significantly increased growth compared to the negative control (Fig. 3.6).

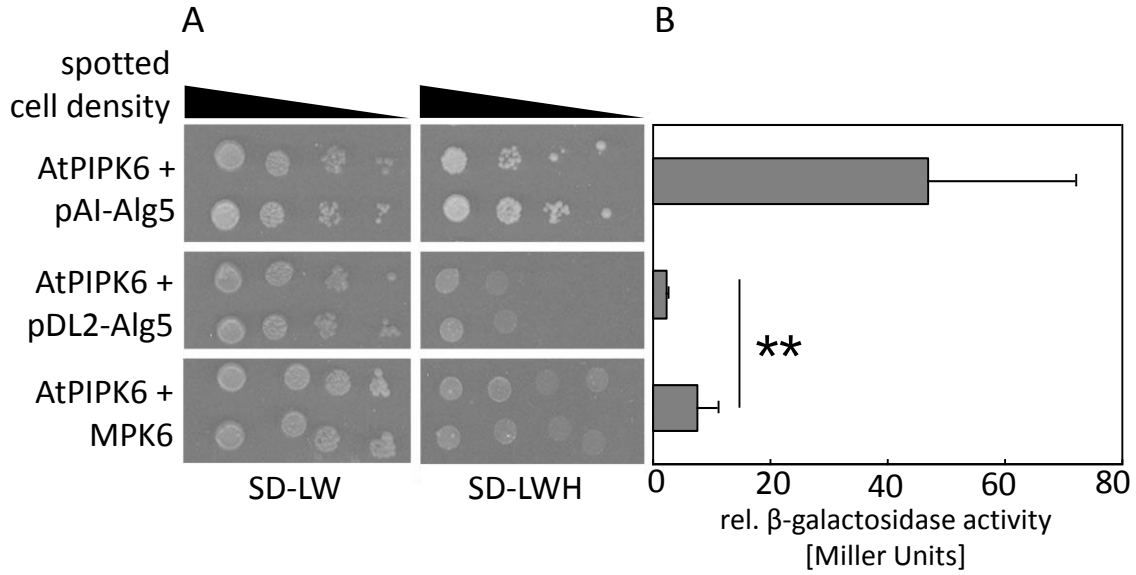

Figure 3.6: PIP5K6 and MPK6 interact in a SUS assay. Yeast was transformed with pBT3C-*OST4-AtPIP5K6* as bait and pAI-*Alg5*, pDL2-*Alg5* and pPR3N-*MPK6* as prey-plasmids. A, the pBT3C-*OST4-PIP5K6* and pPR3N plasmids each bear an auxotrophy selection gene for L and W respectively to control for transformation efficiency and success. For each transformation two individual clones were diluted from OD_{600} 1, 0.5, 0.05 and 0.005 from left to right. Dilutions were plated on SD plates lacking L and W to control for transformation of bait and prey plasmids SD-LW). The interaction of the clones was tested on selection for the histidine auxotrophy marker (SD-LWH). B, quantification of ß-galactosidase activity in Miller Units. Both experiments were performed in triplicates. Error bars resemble the standard deviation, which was calculated based on the entire value population. For statistical analysis a two-tailed t-test was performed. Significance levels are ρ <0.05 (*), ρ <0.01 (**), and ρ <0.001 (***).

To detect an interaction between AtPIP5K6 and MPK6, the co-transformed yeast was selected on histidine-free medium (SD-LWH, without leucine, tryptophan and histidine). Growth on SD-LWH signifies that the yeast is now autotrophic for histidine and indicates an interaction. To evaluate growth, dilutions of single yeast clones were prepared according to the measured OD_{600} and were subjected to selection for the vectors (SD-LW, without leucine and tryptophan) and the interaction (SD-LWH) (Fig.3.6 A).

For the quantification of the interaction of bait and prey can also be measuring the expression level of the reporter gene *LacZ*, coding for a β-galactosidase reporter. Similar to *HIS3*, *LacZ* expression is under the control of the released transcription factors in the yeast strain *NMY51*. For the quantification of β-galactosidase, a colorimetric test is used where *ortho*-nitrophenyl-β-D-galactopyranoside (ONPG) is applied as a substrate. ONPG is hydrolysed by β-galactosidase to galactose and *o*-nitrophenol. *o*-Nitrophenol is yellow and its absorption can be quantified at 420 nm. The uniform, growth of all yeast clones on SD-LW shows that all three vector combinations were successfully transformed and equal amount of cells were plated (Fig. 3.6 A, left). Growth was observed in all dilutions from OD_{600}=1 until 0.005. The test for interaction was performed on SD-LWH (Fig. 3.6 A, right). The positive control showed growth until an OD_{600} of 0.005. In the ONPG-test a relative β-galactosidase-activity of approximately 45 Miller Units was measured. The negative control showed weak basal growth visible until an OD_{600} of 0.05. The ONPG-test showed a relative β-galactosidase activity of two Miller Units. Yeast transformed with AtPIP5K6 and MPK6 also showed growth until an OD_{600} of 0.05. Importantly, the result of the ONPG-assay of seven Miller Units was significantly higher compared to that of the negative control, indicating a weak interaction of MPK6 and AtPIP5K6.

3.4.3 AtPIP5K6 and MPK6 interact at the apical PM in pollen tubes

The SUS assay revealed that there is a weak interaction between AtPIP5K6 and MPK6. To verify protein-protein interaction under physiological conditions *in vivo*, a split-YFP test was performed. This test offers not only the possibility to document the protein-protein interaction in living plant cells, but also characterizes the subcellular localization of the interplay between AtPIP5K6 and MPK6. *AtPIP5K6* fused to the N-terminal part of *YFP* (YFP^N) and *MPK6* fused to the C-terminal part of *YFP* (YFP^C) were transiently expressed in tobacco pollen tubes under the control of a *35S* promoter, which has only minor activity in pollen tubes. As a control, the empty vector containing the corresponding YFP-part was chosen. To identify transformed pollen tubes, all transformations were additionally co-expressing a *lat52* promotor driven *mCherry*-fluorophore (Fig. 3.7).

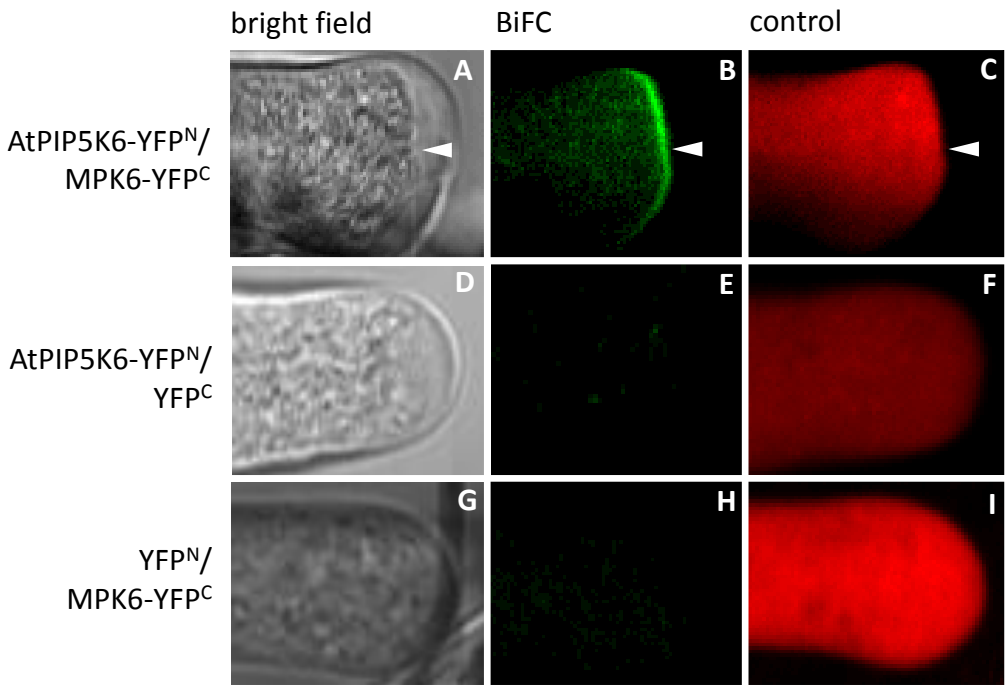

Figure 3.7: AtPIP5K6 and MPK6 interact in a BiFC assay in tobacco pollen tubes. The *lat52::mCherry*, *35S::YFP^N*, *35S::YFP^C*, *35S::AtPIP5K6-YFP^N* and *35S::MPK6-YFP^C* constructs were transiently transformed in tobacco pollen via particle bombardment. Pollen was germinated for 14h. Fluorescence of the proteins was detected by confocal microscopy. Epifluorescence from the interaction between the YFP^N-fusion of AtPIP5K6 and the YFP^C-fusion of MPK6 was observed at the apical PM (B). A YFP^N-fusion of AtPIP5K6 was co-expressed with YFP^C and is shown as a negative control for AtPIP5K6 (E). A YFP^C-fusion of MPK6 was co-expressed with YFP^N and used as a negative control for CPK11 (H). *Lat52:mCherry* was co-expressed with all combinations to identify transformed cells (C, F, I). The white arrowhead indicate the PM in images A, B and C. This experiment was performed three times with comparable results.

Expression of AtPIP5K6-YFP^N together with MPK6-YFP^C gave a YFP-signal in 75 % (n= 10) of the observed pollen tubes. Expression of AtPIP5K6-YFP^N together with YFP^C gave a very low YFP-signal in 10 % (n=10) observed pollen tubes. MPK6-YFP^C expressed together with YFP^N gave a weak cytosolic YFP-signal in 25 % (n=10) of the observed cells. In contrast to the low fluorescence observed for the negative controls, the fluorescence observed for the co-expression of AtPIP5K6 and MPK6 was restricted to the apical PM of the pollen tube. This plasma-membrane localized signal was mainly observed in pollen tubes with AtPIP5K6-specific phenotypes.

The split-YFP experiments are consistent with the SUS data and support interaction between AtPIP5K6 and MPK6 at the apical PM of pollen tubes.

3.4.4 MPK6 phosphorylates pollen-specific PIPKs *in vitro*

From the experiments performed so far, MPK6 emerges as a candidate for a protein kinase possibly responsible for phosphorylating AtPIP5K6. Up to this point, it has remained unclear however, whether MPK6 would really phosphorylate AtPIP5K6 *in vitro*. While the correct

localization in pollen tubes and the physical interaction of the partner proteins are relevant prerequisites for their functional interplay, next it was tested whether MPK6 would specifically phosphorylate AtPIP5K6 or other PI4P 5-kinases. The event of transphosphorylation between a protein kinase and its substrate can be investigated by different methods. To test whether MPK6 not only interacted with, but also added a posttranslational modification to AtPIP5K6, *in vitro* kinase-assays were performed. In these assays the ability of purified and activated MPK6 to phosphorylate four different recombinantly expressed Arabidopsis PI4P 5-kinases was examined. Purified and activated MPK6 was obtained from Pascal Pecher from the group of Dr. Justin Lee (IPB, Halle (Saale)). The kinase reactions were initiated by the addition of 20 µM ATP containing 10 µCi ^{33}P-labeled ATP. After 30 min of incubation, the proteins were separated by SDS-PAGE and the ^{33}P-incorperation was visualized by phosphor imaging. As a control, PI4P 5-kinases were subjected to an autophosphorylation test (Fig. 3.8 A and C).

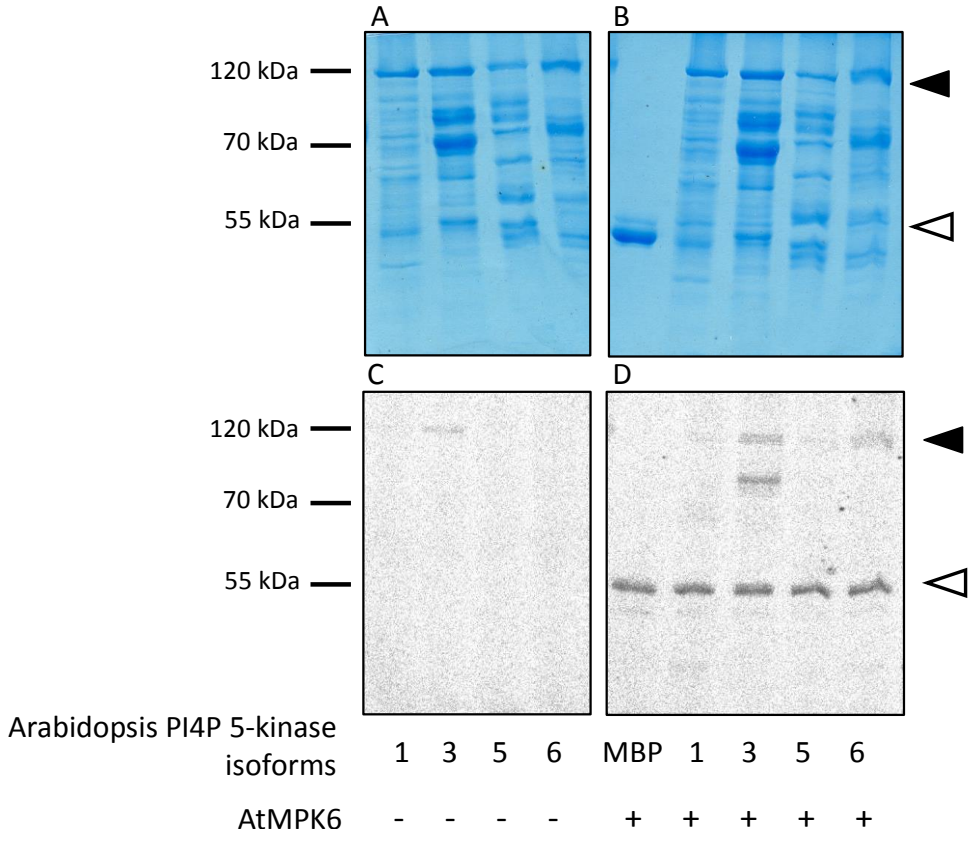

Figure 3.8: MPK6 phosphorylates AtPIP5K6 and AtPIP5K3 in an *in vitro* kinase assay. Recombinant MPB-AtPIP5K1, MBP-AtPIP5K3, MBP-AtPIP5K5 and MBP-AtPIP5K6 were incubated with γ-[^{33}P]-ATP (A, C) to test for protein autophosphorylation. Recombinant MBP, MPB-AtPIP5K1, MBP-AtPIP5K3, MBP-AtPIP5K5 and MBP-AtPIP5K6 was tested together with γ-[^{33}P]-ATP for MPK6 mediated phosphorylation (B, D). Proteins were incubated for 30 min at room temperature, separated by SDS-PAGE and exposed to a phosphorimager screen. The upper part represents the Coomassie-stained gels (A and B); the phosphor images (C and D) are shown in the lower part of the figure. The black arrowhead indicates the sizes of full length MBP-AtPIP5K protein. The open arrowhead marks autophosphorylated MPK6. The gels were dried and exposed for 3 d to a phosphor imager screen. This experiment was performed three times with comparable results.

Fig. 3.8 shows the Coomassie-stained gels (A and B) as a loading control and the corresponding autoradiographs (C and D). Autophosphorylation was only detected for AtPIP5K3, as was already described by Dr. Jennifer Lerche (Dissertation 2013, unpublished data).

Upon incubation with MPK6, AtPIP5K3 and AtPIP5K6 become phosphorylated. The autophosphorylation signal of AtPIP5K3 has to be taken into account when evaluating the intensities of AtPIP5K3 and AtPIP5K6 (D). AtPIP5K3 also shows a phosphorylated fragment at 70 kDa, that intensifies compared to the full length fusion protein. It can be hypothesized that this protein fragment lacked the C-terminal portion that is responsible for autophosphorylation, because the fragment did not exhibit an autophosphorylation signal. The intensified signal can also be explained by a higher number of protein fragments compared to full length fusion protein. AtPIP5K6 was phosphorylated as a full-length protein. The solubility-tag MBP with a size of 40 kDa was not phosphorylated by MPK6. The phosphor band at the size of 55 kDa represents autophosphorylated MPK6 (open arrow) and is present to the same extent in all samples.

The data confirm MPK6 as a protein kinase capable of phosphorylating AtPIP5K6 and are consistent with the data from the in-gel kinase-assay (see section 3.3) and the interaction studies (section 3.4.1 and 3.4.2).

3.4.4.1 Database-aided identification of putative MPK6 phosphorylation sites

To recognize a phosphorylation site MAP-kinases require a proline residue at the position +1 following the phosphorylated S/T (Biondi and Nebreda 2003). The sequence analysis of AtPIP5K1, AtPIP5K3, AtPIP5K5 and AtPIP5K6 revealed MPK6-motif in all four PI4P 5-kinases (Tab. 3.5.).

Table 3.5: Summary of putative MAP-kinase phosphorylation sites in selected PI4P 5-kinases. The amino acid positions listed in this table are putative phosphorylation sites according to the motif S/T-P that is known from MAP-kinase substrates.

PI4P5-kinase	Expressed tissue	Putative MAP-kinase motifs
AtPIP5K1	ubiquitous	T49, T64, T66, T402, S449, S615
AtPIP5K3	Root	S272, S291, S306, T376, S423, T613
AtPIP5K5	Pollen	S359, T431, S478, T650
AtPIP5K6	Pollen and leaf veins	T377, S424, T590, T597
NtPIP5K6	Pollen	T46, S267, T298, T427, S474, T651, T664

The protein sequence of AtPIP5K6 contains four putative MAP-kinase recognition motifs. These motifs are located in close proximity to each other in a variable region within the catalytic domain of AtPIP5K6. The closely related AtPIP5K5 protein also contains four putative MPK6-recognition motifs, distributed within the catalytic region of the enzyme.

AtPIP5K1 and AtPIP5K3 both exhibit six putative MPK6-motifs that are not restricted to the C-terminal portion of the enzymes, like it was observed for the pollen-expressed PI4P 5-kinases AtPIP5K5 and AtPIP5K6.

Experimental data about the phosphorylation status of AtPIP5K6 *in vivo* was collected during the investigation of the Arabidopsis pollen phosphoproteome (Mayank *et al.* 2012; Nakagami *et al.* 2010) and deposited at the PhosphAT 4.0 Database (Heazlewood *et al.* 2008). For AtPIP5K6, four phosphorylation sites have previously been identified, including the two mentioned MAP-kinase motifs, T590 and T597, in the catalytic domain (Tab 3.6).

Tab. 3.6: Summary of experimentally verified phosphorylation sites for AtPIP5K6. The amino acid positions listed in this table are putative phosphorylation sites and were determined by MS analysis. Lin, linker domain; Dim, dimerization domain; Cat, catalytic domain.

Residue	Domain	Identified with	Protein kinase
S71	Lin	Mass spectrometry (PhosPhAT4.0)	unknown
S291	Dim	Mass spectrometry (PhosPhAT4.0)	unknown
T590	Cat	Mass spectrometry (PhosPhAT4.0 and this thesis)	MPK6 (identified in this thesis)
T597	Cat	Mass spectrometry (PhosPhAT4.0 and this thesis)	MPK6 (identified in this thesis)

The protein sequence analysis of AtPIP5K6 revealed that there are four putative MPK6-recognition motifs within the catalytic domain. Two of these four MPK6-motifs were identified by an undirected approach of the Arabidopsis pollen proteome as sites phosphorylated *in vivo* (Mayank *et al.* 2012).

3.4.4.2 Identification of AtPIP5K6 amino acid residues phosphorylated by MPK6

To analyse which phosphorylation sites are targeted in AtPIP5K6 by MPK6 *in vitro*, a kinase assay was performed without radiolabeled ATP, as described in section 2.14. The AtPIP5K6 band was excised, the protein was cleaved with trypsin and phosphorylated peptides were identified by a targeted MS-MS analysis, according to the masses of the predicted phosphorylated and non-phosphorylated peptides, in cooperation with Dr. Wolfgang

Hoehenwarter (Proteome Analytics, IPB, Halle (Saale)) using HR/AM LC-MS with an Orbitrap Velos Pro System (Thermo Scientific, Dreireich, Germany). See detailed description under section 2.16. The analysed peptides cover around 70 % of the AtPIP5K6 protein (see Appendix, Fig. 7.1). The identified phosphorylation sites are two threonine residues at position T590 and T597 when AtPIP5K6 was incubated with active MPK6 *in vitro* (Tab. 3.7). The site T590 was already determined to be phosphorylated by the complex pollen tube extract (see Tab. 3.2). The protein sequence neighbouring T590 and T597 contains several lysine (K) and arginine (R) residues that are potential cleavage sites for trypsin. If trypsin cleavage is complete, the resulting peptides are, with a size of 10 amino acids, too small for detection by MS analysis. It was observed, that T590 was detected when there was a miscleavage at position K586 (Tab. 3.7, first line). The second site T597 was detected, but could not be as confidently mapped as the first residue. Phosphopeptides containing both sites were detected with high numbers of peptide spectral matches (#PSMs; Tab. 3.7, first and second line). This is a semi-quantitative index and indicates high levels of phosphorylation at these sites following the *in vitro* kinase assay of AtPIP5K6 with activated MPK6. The phosphopeptide spectra are shown in Fig. 7.8 (see appendix).

3.4.5 Site-directed mutagenesis of the residues T590 and T597 of PIP5K6

To validate the two phosphorylation sites of AtPIP5K6 in the previous section, further experiments were performed. A tool to analyse the effect of such a phosphorylation on protein level, to prevent the phosphorylation, is the introduction of a small neutral amino acid, for example alanine (A), by site-directed mutagenesis of the corresponding cDNA and the study of the effects of this substitution.

3.4.5.1 *In vitro* phosphorylation of PIP5K6 variants

To show that AtPIP5K6 gets phosphorylated specifically at the MAPK-kinase motifs introduced above, recombinantly expressed and enriched fractions of AtPIP5K6, AtPIP5K6 T590A, AtPIP5K6 T597A and the double mutant variant AtPIP5K6 T590A T597A were incubated with MPK6 to test for phosphorylation of these AtPIP5K6 variants. After incubation with MPK6, the proteins were separated and the amount of ^{33}P-incorporation was detected using phosphor imaging and quantifications with TINA software (Raytest, Straubenhardt, Germany). The Coomassie-stained loading control (Fig. 3.9, A) shows the amounts of protein that were applied for each variant. To quantify the extent of phosphorylation, protein amounts and

^{33}P-incorporation were normalised to the amount of wild type AtPIP5K6 fusion protein (Fig. 3.9, B).

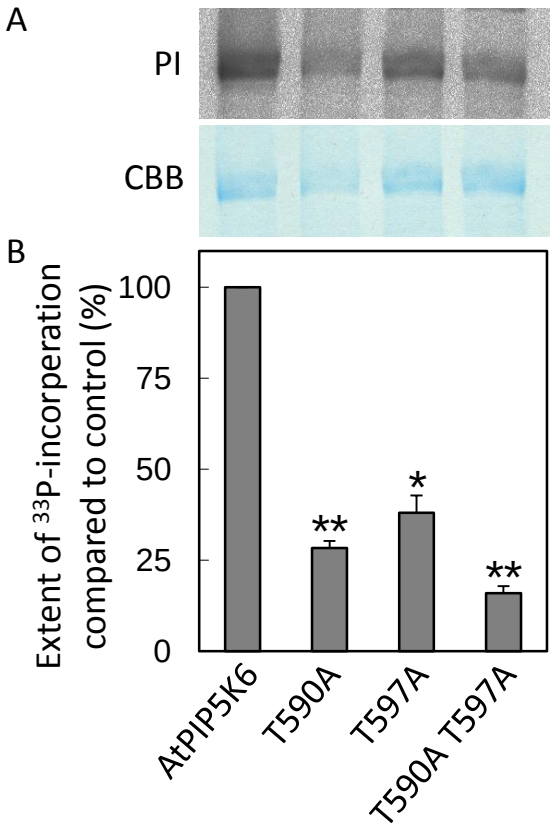

Figure 3.9.: *In vitro* phosphorylation of MPB-AtPIP5K6 T590A and MBP-AtPIP5K6 T597A. MBP-AtPIP5K6 T590A, MBP-AtPIP5K6 T597A and the double variant MBP-AtPIP5K6 T590A T597A were tested for phosphorylation by recombinant and activated MPK6 and γ-[^{33}P]-ATP. Proteins were separated by SDS-PAGE and the incorporation of ^{33}P was visualized by phosphor image technology. A, section of a phosphorimage (PI, top) and the corresponding Coomassie-stained gel (CBB, bottom). B, level of ^{33}P-incorporation was normalized to protein amounts of the wild type control. The bars resemble the mean values of a triplicate measurement. Error bars resemble the standard deviation, which was calculated based on the entire value population. The experiment was performed in three independent experiments with similar results. For statistical analysis a two-tailed t-test was performed. Significance levels are ρ <0.05 (*), ρ <0.01 (**), and ρ <0.001 (***).The gel was dried and exposed for 3 d to a phosphor imager screen. The experiment was performed three times with similar results.

The quantification shows that the wild type AtPIP5K6 exhibits the strongest phosphorylation signal compared to all other lanes. The single exchange mutants AtPIP5K6 T590A and AtPIP5K6 T597A displayed reduced incorporation of phosphate, and the double mutant AtPIP5K6 T590A T597A had the weakest phosphorylation signal detected. To further validate these patterns, AtPIP5K6 A-variants were incubated with MPK6 and ATP and were subjected to tryptic digestion and phosphopeptide identification in cooperation with Dr. Wolfgang Hoehenwarter (Proteome Analytics, IPB, Halle (Saale)) using HR/AM LC-MS with an Orbitrap Velos Pro System (Thermo Scientific, Dreireich, Germany). See detailed description under section 2.15 and 2.16. For T590A phosphorylation was detected at position T597. The reciprocal effect was detected for T597A, where the phosphorylation of T590 was still detectable. For the two single variants

no additional phosphopeptides were identified, whereas for the double variant AtPIP5K6 T590A T597A low levels of unspecific phosphorylation were detected at position T592 in agreement with the basal signal level on the phosphorimage (Fig. 3.12). These signals were never observed in analysis with other protein variants and may be non-specific residual phosphorylation by the recombinant MPK6 in the absence of its preferred target motifs and commonly observed for *in vitro* kinase assays. Based on the analysis done, it can be concluded that both T590 and T597 are relevant phosphorylation sites of AtPIP5K6 that are modified by MPK6.

Table 3.7: Summary of identified phosphopeptides. The peptides listed were identified from AtPIP5K6 and variants incubated with MPK6 by HR/AM LC-MS by Dr. Wolfgang Hoehenwarter (Proteome Analytics, IPB, Halle (Saale)). p in a peptide sequence indicates a phosphorylated residue, #PSM numbers of peptide spectral matches. P-site, amino acid residue in the protein sequence of AtPIP5K6 with the highest probability of all possible positions within the peptide. Probability is based on the probability of all possible phosphorylation sites in the peptide sequence based on interpretation of the MS/MS fragment ion pattern by the phosphoRS software (Mascot software v.2.5).

Protein substrate	Sequence	#PSMs	P-site	Probability %
AtPIP5K6	EAAIKDSA**p**TPTSGAR	108	T590	95
AtPIP5K6	DSATPTSGAR**p**TPTGNSETR	321	T597	11.5
AtPIP5K6 T590A	DSAAPTSGAR**p**TPTGNSETR	113	T597	99
AtPIP5K6 T590A	EAAIKDSAAPTSGAR**p**TPTGNSETR	18	T597	78.8
AtPIP5K6 T597A	EAAIKDSA**p**TPTSGAR	148	T590	95.6
AtPIP5K6 T590A T597A	EAAIKDSAAP**p**TSGAR	17	T592	88.2

3.4.6 Effects of MPK6 on the catalytic activity of AtPIP5K6 *in vitro*

Phosphorylation as a posttranslational modification is known to be a fast and potent regulatory mechanism to control protein activity. The data so far establish that MPK6 phosphorylates AtPIP5K6 at typical MAP-kinase recognition motifs, raising the question, whether the phosphorylation has a regulatory effect on AtPIP5K6. To investigate if phosphorylation by MPK6 has an effect on AtPIP5K6 activity, both recombinant enzymes were pre-incubated together, enabling phosphorylation of AtPIP5K6 by MPK6 and the PI4P 5-kinase activity of the phosphorylated AtPIP5K6 protein was then analysed by monitoring the phosphorylation of the inositol head group of the lipid substrate PtdIns4P in the presence of γ-[^{33}P]-ATP (Fig. 3.10). To ensure phosphorylation of the MBP-AtPIP5K6 fusion the identical experimental setup for the kinase assay was used as described in section 2.14 and 3.3.4. The results of the activity test were compared to an equally treated sample containing identical amounts of the same AtPIP5K6 preparation without prior incubation with MPK6 (Fig. 3.9). Compared to the activity of the control, the activity of AtPIP5K6 treated with MPK6 was

significantly decreased by ~55 % (ρ= 0.0092). The inhibitory effect of MPK6 mediated phosphorylation on AtPIP5K6 activities corresponds well with previous reports that phosphorylation inhibits PI4P 5-kinase activity, and with the location of the phosphorylation site within the catalytic domain of AtPIP5K6.

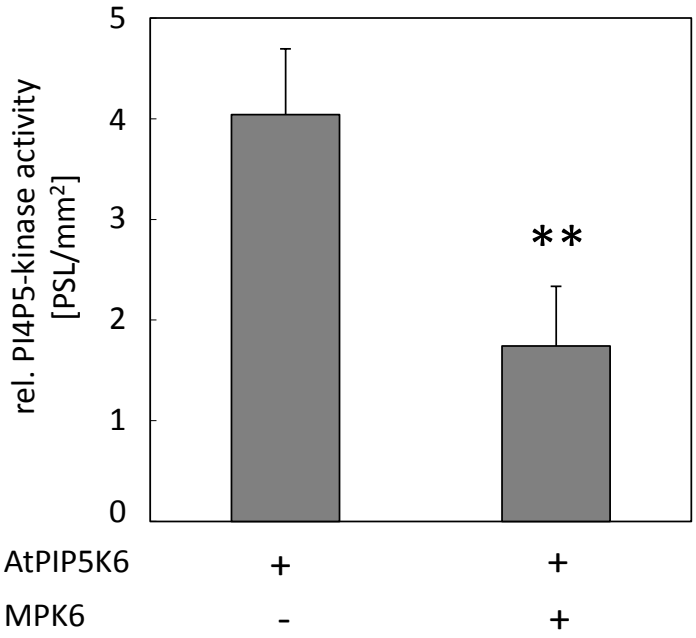

Figure 3.10: MPK6 lowers catalytic activity of AtPIP5K6 *in vitro*. Recombinant MBP-AtPIP5K6 was pre-incubated with and without 1 µg purified and activated MPK6 protein and 20 µM ATP for 30 min at 22°C. The such treated MBP-AtPIP5K6 fusion protein was subsequently mixed with PI4P and 10 µCi γ-[^{33}P]-ATP and 1 mM cold ATP for 1h to examine residual PI4P 5-kinase activity. Synthesized PtdIns(4,5)P_2 was isolated by acidic lipid extraction and separated with thin layer chromatography. ^{33}P-incorporation was detected with phosphor image technology and calculated with TINA-software. Error bars resemble the standard deviation, which was calculated based on the entire value population. For statistical analysis a two-tailed t-test was performed. Significance levels are ρ <0.05 (*), ρ <0.01 (**), and ρ <0.001 (***). The experiment was performed twice with similar results.

3.4.7 MPK6 does not affect AtPIP5K6 T590A T597A activity *in vitro*

Next it was tested, whether activated MPK6 still modulates the PI4P 5-kinase activity of the AtPIP5K6 T590A T590D variant. The experiment was performed according to the description in sections 2.6.2 and 3.4.6. Recombinantly expressed and purified AtPIP5K6 T590A T597A protein was pre-incubated with 1 µg MPK6 for 30 min and PI4P 5-kinase activity was measured in a subsequent activity test (see section 2.13.14.) The results are summarized together with the data of section 3.4.6 as percentage of control PI4P 5-kinase activity in figure 3.11. Whereas AtPIP5K6 activity was diminished by the incubation with MPK6 by ~55 %, the activity of AtPIP5K6 T590A T597A activity was not affected by the incubation with MPK6. Importantly, the AtPIP5K6 T590A T597A variant was fully active. In fact, the activity of the variant enzyme was higher than that of the wild type (see for comparison Fig. 7.4).

These data demonstrate that the phosphorylation of AtPIP5K6 in positions T590 and T597A by MPK6 were responsible for the inhibition of catalytic activity observed after incubation of the enzyme with MPK6.

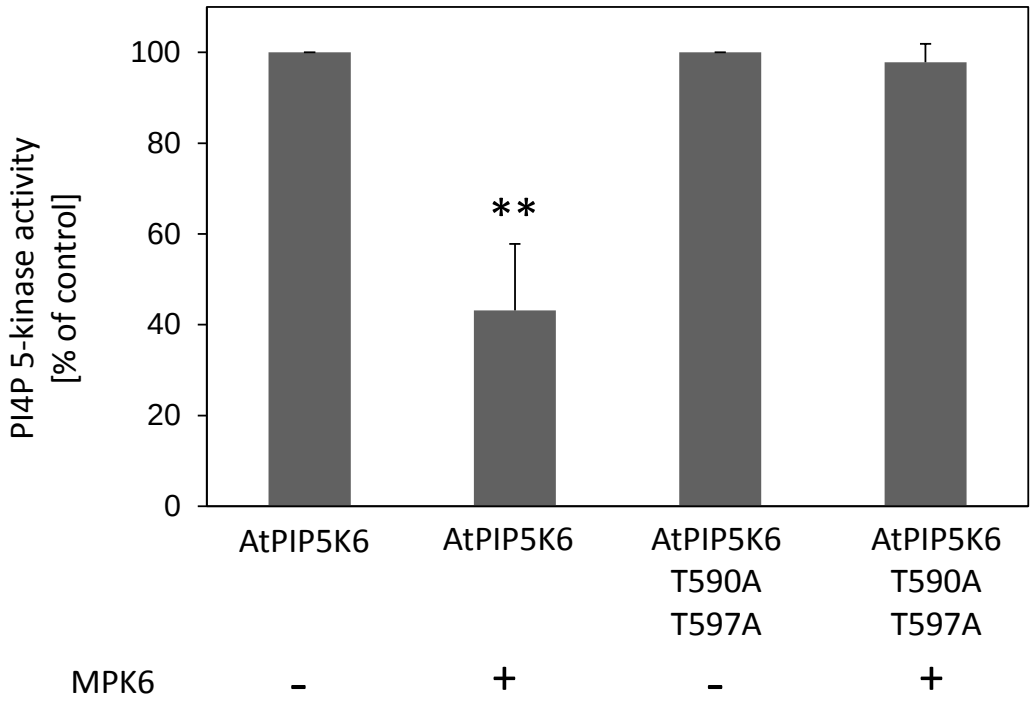

Figure 3.11: MPK6 does not affect catalytic activity of AtPIP5K6 T590A T597A *in vitro*. Recombinant MBP-AtPIP5K6 was pre-incubated with and without 1 µg purified and activated MPK6 protein and 20 µM ATP for 30 min at 22°C. The such treated MBP-AtPIP5K6 fusion protein was subsequently mixed with PI4P and 10 µCi γ-[^{33}P]-ATP and 1 mM cold ATP for 1h to examine residual PI4P 5-kinase activity. Synthesized PtdIns(4,5)P_2 was isolated by acidic lipid extraction and separated with thin layer chromatography. ^{33}P-incorporation was detected with phosphor image technology and calculated with TINA-software. Values were transformed to percent for reasons of comparison. Error bars resemble the standard deviation, which was calculated based on the entire value population. For statistical analysis a two-tailed t-test was performed. Significance levels are ρ <0.05 (*), ρ <0.01 (**), and ρ <0.001 (***).The experiment was performed twice in triplicates with similar results.

3.4.8 Effects of MPK6 on the functionality of AtPIP5K6 *in vivo*

The data so far demonstrate a clear effect of MPK6 on AtPIP5K6 function *in vitro*, raising the question whether these observations have relevance for *in vivo* functions of AtPIP5K6 and pollen tube growth. The phenotypes induced by overexpression of AtPIP5K6 as a result of enhanced production of PtdIns(4,5)P_2 have been described in detail in section 1.3. The incidence of the branched and stunted phenotypes is an indication for the functionality of PI4P 5-kinases with roles for in the control of secretion (Ischebeck *et al.* 2010). To investigate the influence of MPK6 on AtPIP5K6 *in vivo*, AtPIP5K6-YFP was co-expressed in tobacco pollen tubes either with an mCherry control or with MPK6 fused to mCherry (Fig. 3.12). Upon co-expression of these combinations, the incidence of normal, branched and stunted phenotypes was

quantified as it has been used in prior studies for quantitative statements (Ischebeck *et al.* 2010). When AtPIP5K6 was co-expressed with mCherry, a characteristic distribution of phenotypes was observed (Fig. 3.10, white bars). Normal growing pollen tubes usually comprised ~10 % of transformed cells, likely those with low expression levels (Ischebeck *et al.* 2008). The intermediate phenotype, represented by branched pollen tubes, accounted for ~25 %. The residual ~65 % were allocated to the most severe phenotype, stunted pollen tubes (Fig. 3.14, white bars). The distribution of the phenotypes observed upon co-expression of AtPIP5K6 with MPK6-mCherry was shifted from the pattern of the controls (Fig 3.12, grey bars). While the number of normal growing pollen tubes did not differ from the number observed for AtPIP5K6 co-bombarded with mCherry, the number of branched pollen tubes increased by ~30 %, compared to the control (ρ=0,032). Concomitantly, the number of stunted pollen tubes decreased by ~20 % compared to the control (ρ=0,023). This change was found to be statistically significant based on a two tailed student's t-test.

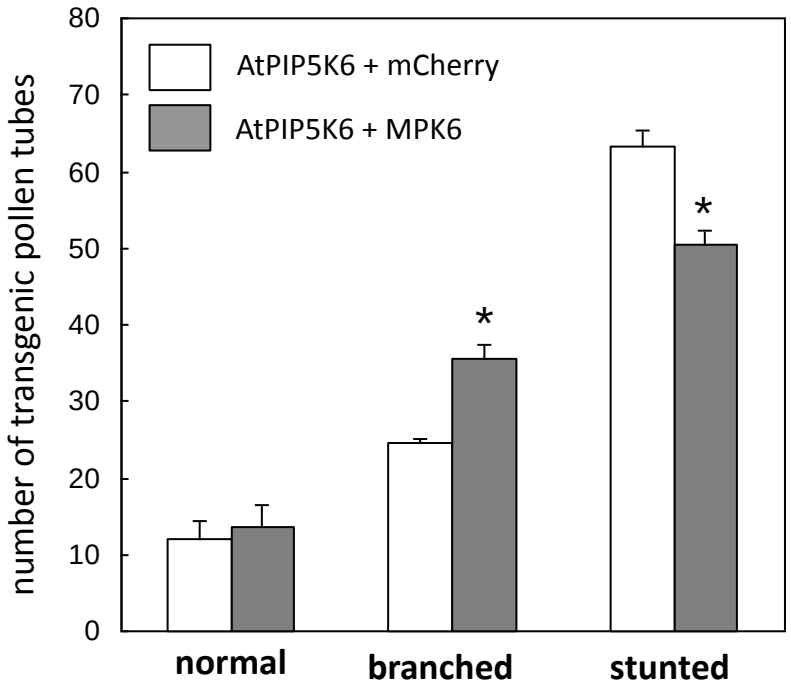

Figure 3.12.: Statistic analysis of phenotype distribution upon co-expression of AtPIP5K6-YFP with MPK6-mCherry. The values show the distribution of phenotypes upon transient overexpression of AtPIP5K6 with mCherry (white) and AtPIP5K6-YFP with MPK6-mCherry (grey) expressed as numbers, in tobacco pollen tubes. Pollen was grown for 6-8h. The data is the result of three individual experiments. For each experiment 100 pollen tubes were scored. Error bars resemble the standard deviation, which was calculated based on the entire value population. For statistical analysis a two-tailed t-test was performed. Significance levels are ρ <0.05 (*), ρ <0.01 (**) and ρ <0.001 (***).

The data indicate that upon co-expression of AtPIP5K6 and MPK6, there was a shift of the phenotypic distribution towards a weaker manifestation of the AtPIP5K6-mediated changes. This observation is consistent with reduced AtPIP5K6-activity upon co-incubation with

recombinant, activated MPK6, supporting the notion of an inhibitory effect of MPK6 on AtPIP5K6.

3.5 AtPIP5K6 and MPK6 have close homologs in *N. tabacum*

The previous sections illustrated a functional link between Arabidopsis MPK6 and AtPIP5K6 *in vitro* and in the heterologous tobacco pollen system. To exclude possible artefacts arising from the heterologous enzymes in tobacco pollen tubes, additional analyses were performed with homologous enzymes from *N. tabacum* (Fig. 3.13).

3.5.1 NtPIP5K6 is a close homolog of AtPIP5K6

A tobacco homolog *NtPIP5K6* of *AtPIP5K6* was isolated in a previous study by Dr. Irene Stenzel based on a tobacco pollen tube cDNA library (Stenzel *et al.* 2012). It was termed *NtPIP5K6* after its closest Arabidopsis relative, AtPIP5K6. The newly identified *NtPIP5K6* was classified as a type B PI4P 5-kinase and overexpression of *NtPIP5K6* also resulted in a secretion phenotype. Sequence identity between AtPIP5K6 and NtPIP5K6 is 66 % and higher than the sequence identity between, for example, AtPIP5K6 and AtPIP5K4 (62.5 %)/AtPIP5K5 (63 %) (Stenzel *et al.* 2012), which are also highly expressed in pollen and important for the development of pollen tubes (Ischebeck *et al.* 2008).

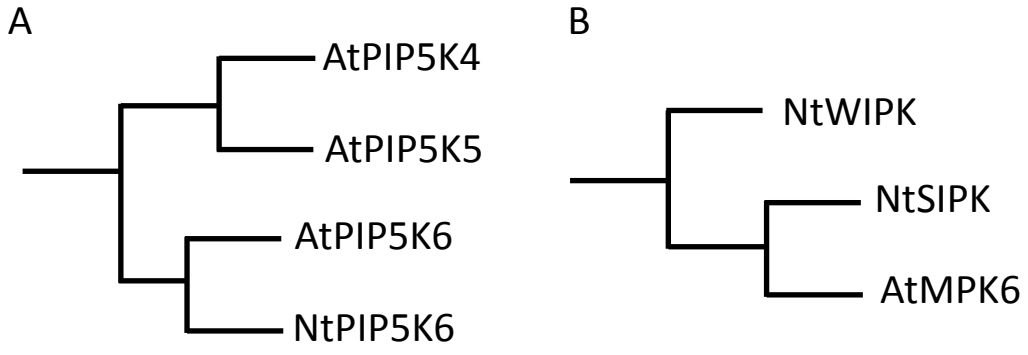

Figure 3.13.: Phylogenetic tree of AtPIP5K6 and MPK6-homologs in *N. tabacum*. A, *Arabidopsis* AtPIP5K4, AtPIP5K5 and AtPIP5K6 are very similar in sequence. Although AtPIP5K6 and NtPIP5K6 are heterologs, they show higher sequence similarity than AtPIP5K6 and any PI4P 5-kinase from *Arabidopsis* (modified, Stenzel *et al.* 2012). B, The homolog proteins of MPK6 in tobacco are salicylic acid-induced protein kinase (SIPK) and the wound-induced protein kinase (WIPK). Dendrogram modified from Zhang *et al.* 2013.

3.5.2 *In vitro* phosphorylation of purified recombinant MBP-PIP5K6 by a protein extract prepared from tobacco pollen

To test whether recombinantly expressed NtPIP5K6 is phosphorylated by kinase activity of tobacco pollen tube extract, NtPIP5K6 was incubated with pollen tube extract (for detailed description see section 2.14). NtPI5K6 does not exhibit autophosphorylation activity (Fig. 3.14). When co-incubated with pollen tube extract and γ-[^{33}P]-ATP for 30 min, NtPIP5K6 becomes phosphorylated by endogenous protein kinases from the extract which was also observed for AtPIP5K6 (see section 3.2).

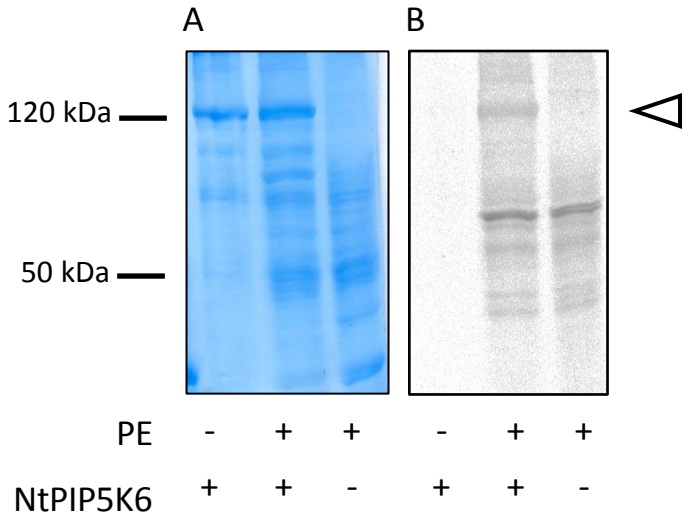

Figure 3.14: Recombinant MBP-NtPIP5K6 is phosphorylated by an extract prepared from tobacco pollen tubes. Recombinant MBP-NtPIP5K6 was incubated with (+) or without (-) pollen tube extract (PE) for 30 min at 22 °C. Proteins were incubated with γ- [^{33}P]-ATP and separated by SDS-PAGE (A). Phosphorylated bands were visualised by a phosphorimager (B). In the first lane MBP-NtPIP5K6 is incubated in the presence of γ-[^{33}P]-ATP. In the second lane MBP-NtPIP5K6 was co-incubated with PE and γ-[^{33}P]-ATP. The last lane shows pollen tube extract autophosphorylation pattern. The white arrowhead indicates the size of the MBP-NtPIP5K6 fusion protein. The gel was dried and exposed for 2 d to a phosphor imager screen. The experiment was performed three times with comparable results.

Similarly to the results obtained for AtPIP5K6, NtPIP5K6 was phosphorylated by protein kinase activity from pollen tube extract. To determine whether NtPIP5K6 is regulated by MAP-kinase activity, as it was observed for AtPIP5K6, a suitable tobacco homolog of MPK6 was chosen and tested in the following sections.

3.5.3 NtSIPK is a close homolog of MPK6

MAP-kinase signalling is a conserved signalling mechanism in all eukaryotes. Two tobacco genes coding for MAP-kinases in tobacco were previously identified by Zhang and Klessig (Zhang and Klessig 1997; 1998): salicylic acid-induced protein kinase (*SIPK*) and wound-induced protein kinase (*WIPK*). *SIPK*, similar to *MPK6*, belongs to the A2 subgroup of MAP-kinases,

whereas *WIPK* belongs to subgroup A1 (MAPK Group, 2002, Fig., 3.13). WIPK activity is regulated on the mRNA level after wounding (Zhang and Klessig 1997). SIPK activity was observed to be directly modulated by fungal elicitors and has been designated a tobacco ortholog of MPK6 (Zhang and Klessig 1998). For this reason, *NtSIPK* was cloned and used to analyse if the findings presented in chapter 3.4 for MPK6 and AtPIP5K6 could be confirmed for their tobacco homologs, NtSIPK and NtPIP5K6.

3.5.4 Protein-protein interaction between salicylic acid-induced protein kinase (SIPK) and NtPIP5K6

To test whether NtPIP5K6 and SIPK proteins interact, as observed for their Arabidopsis homologs, a SUS assay was performed. The coding sequences of *NtPIP5K6* and *NtSIPK* were cloned in the corresponding bait and prey vectors as described in section 2.12.2.

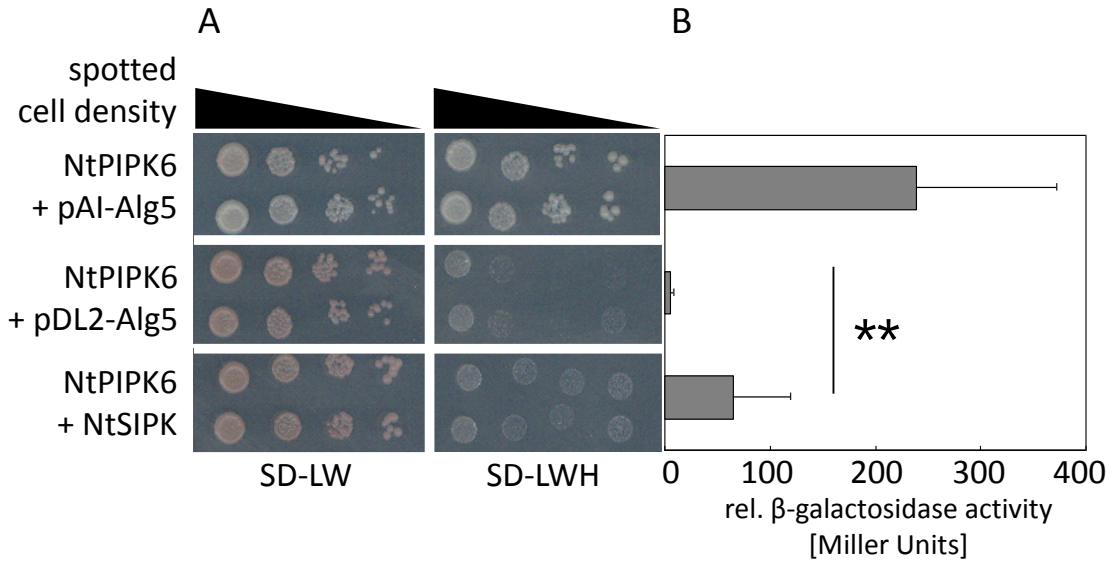

Figure 3.15: NtPIP5K6 and NtSIPK interact in a SUS assay. Yeast strain NMY51 was transformed with pBT3C-*OST4-NtPIP5K6* as bait and pAI-*Alg5*, pDL2-*Alg5* and pPR3N-*NtSIPK* as prey-plasmids. A, the pBT3C-*OST4-NtPIP5K6* and pPR3N plasmids each bear an auxotrophy selection gene for L and W respectively to control for transformation efficiency and success. For each transformation two individual clones were diluted from OD_{600} 1, 0.5, 0.05 and 0.005 from left to right. Dilutions were plated on SD plates lacking L and W to control for transformation of bait and prey plasmids SD-LW). The interaction of the clones was tested on selection for the histidine auxotrophy marker (SD-LWH). B, ONPG-test in Miller Units. Both experiments were performed in triplicates. B is the mean of three individual experiments. Error bars resemble the standard deviation, which was calculated based on the entire value population. For statistical analysis a two-tailed t-test was performed. Significance levels are $\rho < 0.05$ (*), $\rho < 0.01$ (**), and $\rho < 0.001$ (***).

The uniform growth of all yeast clones on SD-LW showed that all three vector combinations were successfully transformed and equal amount of cells were plated (Fig. 3.15 A, left). Growth was observed in all dilutions from OD_{600}=1 until 0.005. The test for interaction was performed

on SD-LWH (Fig. 3.15, right). The positive control showed growth until an OD_{600} of 0.005. In the ONPG-test a relative β-galactosidase-activity of 100 Miller Units was measured. The negative control showed weak basal growth clearly visible until an OD_{600} of 0.05. The ONPG-test showed a relative β-galactosidase activity of 1 Miller Units. Yeast transformed with *NtPIP5K6* and *NtSIPK* showed weak growth until an OD_{600} of 0.005. Importantly, the result of the ONPG-assay of approximately 70 Miller Units was significantly higher compared to the negative control. The data indicate a weak interaction of NtSIPK with NtPIP5K6.

3.5.5 MPK6 phosphorylates NtPIP5K6 *in vitro*

The results from the sections above support that NtPIP5K6 interacts with NtSIPK, similar to the observation for AtPIP5K6 and MPK6 made in section 3.4.2. Under physiological conditions, NtSIPK is phosphorylated and simultaneously activated by MEK2, a MAPKK. It was attempted in this work to activate recombinantly expressed NtSIPK with recombinantly expressed MPK2 *in vitro* but, failed to obtain activated NtSIPK protein (data not shown). Therefore an *in vitro* kinase assay, described in section 2.14, was performed with activated MPK6 protein from Arabidopsis (Fig. 3.16) to support the hypothesis, that NtPIP5K6 is a putative substrate of MAP-kinase signaling,

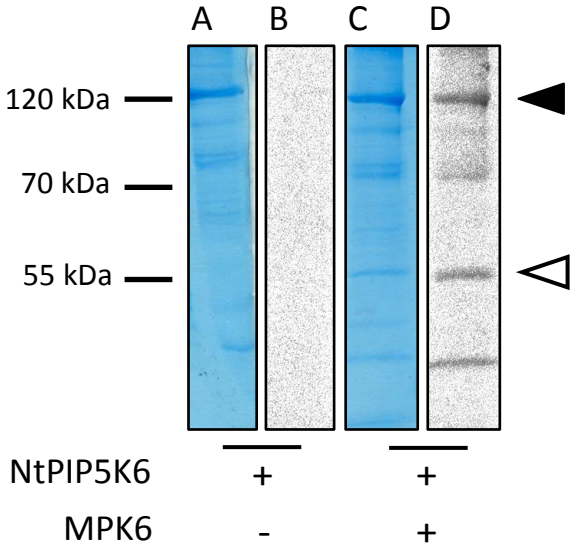

Figure 3.16: Recombinant MBP-NtPIP5K6 is phosphorylated by activated MPK6. Recombinant MBP-NtPIP5K6 was incubated with γ-[^{33}P]-ATP with (+) or without (-) activated MPK6 for 30 min at 22 °C. Proteins were separated by SDS-PAGE and phosphorylated bands were visualised by phosphorimager technologie. A and C show the Coomassie-stained loading controls, B and D show the corresponding phosphorimages. A and B show the autophosphorylation control of MBP-*Nt*PIP5K6. C and D show MBP-*Nt*PIP5K6 phosphorylation. The white arrowhead indicates the size of MPK6; the black arrow head indicate the full length MBP-NtPIP5K6 fusion protein. The gels were dried and exposed for 3 d to a phosphor imager screen. The experiment was performed three times with comparable results.

Similarly to AtPIP5K6, NtPIP5K6 does not show autophosphorylation (Fig. 3.16, lane A and B). When recombinantly expressed MBP-NtPIP5K6 protein was incubated in the presence of activated MPK6 protein, full-length MBP-NtPIP5K6 protein with a size of 120 kDa as well as a protein fragment of ~70 kDa are phosphorylated. A control for MBP phosphorylation was also performed (data shown in section 3.4.4) and excludes phosphorylation of the solubility tag. Taken together, NtPIP5K6 interacts with NtSIPK *in vitro* and becomes phosphorylated by MPK6, consistent with the results obtained for AtPIP5K6 and MPK6.

3.5.6 Co-expression of NtSIPK with NtPIP5K6 inhibits effects of NtPIP5K6 *in vivo*

So far, selected experiments performed with NtPIP5K6 and NtSIPK support the observation that the enzymes are functionally linked, as it was observed for the Arabidopsis homologs. Another important aspect to address was the verification of possible inhibitory effects of phosphorylation on PI4P 5-kinase function using the homologous tobacco enzymes NtSIPK and NtPIP5K6 *in vivo*. NtPIP5K6 localizes at the apical PM of growing pollen tubes (Stenzel *et al.* 2012), whereas NtSIPK is localized predominantly in the nucleus (Dahan *et al.* 2009; Hoser *et al.* 2013).

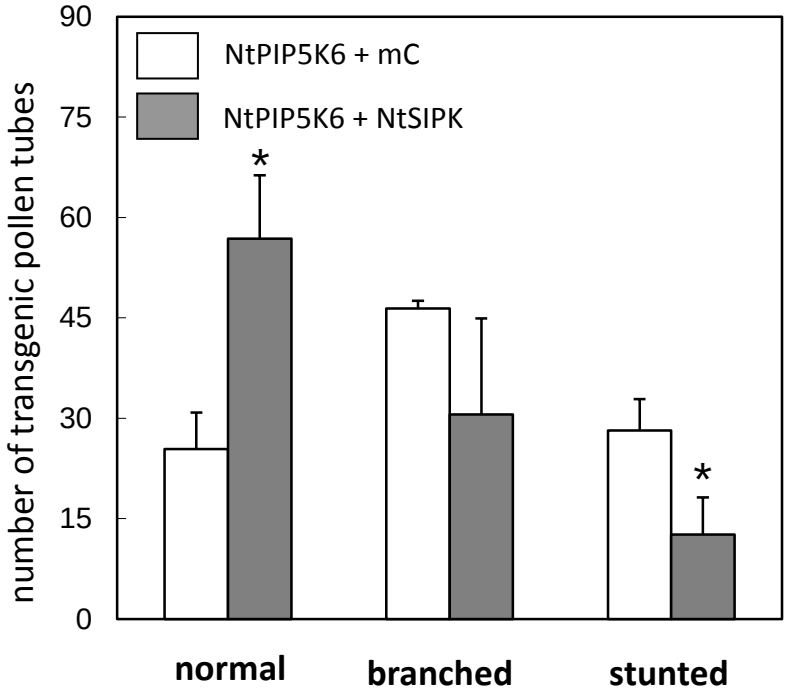

Figure 3.17: Phenotypic distribution of pollen tube morphologics. The values show the distribution of phenotypes upon transient overexpression of NtPIP5K6 with mCherry (white) and AtPIP5K6 with NtSIPK (grey) expressed as numbers, in tobacco pollen tubes. Pollen were grown for 7-9h. The data is the result of three individual experiments. For each experiment 100 pollen tubes were scored. Error bars resemble the standard deviation, which was calculated based on the entire value population. For statistical analysis a two-tailed t-test was performed. Significance levels are $\rho < 0.05$ (*), $\rho < 0.01$ (**), and $\rho < 0.001$ (***).

The incidence of NtPIP5K6 overexpression phenotypes was assessed upon co-expression of the enzyme with either an mCherry control or with NtSIPK (Fig. 3.17). The phenotypic distribution for NtPIP5K6 co-expressed with mCherry showed a similar amount of normal and stunted pollen tubes, while the majority of pollen tubes were in the branched category (Fig. 3.17, white bars). Upon co-bombardment of NtPIP5K6 with NtSIPK, the distribution strongly shifted and the number of tubes displaying normal growth was increased by ~60 % (ρ=0,015), with the number of overall altered tubes decreased (Fig. 3.17, grey bars). This change was found to be statistically significant based on a two tailed student's t-test. The portion of branched pollen tubes was diminished by ~30 % and the number of stunted pollen tubes reduced by 50 % (ρ=0.038). Overall this pattern indicates a shift towards attenuated effects of NtPIP5K6 overexpression upon co-expression with NtSIPK. This observation confirms the findings presented in figure 3.12 for Arabidopsis MPK6 and AtPIP5K6 using homolog tobacco enzymes in tobacco pollen tubes.

3.5.7 Effects of NtPIP5K6 overexpression on the growth of pollen tubes of tobacco plants with reduced NtSIPK expression

The data so far indicate that MPK6 and NtSIPK phosphorylate and thereby inhibit PIP5K6 isoforms from Arabidopsis and tobacco, respectively, and that this inhibition has effects on the performance of PIP5K6 *in vivo*. If the reduced effect of PIP5K6 overexpression in the pollen tubes co-expressing the MAPKs was really due to a functional effect of the MAPKs on their PIP5K6 substrates, than – reciprocally – reduced MAPK expression should result in enhanced effects of PIP5K6. In 2007, Seo and coworkers generated plants with RNAi constructs against *SIPK* and *WIPK*, two MAPKs with high sequence identity (Seo *et al.* 2007). The reduction of SIPK and WIPK led to an altered pathogen response, but data on the phosphoprotein profile were not collected. The RNAi transgenics were kindly provided by Dr. Shinpei Katou (National Institute of Agrobiological Sciences, Tsukuba, Ibaraki, Japan) to serve as a genetic background to test the hypothesis that inhibition of MAPK-activity might enhance PI4P 5-kinase effects *in vivo.* Fluorescence-tagged NtPIP5K6 was transiently expressed in pollen of *SIPK/WIPK* RNAi plants and the incidence of morphological changes to pollen tubes was monitored. Pollen from plants holding only the empty RNAi vctor, but not expressing a RNAi construct, were used as controls (Fig. 3.18).

The distribution of pollen tube phenotypes upon overexpression of NtPIP5K6 in the vector control (Fig. 3.18, white bars) was similar to that observed for pollen expressing NtPIP5K6 in the wild type background (Fig. 3.17): Pollen tubes exhibiting the branched phenotype were

most abundant with ~55 % and stunted pollen tubes represented ~30 % of observed cells. The remaining ~15 % were pollen tubes that did not show a distinct phenotype. In contrast, when NtPIP5K6 was overexpressed in either of the two RNAi lines, there was a statistically significant decrease of ~25 % (WS2 ρ=0,017, WS3 ρ=0,012) in the number of branched pollen tubes concomitant with an increased number of stunted pollen tubes by ~10 % in WS2 (ρ=0,032) and even ~25 % in WS3 (ρ=0,004). Both changes were significant compared to the vector control. The drop in the number of branched pollen tubes and the concurrent increase of stunted pollen tubes indicates enhanced functionality of NtPIP5K6 in the pollen tubes with reduced levels of SIPK and WIPK.

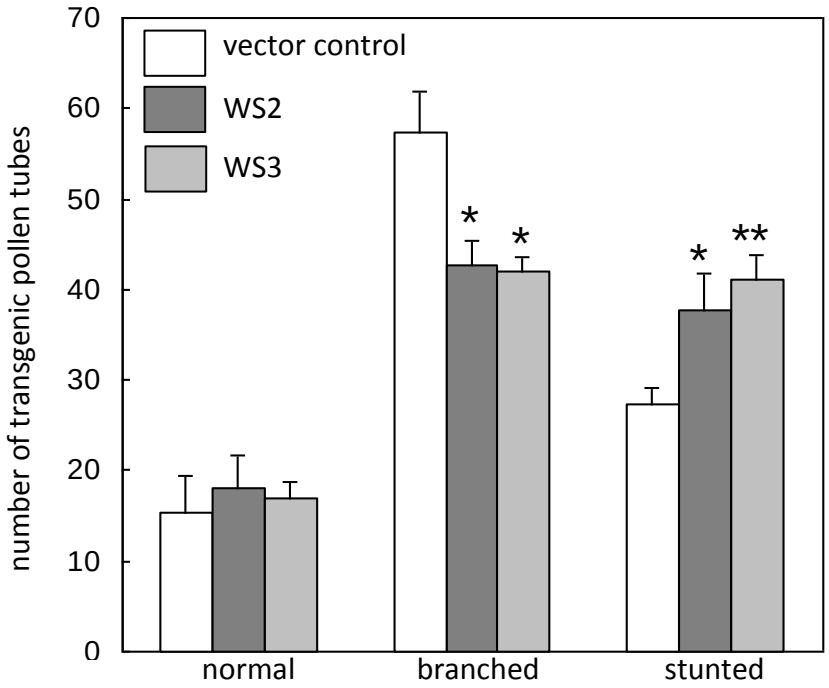

Figure 3.18: Phenotypic distribution of pollen tube morphologies NtPIP5K6 overexpression in *wipk/sipk* RNAi lines. Pollen from tobacco plants modified with an empty vector and two individual *wipk/sipk* (WS2, WS3) RNAi-lines were transiently transformed with *lat52::mCherry* and *lat52::NtPIP5K6-EYFP*. The values show the distribution of overexpression phenotypes. The vector control is depicted in white and the two RNAi-lines in dark and light grey, respectively. The data is the result of three individual experiments. For each experiment 100 pollen tubes were scored. Error bars resemble the standard deviation, which was calculated based on the entire value population. For statistical analysis a two-tailed t-test was performed. Significance levels are ρ <0.05 (*), ρ <0.01 (**), and ρ <0.001 (***).

3.6 A new link between CPK11 signaling and AtPIP5K6 function

Besides MPK6, another protein kinase, CPK11, was identified in the in-gel kinase-assay (Fig. 3.4) as a candidate from pollen extract capable of phophorylating AtPIP5K6. CPK11 has previously been characterized by Zhao and coworkers as a negative regulator of pollen tube growth (Zhao *et al.* 2013). Furthermore, together with CPK24, CPK11 indirectly modulates the shaker-type pollen inward K^+ (SPIK)-channel. A number of CDPKs were identified that affect pollen tube growth by the modulation of ion channels (Gutermuth *et al.* 2013; Myers *et al.* 2009). This observation is particular interesting, because it is known that PtdIns(4,5P)$_2$ can also activate and modulate shaker-type K^+ channels (Liu *et al.* 2005). The first test for a functional connection was the test for *in vivo* localisation of both proteins.

3.6.1 Subcellular localisation of CPK11

To test the subcellular localization of CPK11 and AtPIP5K6 in relation to each other, *CPK11-mCherry* was fused to *mCherry* and *AtPIP5K6-EYFP* were transiently expressed in tobacco pollen tubes (Fig 3.19).

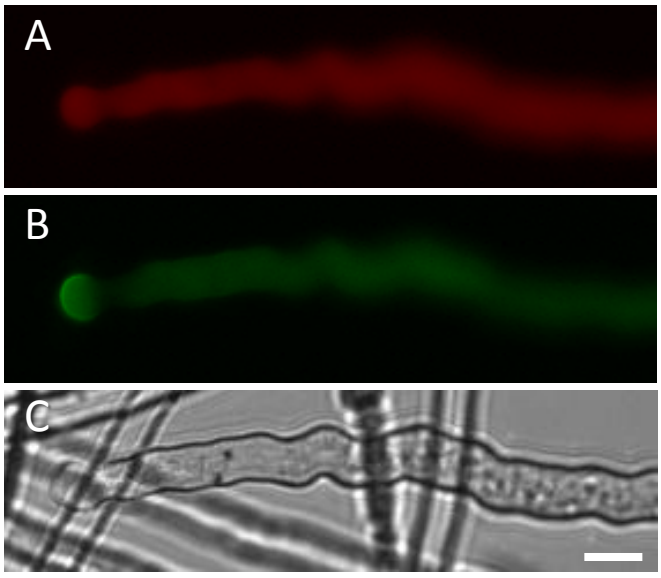

Figure 3.19: Subcellular localization AtPIP5K6-EYFP and CPK11-mCherry fusion proteins. Transient transformation of tobacco pollen tubes with lat52:CPK11-mC and lat52:AtPIP5K6-EYFP. A, Subcellular localization of CPK11-mCherry. B, Subcellular localization of AtPIP5K6-EYFP. C, Bright field image. Bar = 10 µm.

Both protein fusions, CPK11-mCherry and AtPIP5K6-EYFP, showed distinct localization of the proteins *in vivo*. CPK11-mCherry was observed in the cytosol of pollen tubes (Fig. 3.19 A). This confirmed the observations made by Gutermuth and coworkers (Gutermuth *et al.* 2013). In contrast, AtPIP5K6-EYFP localized to the cytosol and the apical PM (Fig. 3.19 B), which has

been previously reported for AtPIP5K6 (Zhao *et al.* 2010) and other PI4P 5-kinases (Ischebeck *et al.* 2008; Ischebeck *et al.* 2011; Ischebeck *et al.* 2010b; Sousa *et al.* 2008). The localization studies revealed that CPK11 and AtPIP5K6 showed a defined localization *in vivo* and overlap in their cytosolic localization.

3.6.2 Protein-protein interaction between CPK11 and AtPIP5K6

Based on the information gained from the localization studies of CPK11 and AtPIP5K6 a protein-protein interaction between the proteins appears possible within the cytosol or/and at the interface between PM and cytosol. A SUS assay was performed to test for physical interaction of CPK11 and AtPIP5K6. The coding sequences *CPK11* of *AtPIP5K6* were cloned in the corresponding bait and prey vectors as described in more detail in section 2.17 and 3.4.2. Yeast was transformed and selected on the appropriate media for interaction between the two protein partners (Fig. 3.20).

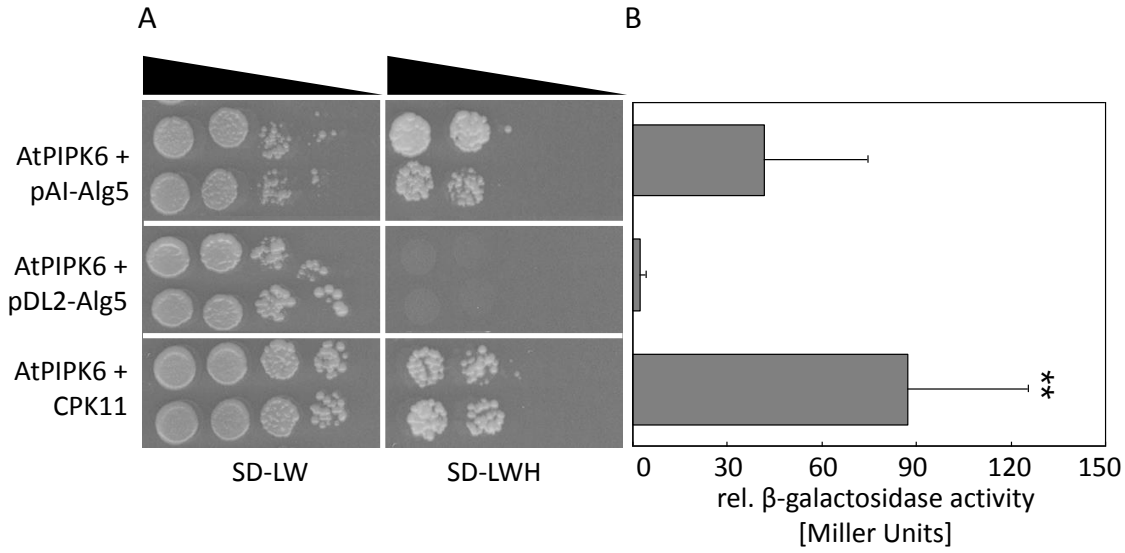

Figure 3.20: AtPIP5K6 and CPK11 interact in a SUS assay. Yeast strain *NMY51* was transformed with pBT3C-*OST4-AtPIP5K6* as bait and pAI-*Alg5*, pDL2-*Alg5* and pPR3N-*CPK11* as prey-plasmids. A, the pBT3C-*OST4-AtPIP5K6* and pPR3N plasmids each bear an auxotrophy selection gene for L and W respectively to control for transformation efficiency and success. For each transformation two individual clones were diluted from OD_{600} 1, 0.1, 0.01 and 0.001 from left to right. Dilutions were plated on SD plates lacking L and W to control for transformation of bait and prey plasmids SD-LW). The interaction of the clones was tested on selection for the histidine auxotrophy marker (SD-LWH). B, ONPG-test in Miller Units. Both experiments were performed in triplicates. B is the mean of three individual experiments. Error bars resemble the standard deviation, which was calculated based on the entire value population. For statistical analysis a two-tailed t-test was performed. Significance levels are $\rho < 0.05$ (*), $\rho < 0.01$ (**), and $\rho < 0.001$ (***).

The uniform growth of all yeast clones on SD-LW showed that all three vector combinations were successfully transformed and equal amount of cells were plated (Fig. 3.20 A, left). Growth was observed in all dilutions from OD_{600}=1 until 0.001. The test for interaction was performed on SD-LWH (Fig. 3.20, right). The positive control showed growth until an OD_{600} of 0.01. In the ONPG-test a relative β-galactosidase-activity of ~45 Miller Units was measured. The negative control showed no growth. This is underlined by the results of the ONPG-test that showed a relative β-galactosidase activity of 1 Miller Units. Yeast transformed with AtPIP5K6 and CPK11 showed strong growth until an OD_{600} of 0.01. Importantly, the result of the ONPG-assay of approximately 90 Miller Units was significantly higher compared to the negative control. The data indicate an interaction of CPK11 with AtPIP5K6.

3.6.3 CPK11 and AtPIP5K6 interact at the apical PM of pollen tubes

The results of the experiments described in the sections above support the finding that there is a possible functional connection between CPK11 and AtPIP5K6, which was underlined by the physical interaction of the proteins in the SUS assay. To verify this interaction under physiological conditions *in vivo*, a split-YFP test was performed (Fig. 3.21, see detailed description in sections 2.17 and 3.4.3). Expression of AtPIP5K6-YFP^N together with CPK11-YFP^C gave a YFP-signal in 75 % (n= 8) of the observed pollen tubes. Expression of AtPIP5K6-YFP^N together with YFP^C gave a very low YFP-signal in 10 % (n=10) observed pollen tubes. CPK11-YFP^C expressed together with YFP^N gave a weak cytosolic YFP-signal in 30 % (n= 9) of the observed cells. In contrast to the low background fluorescence observed for the negative controls, the fluorescence observed for the co-expression of AtPIP5K6 and CPK11 was restricted to the apical PM of the pollen tube. Positive transformants were identified in all cases by the red fluorescence of an expressed mCherry protein, which displayed equivalent florescence intensities in all cases (Fig. 3.21). The split-YFP experiments are consistent with the SUS data and support an interaction between AtPIP5K6 and CPK11 at the apical PM of pollen tubes.

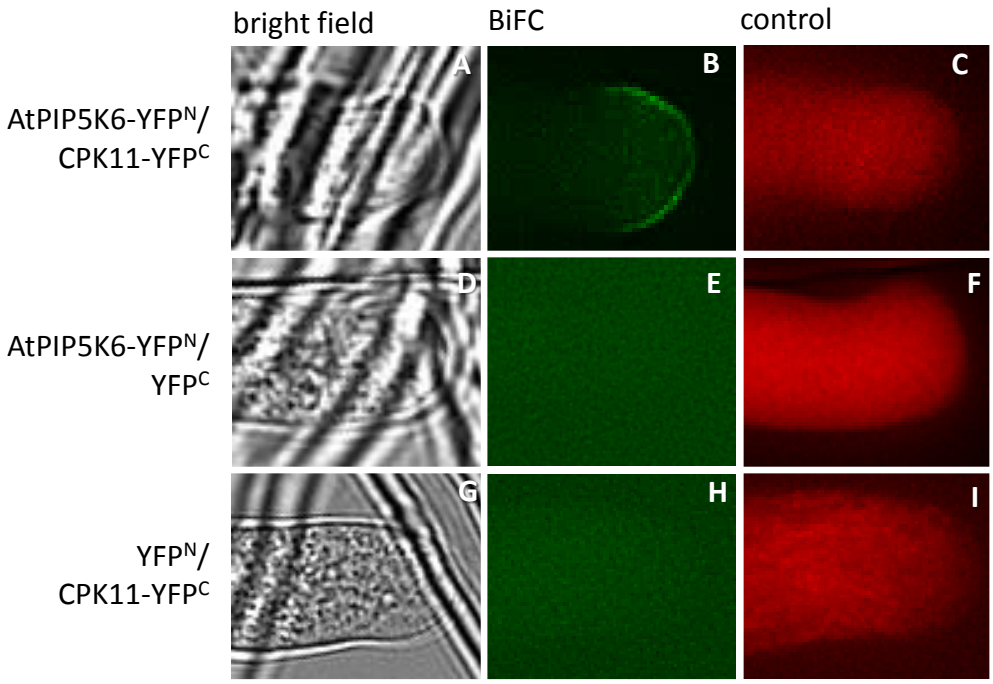

Figure 3.21: AtPIP5K6 and CPK11 interact in a BiFC assay in tobacco pollen tubes. The *lat52::mCherry*, *35S:YFP^N*, *35S:YFP^C*, *35S:AtPIP5K6-YFP^N* and *35S:CPK11-YFP^C* constructs were transiently transformed in tobacco pollen via particle bombardment. Pollen was germinated for 14h. Fluorescence of the proteins was detected by epifluorescence microscopy. A, D and G show bright field images of the corresponding pollen tubes. Epifluorescence from the interaction between the YFP^N-fusion of AtPIP5K6 and the YFP^C-fusion of CPK11 was observed at the apical PM (B). A YFP^N-fusion of AtPIP5K6 was co-expressed with YFP^C and is shown as a negative control for AtPIP5K6 (E). A YFP^C-fusion of CPK11 was co-expressed with YFP^N and used as a negative control for CPK11 (H). *Lat52:mCherry* was co-expressed with all combinations to identify transformed cells (C, F, I). This experiment was performed three times with comparable results.

3.6.4 CPK11 phosphorylates Arabidopsis PIPKs *in vitro*

From the experiments performed so far, CPK11 emerges as a candidate for a protein kinase possibly responsible for phosphorylating AtPIP5K6 in pollen tubes.

While the correct localization in pollen tubes and the physical interaction of the partner proteins are relevant prerequisites for their functional interplay, next it was tested whether recombinant CPK11 would specifically phosphorylate AtPIP5K6 or other PI4P 5-kinases *in vitro*. In *in vitro* kinase assays the ability of CPK11 from bacterial crude extract to phosphorylate four different recombinant expressed *Arabidopsis* PI4P 5-kinases was examined. In contrast to MPK, CPK11 is a calcium-dependent protein kinase, therefore the kinase assays were performed in the presence of calcium. Please note that the assay conditions are different from those for MPK6. The kinase reactions were initiated by the addition of 20 µM ATP containing 10 µCi ^{33}P-labeled ATP and the addition of 0.55 mM $CaCl_2$. After 30 min of incubation, the proteins were separated by SDS-PAGE and the ^{33}P-incorperation was visualized by phosphor imaging. As a

control, PI4P 5-kinases were subjected to an autophosphorylation test (Fig. 3.22 A and C). Fig. 3.22 shows the Coomassie-stained gels (A and B) as a loading control and the corresponding autoradiographs (C and D). Autophosphorylation was only detected for AtPIP5K3, as was already described by Dr. Jennifer Lerche (Dissertation 2013, unpublished data).

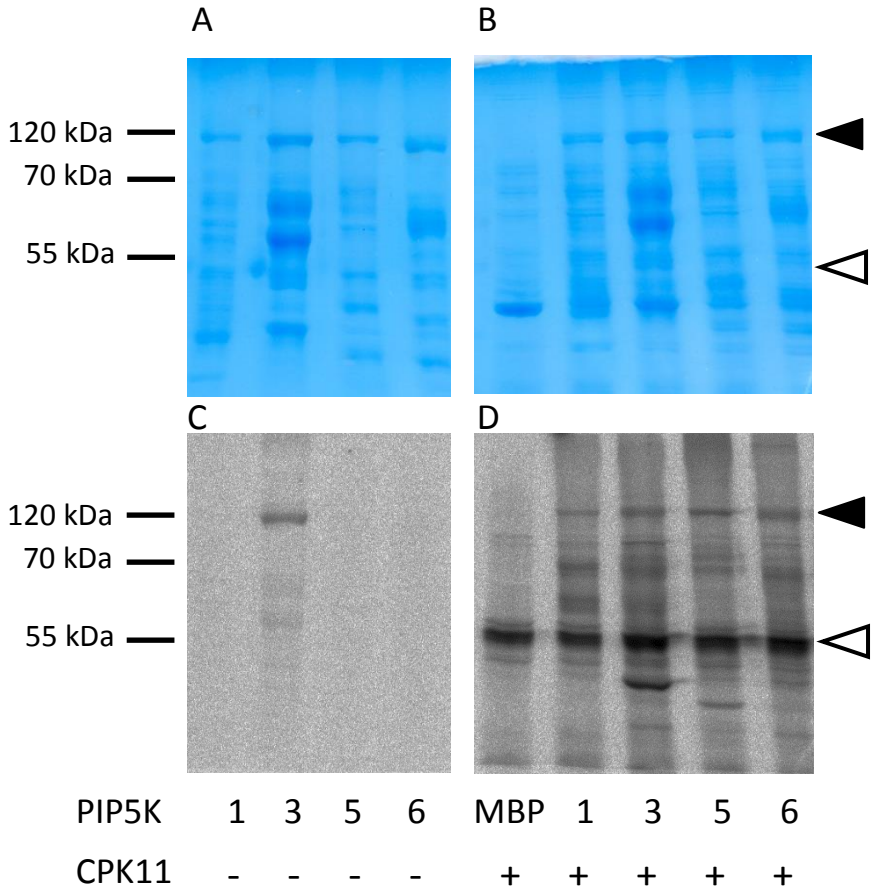

Figure 3.22: CPK11 phosphorylates AtPIP5Ks in an *in vitro* kinase assay. Recombinant MPB-AtPIP5K1, MBP-AtPIP5K3, MBP-AtPIP5K5 and MBP-AtPIP5K6 were incubated with γ-[^{33}P]-ATP (A, C) to test for protein autophosphorylation. Recombinant MBP, MPB-AtPIP5K1, MBP-AtPIP5K3, MBP-AtPIP5K5 and MBP-AtPIP5K6 was tested together with γ-[^{33}P]-ATP for CPK11 mediated phosphorylation (B, D). Proteins were incubated for 30 min at room temperature in the presence of 0.55 mM $CaCl_2$, separated by SDS-PAGE and exposed to a phosphorimager screen. The upper part represents the Coomassie-stained gels (A and B); the phosphor images (C and D) are shown in the lower part of the figure. The black arrowhead indicates the sizes of full length MBP-PIP5K proteins. The white arrowhead marks the autophosphorylated CPK11. The gels were dried and exposed for 4 d to a phosphor imager screen. This experiment was performed three times with comparable results.

Upon incubation with CPK11 from *E. coli* crude extract, all PI4P 5-kinases included in the assay become phosphorylated. The phosphorylated bands appearing from the sample where MBP was co-incubated with CPK11 crude extract, show phosphorylated bands with a protein size of ~100 kDa and ~55 kDa, but no phosphorylated band at 40 kDa, the size of MBP. AtPIP5K1, AtPIP5K3, AtPIP5K5 and AtPIP5K6 show a phosphor signal at around 120 kDa, according to the

size of the full length MBP-fusion protein (Fig 3.22 D). Furthermore, all protein fusions of minor size (premature translational break-down) visible by Coomassie-staining in the loading control were phosphorylated by CPK11 *in vitro*. To test whether or not phosphorylation of Arabidopsis PI4P 5-kinases is calcium dependent, a similar kinase assay was performed for AtPIP5K6 in the absence of calcium and with the catalytic inactive variant CPK11 D150A (DN) to exclude protein kinase activity from the *E. coli* extract (Fig. 3.23).

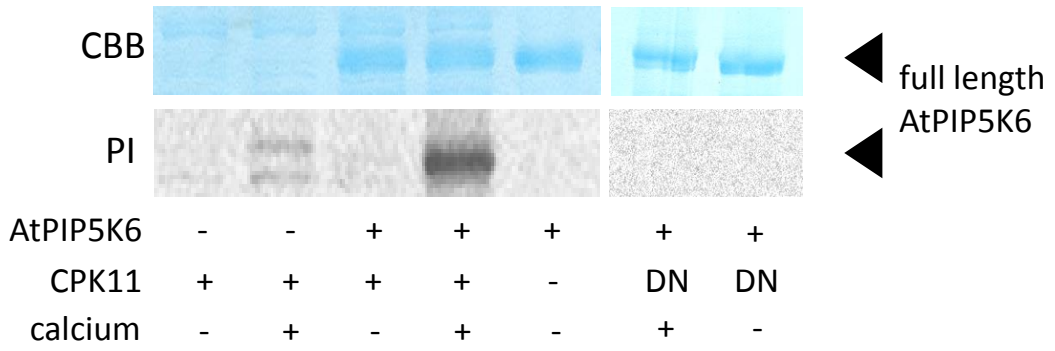

Figure 3.23: CPK11 phosphorylates AtPIP5K6 in a calcium-dependent way. Recombinant MPB-AtPIP5K6, was incubated with γ-[^{33}P]-ATP in the present and absence of calcium for 30 min at room temperature to test for protein phosphorylation. Proteins were separated by SDS-PAGE and exposed to a phosphorimager screen. MBP-AtPIP5K6 was tested together CPK11 and a dominant negative (DN, D150A) variant of CPK11, to test for calcium-dependency. The upper part represents the Coomassie-stained gels; the phosphor images are shown in the lower part of the figure. The gels were dried and exposed for 2 d to a phosphor imager screen. This experiment was performed twice with comparable results.

In the presence of calcium, CPK11 showed two weak autophosphorylation bands at sizes of ~110 and ~130 kDa, which are probably caused by aggregation of the auto activated protein (Fig. 3.23, lane two). These bands are absent when CPK11 was incubated in the absence of calcium, confirming that calcium is necessary for auto activation of the enzyme (Fig. 3.23, lane one). AtPIP5K6 was phosphorylated by CPK11 in the presence of calcium, but not in the absence of calcium (Fig. 3.23, lane three and four). The incubation of AtPIP5K6 with a catalytic inactive variant in the presence and absence of calcium did not lead to phosphorylated protein, suggesting that the phosphorylation of AtPIP5K6 by CPK11 is dependent on activated and catalytically active CPK11 protein.

3.6.5 Analysis of phosphorylation sites by phosphoproteomics

To identify phosphorylation sites within AtPIP5K6, recombinantly expressed AtPIP5K protein was incubated with CPK11 crude extract in the presence of 0.55 mM $CaCl_2$ and 1 mM ATP (see section 2.14) to conduct *in vitro* phosphorylation. To assess relevant phosphorylation sites, the protein mixture was separated by SDS-PAGE and full-length AtPIP5K6 protein was excised. For

mass spectrometric analysis, the protein was digested with trypsin and peptides were desalted (section 2.15). Phosphorylated peptides were identified by a targeted MS-MS analysis, according to the masses of the predicted phosphorylated and non-phosphorylated peptides, in cooperation with Dr. Wolfgang Hoehenwarter (Proteome Analytics, IPB, Halle (Saale)) using HR/AM LC-MS with an Orbitrap Velos Pro System (Thermo Scientific, Dreireich, Germany). See detailed description under section 2.16.

The coverage for AtPIP5K6 was ~60 % and two phosphorylation sites were identified with low confidence. The amino acid residues T604 and S607 were mutagenized to alanine to test if variant AtPIP5K6 protein phosphorylation intensity is altered compared to AtPIP5K6 wild type protein in an *in vitro* protein phosphorylation assay. The experiment did not show any difference in the phosphorylation status of the mutant AtPIP5K6 variants and the phosphorylation site(s) was not confirmed (see appendix Fig. 7.5).

3.6.6 Effects of CPK11 on the catalytic activity of AtPIP5K6 *in vitro*

The data so far establish that CPK11 can phosphorylate AtPIP5K6 *in vitro*, but a possible phosphorylation site was not identified. Nevertheless, the identification of clear phosphorylation bands and the results of the interaction studies point to a functional connection between CPK11 and AtPIP5K6. To investigate if CPK11 has a calcium-dependent influence on AtPIP5K6 activity, both recombinant proteins were pre-incubated together in the presence and absence of calcium and the PI4P 5-kinase activity of the phosphorylated AtPIP5K6 protein, immobilised to MBP-agarose beads, was analysed by monitoring the phosphorylation of the inositol head group of the lipid substrate PtdIns4P in the presence of γ-[^{33}P]-ATP (Fig. 3.24).

During the pre-incubation the MBP-AtPIP5K6 fusion protein should be phosphorylated. This cannot be tested within the same experiment, but the identical setup was used as for all other kinase assays before, where phosphorylation of AtPIP5K6 was observed (Fig. 3.22 and 3.23).

The analysis of the effects of calcium-dependent phosphorylation on PI4P 5-kinases activity is not trivial, because the presence of calcium perturbs the lipid-phosphorylation assay in the presence of 0.55 mM $CaCl_2$, an inhibition of the substrate conversion was observed (see appendix). This complicates interpretation, as effects of calcium and CPK11 may not be distinguished. To enable comparison of AtPIP5K6 activity after incubation with CPK11 in the presence and absence of calcium, a different setup was chosen: AtPIP5K6 immobilised on beads coated with amylose was incubated with CPK11 and calcium in the presence and absence of EGTA, which chelates calcium.

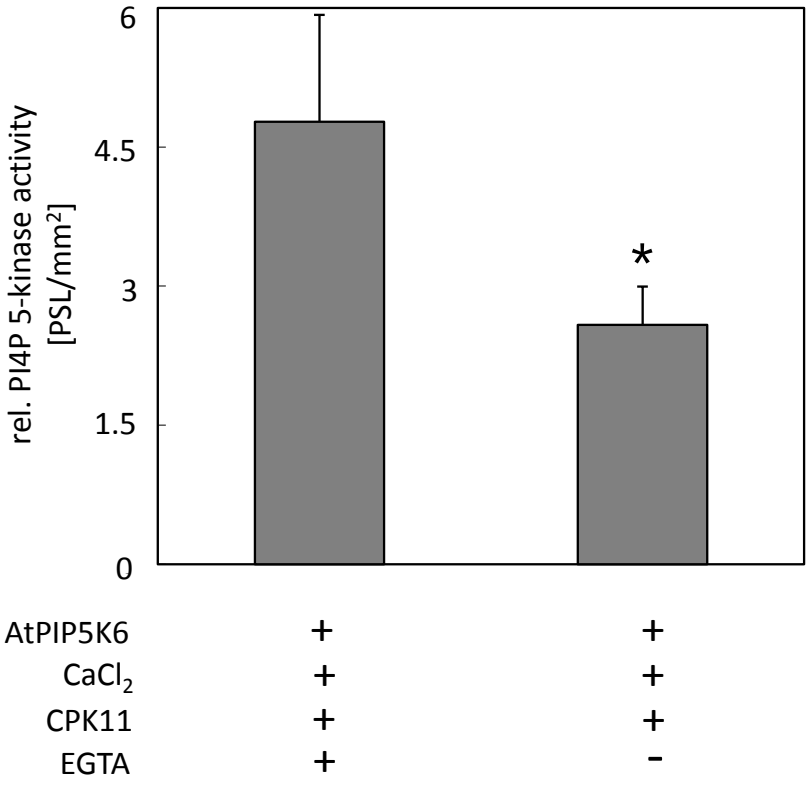

Figure 3.24: CPK11 lowers catalytic activity of AtPIP5K6 *in* vitro in a calcium-dependent way. Recombinant MBP-AtPIP5K6 was immobilised to beads and pre-incubated with and without 1 µg recombinant CPK11 from crude extract and 20 µM ATP, 0.55 mM $CaCl_2$ and 1 mM EGTA for 30 min at 22°C. The such treated MBP-AtPIP5K6 fusion protein was subsequently mixed with PI4P and 10 µCi γ-[^{33}P]-ATP and 1 mM cold ATP for 1h to examine residual PI4P 5-kinase activity. Synthesized PtdIns(4,5)P_2 was isolated by acidic lipid extraction and separated with thin layer chromatography. ^{33}P-incorporation was detected with phosphor image technology and calculated with TINA-software. Error bars resemble the standard deviation, which was calculated based on the entire value population. For statistical analysis a two-tailed t-test was performed. Significance levels are $\rho < 0.05$ (*), $\rho < 0.01$ (**), and $\rho < 0.001$ (***). The experiment was performed twice in triplicates with similar results.

To remove calcium, interfering with the lipid kinase assay, beads were washed and submitted to the lipid kinase assay in a buffer without calcium supply. Using this setup, a significantly higher activity was observed in the presence of EGTA then in the absence of EGTA, indicating a calcium-dependent inhibition of AtPIP5K6 by CPK11.

When CPK11 was activated by calcium during the pre-incubation, the reduction of activity compared to the control with CPK11 and EGTA accounted for 50 % (ρ= 0.031). This drop in activity is statistically significant. Therefore, the inhibitory effect of CPK11 on AtPIP5K6 activity is calcium dependent. Though, phosphoproteomics did not reveal feasible results, the calcium-dependent inhibition of CPK11 on AtPIP5K6 activities points to a changed activity of AtPIP5K6 upon incubation with CPK11 and calcium.

3.6.7 Effects of CPK11 on the functionality of AtPIP5K6 *in vivo*

The data so far demonstrate a clear effect of CPK11 on AtPIP5K6 activity *in vitro*, raising the question whether these observations have relevance for *in vivo* functions of AtPIP5K6 and pollen tube growth. To investigate the influence of CPK11 on AtPIP5K6 *in vivo*, AtPIP5K6-YFP was co-expressed in tobacco pollen tubes either with an mCherry control or with CPK11 fused to mCherry (Fig. 3.25). Upon co-expression of these combinations, the incidence of normal, branched and stunted phenotypes was quantified as it has been described in prior studies for quantitative statements on PI4P 5-kinase function (Ischebeck *et al.* 2010b). The distribution of phenotypes for AtPIP5K6 co-expressed with mCherry is indicated in Fig. 3.25 (white bars). Normal growing pollen tubes usually compromised ~15 % of transformed cells, likely these with low expression levels (Ischebeck *et al.* 2008). The intermediate phenotype, represented by branched pollen tubes, accounted for ~25 %. The residual ~60 % were allocated to the most severe phenotype, stunted tubes with trapped protoplast (Fig 3.25, white bars). The distribution of the phenotypes observed upon co-expression of AtPIP5K6 with CPK11-mCherry changed to a low number of stunted pollen tubes to a high number of branched pollen tubes (Fig 3.25, grey bars). In contrast to the number of normal growing pollen tubes did not differ from the number observed for AtPIP5K6 co-bombarded with mCherry. The number of branched pollen tubes increased by ~50 % ($\rho < 0.001$), compared to the control. Concomitantly, the number of stunted pollen tubes decreased by ~55 % compared to the control. This changes were found to be statistically highly significant based on a two tailed students t-test ($\rho < 0.001$).

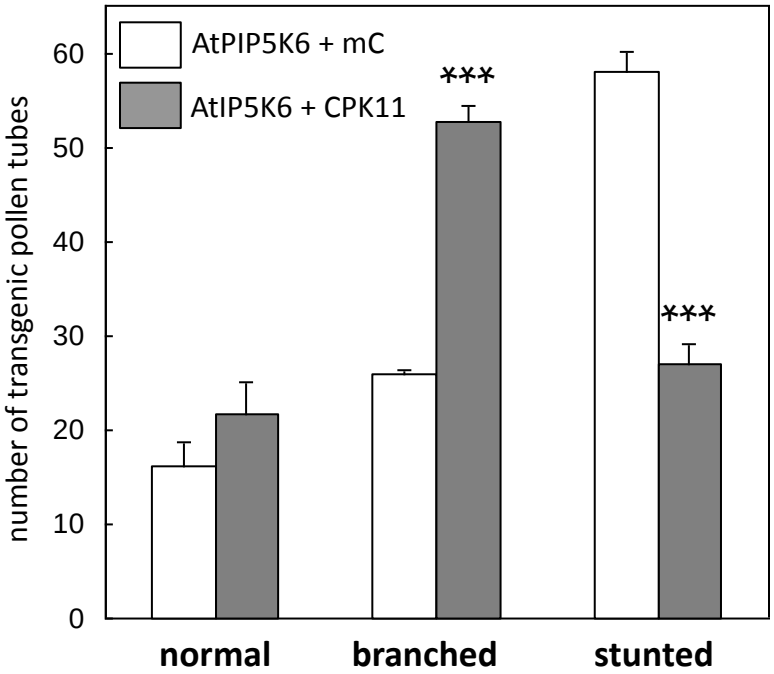

Figure 3.24.: Phenotypic distribution pf pollen tube morphologies upon co-expression of AtPIP5K6 with CPK11. The values show the distribution of phenotypes upon transient overexpression of *lat52::AtPIP5K6-EYFP* with *lat52::mCherry* (white) and *lat52::AtPIP5K6-EYFP* with *lat52:CPK11-mCherry* (grey) expressed as numbers, in tobacco pollen tubes. Pollen was germinated for 6-8 h. The data is the result of three individual experiments. For each experiment 100 pollen tubes were scored. Error bars resemble the standard deviation, which was calculated based on the entire value population. For statistical analysis a two-tailed t-test was performed. Significance levels are $\rho < 0.05$ (*), $\rho < 0.01$ (**) and $\rho < 0.001$ (***).

The data indicate that upon co-expression of AtPIP5K6 and CPK11, there was a significant shift of the phenotypic distribution towards a weaker manifestation of the AtPIP5K6-mediated changes. This observation is consistent with reduced AtPIP5K6-activity upon co-incubation with recombinant, activated CPK11, supporting the notion of an inhibitory effect of CPK11 on AtPIP5K6.

4 Discussion

Phosphorylation as a mechanism of posttranslational modification is a fast and reversible means to modify protein activity, localization and interactions of an enzyme with other proteins. In the context of this thesis, phosphorylation of AtPIP5K6 was observed and MPK6 and CPK11 were identified as responsible protein kinases. Both kinases interact with AtPIP5K6 at the apical PM of growing pollen tubes. Phosphorylation of AtPIP5K6 by either kinase resulted in the inhibition of the catalytic activity *in vitro* and negatively influenced the functionality of AtPIP5K6 *in vivo*. Additionally, two phosphorylation sites that are recognized by MPK6 were identified by MS analysis.

4.1 *In vitro* phosphorylation of AtPIP5K6 by pollen tube extract

In the present work, tobacco pollen was used for the preparation of pollen tube protein extract and transient transformation of pollen tubes. While Arabidopsis is the best characterized model organism for molecular plant science, tobacco pollen tubes are a well-studied model system for the investigation of polar growth. Furthermore, the amounts of pollen necessary for the preparation of a pollen tube extract are easier to obtain from tobacco flowers than from the much smaller Arabidopsis flowers. Arabidopsis and tobacco are closely related and belong to the family of brassicacea. Furthermore, many protein kinase families are evolutionary conserved in eukaryotes and share common structural features.

Previous studies by Westergren and coworkers (Westergren *et al.* 2001) and Dr. Jennifer Lerche (Dissertation 2013, data unpublished) showed that Arabidopsis PI4P 5-kinases AtPIP5K1, AtPIP5K2 and AtPIP5K3 are phosphorylated by a protein extract prepared from Arabidopsis leafs. A similar result was obtained in this thesis when pollen specific AtPIPI5K6 (Fig. 3.3) and its closely related tobacco homolog NtPIP5K6 (Fig. 3.14) were incubated as recombinantly expressed proteins and co-incubated with a protein extract prepared from tobacco pollen tubes. A phosphorylation kinetic showed that the kinase reaction was the fastest in the first five minutes of incubation and then rapidly slowed down (Fig. 3.2). This can be explained by the decreasing availability of the non-phosphorylated substrate protein, the stability of the protein kinases in the presence of ATP or with an increasing action of phosphatases, leading to equilibrium of phosphorylation and dephosphorylation. Furthermore, there could be phosphorylation sites which are easier to access for the kinases responsible and

are therefore phosphorylated faster. Other sites in AtPIP5K6 which are less exposed and thus more difficult to access might be phosphorylated more slowly. Additionally, it is possible that different protein kinases have different affinities for the substrate protein AtPIP5K6, where one acts faster than the other, explaining the difference in phosphate incorporation. The abundance of different protein kinases on protein level in the pollen tube extract might also vary, and a phosphorylation signal from a protein kinase with a high affinity for AtPIP5K6 but low abundance may be similar to that of a protein kinase that is highly abundant, but exhibits only low affinity for AtPIP5K6. In the pollen tube protein extract itself, a number of phosphorylated proteins were observed under our test conditions which probably represent autophosphorylated proteins and proteins that are themselves substrates of endogenous protein kinases from the extract.

Based on the complexity of the pollen tube extract, no assumptions can be drawn about the protein kinases responsible for phosphorylation of AtPIP5K6. One possibility to gain more insight in the nature of the relevant protein kinases would have been the use of different kinase buffer conditions favoring or discriminating specific protein kinase classes. For instance, the use of a chelating agent like EGTA for the chemical reduction of the availability of calcium ions would potentially diminish the kinase activity of calcium-dependent protein kinases. Overall, the experiments using tobacco pollen extract establish that there are protein kinase activities present that are capable of phosphorylating AtPIP5K6 but the specific protein kinase(s) remain(s) unknown.

4.2 Identification of putative upstream protein kinases of AtPIP5K6

To identify putative upstream protein kinases of AtPIP5K6 from the complex tobacco pollen tube protein extract, the in-gel kinase-assay (IGKA) was designed. To date, no endogenous protein kinase was known to interact and/or phosphorylate an Arabidopsis PI4P 5-kinase. The principle of the assay is the phosphorylation of the AtPIP5K6 substrate by protein kinases from the extract. The identification of putative protein kinases was performed according to the size of phosphor signals after the separation of the proteins from pollen tube extract by SDS-PAGE. Protein bands displaying phosphorylation signals in the IGKA (Fig. 3.4) were excised and analyzed by a highly sensitive data independent MS^E approach. The mapping of peptides from tobacco to the Arabidopsis TAIR10 database resulted in the identification of seven candidate protein kinases (Tab. 3.3).

In the denaturing environment of an SDS-PAGE, proteins at least partially unfold and presumably loose activity-relevant cofactors like calcium or magnesium. To anticipate reduced

kinase activity, the reaction mix in the final step of the IGKA contained an excess of calcium and magnesium ions. The phosphorylation of protein kinases by upstream kinases, like it is known for MAPK-kinases, is also a relevant factor for the maintenance of protein kinase activity and was anticipated by the inclusion of potent phosphatase inhibitors during all steps of the assay. Based on the successful phosphorylation, it can be assumed that protein kinases renature during the assay and regain activity. It can, however, not be ruled out that the reactivation is only partial and will not equally occur for all protein kinases in the assay.

The success of the IGKA was first evaluated when the control gel was compared to the gel containing MBP-AtPIP5K6 fusion protein. Phosphobands in the control gel are likely due to protein kinase autophosphorylation, being an indicator for the successful refolding and incorporation of ^{33}P of protein kinase with a size of 45 to 55 kDa. Autophosphorylation has, for instance, been described for calcium-dependent kinases upon calcium-binding (Boudsocq *et al.* 2012). Importantly, when MBP-AtPIP5K6 was copolymerized in the gel, several phosphobands intensified, indicating the introduction of radiolabelled phosphate in the MBP-AtPIP5K6 fusion protein. It is important to note that the experimental setup is valid only for the identification of monomeric protein kinases. Protein kinases that act in complexes, for example the CBLs/CIPKs, can, due to the spatial separation in the IGKA, not lead to a phospho signal under these conditions.

The annotation of precursor ions from the MS^E-analysis to Arabidopsis proteins was performed according to approved requirements (Helm *et al.* 2014) to ensure the annotation of the proteins identified. Additionally, the annotation is supported by the high the sequence similarity of MPK6 and CPK11 and their tobacco orthologs NtSIPK and NtCPK, respectively. Furthermore, the protein sizes of NtSIPK (45 kDa) and NtCPK (56 kDa) are consistent with sizes of the phosphobands detected in the IGKA. Both enzymes are active as monomeric protein kinases. NtSIPK as well as MPK6 are activated by phosphorylation by an MAPKK, therefore activity need to be retained by prevention of phosphatase action. In contrast to that, CDPKs perform auto activation in the presence of calcium, which was supplied in the IGKA.

Generally, IGKAs are mostly used to confirm protein kinase-substrate interactions. In contrast, in this thesis the IGKA approach was adapted to screen for upstream protein kinases, so there is no data available to compare the output of previous investigations with the results obtained in this thesis. Two classes of protein kinases, namely MAPKs and calcium-dependent protein kinases, were identified from the IGKA. The candidate protein kinases MPK6 and CPK11 were chosen for further investigation upon transcription data for pollen and pollen tubes (eFP Browser, Winter *et al.* 2007) as well the evidence from current literature that supported possible interconnections with PI-signaling.

4.3 Verification of MPK6 and AtPIP5K6 protein-protein interaction

The identification of the candidate protein kinase MPK6, opened new avenues of investigation and appears sensible for the control of pollen tube growth. While AtPIP5K6 plays an important role in membrane trafficking and delivery of vesicles loaded with cell wall material in growing pollen tubes (Stenzel *et al.* 2012; Zhao *et al.* 2010), MPK6 seems to influence pollen tube growth rather in a directional way (Guan *et al.* 2014). The subcellular localization of both proteins in the growing pollen tube showed that localization of AtPIP5K6 and MPK6 overlaps in the cytosol, probably increased in the cytosol adjacent to the PM (Fig. 3.5). While AtPIP5K6 is mainly localized to the apical PM (Stenzel *et al.* 2012), MPK6 was predominantly localized to the nucleus, which was already described by (Guan *et al.* 2014). The interaction of AtPIP5K6 and MPK6 was subsequently tested *in vivo* by BiFC-studies in growing pollen tubes and the data suggests that interaction of AtPIP5K6 and MPK6 takes place at the apical PM. The results of other groups with cytosolic substrate proteins of MPK6 showed an YFP-complementation signal mainly in the nucleus and the cytosol (Perez-Salamo *et al.* 2014; Wang *et al.* 2014). The protein-protein interaction of AtPIP5K6 and MPK6 in the SUS was very weak. In other reports yeast-two hybrid analysis of MPK6 revealed strong interaction with its substrates (Pecher *et al.* 2014; Perez-Salamo *et al.* 2014). In contrast to SUS used in this thesis, other studies used a nuclear-based yeast two-hybrid system. Since MPK6 is mainly localized in the nucleus and AtPIP5K6 is anchored to the ER-membrane by an OST4-tag in the SUS, the probability of the encounter of AtPIP5K6 and MPK6 might be suboptimal. Since nuclear transport of Arabidopsis PI4P 5-kinases is not fully understood (personal communication, Dr. Mareike Heilmann, MLU Halle-Wittenberg) and PI4P 5-kinases are primarily PM associated proteins, the use of the nuclear-based yeast two hybrid system is not feasible.

The data presented here indicate that a relevant interaction of MPK6 with AtPIP5K6 take place outside the nucleus. It is possible that MPK6 is recruited to the PM by AtPIP5K6 or by binding of PIs.

4.4 Phosphorylation of AtPIP5K6 by MPK6

The key question at this point was whether the IGKA-based identification of MPK6 as an upstream protein kinase acting on AtPIP5K6 was supported by additional data. Before the work on this project was initiated, no information about phosphorylation of AtPIP5K6 was available. In 2012, Mayank *et al.* analyzed the pollen phosphoproteome and identified two phosphorylation sites within a peptide from AtPIP5K6 containing the amino acid residues T590

and T597 (Mayank *et al.* 2012). These findings were deposited in the Arabidopsis phosphorylation database PhosphAt 4.0 (Heazlewood *et al.* 2008).

The MAPK MPK6 was identified in this work by an IGKA and its activity towards AtPIP5K6 was confirmed by a kinase assay using purified and activated MPK6 protein. The targeted determination of phosphorylation sites introduced to AtPIP5K6 by MPK6 by MS analysis resulted in the identification of two phosphorylation sites, residues T590 and T597 (Tab. 3.7). These residues are located within distinct MAP-kinase recognition motifs, +1 amino acid of a proline residue. Interestingly, peptides containing the above mentioned phosphothreonine residues could only be detected when a minimum of one missed cleavages occurred. The incidence of this incomplete trypsin digestion cannot be estimated with certainty. Compared to the identification of the phosphorylation site T590, the assignment of the second phosphorylation site was more difficult and occurred predominantly in measurements performed with the ablation variant AtPIP5K6 T590A (Tab. 3.7).

Experiments performed in this work revealed that AtPIP5K6 is phosphorylated by an extract prepared from tobacco pollen tubes, leading to the identification of two phosphorylation sites: S588 and T590. The identification of the site T590, which had already been determined before (Mayank *et al.* 2012), showed that protein extract prepared from tobacco pollen tubes contained protein kinase activity equivalent to that in Arabidopsis pollen tubes.

The phosphoablation variants AtPIP5K6 T590A, AtPIP5K5 T597A and AtPIP5K6 T590A T597A were used to confirm the phosphorylation sites identified by MS analysis. Phosphorylation of the single variants AtPIP5K6 T590A and AtPIP5K5 T597A by MPK6 in a kinase assay was reduced by ~60-70%, whereas the double variant AtPIP5K6 T590A T597A showed only residual phosphorylation that accounted for 15 % (Fig. 3.9). Concurrent MS analysis of the variant proteins confirmed these observations. Residual phosphorylation of AtPIP5K6 T590A T597A showed that a phosphorylation site was identified at position T592 which is in proximity to a proline residue (-1 amino acid), but is not part of an MAPK-motif. Additionally, this peptide was, compared to the peptides found for the single variants, only present in low abundance. The residual phosphorylation outside a MAPK-motif points out to unspecific performed transphosphorylation. This reaction might be favored by a high amount of substrate protein in the absence of the initial phosphorylation motifs and argues against a third phosphorylation site. Phosphoablation studies of other MPK6 substrate proteins showed also low residual phosphorylation for MVQ1 with alanine exchanges for all determined phospho sites (Pecher *et al.* 2014), while for another substrate, ERF6, phosphorylation was nearly completely abolished in the total phosphoablation variant (Liu and Zhang 2004).

A partial alignment of all nine type B PI4P 5-kinases and the tobacco homolog NtPIP5K6 shows that the region flanking AtPIP5K6 T590 and T597 is only present in pollen-expressed PIP5Ks:, AtPIP5K5, AtPIP5K6 and NtPIP5K6. In this stretch of the catalytic domain right behind the MDYSL-motif, where aspartate is responsible for substrate conversion as a catalytic base, the amino acid sequence is variable. While the MAPK-motif at position T590 is only present in AtPIP5K6, the motif at position T597 is conserved for all pollen-specific PI4P 5-kinases. The *in silico* analysis of MAPK-motifs within the protein sequence of selected PI4P 5-kinases (Fig 3.5) revealed that PIP5Ks possess between 4-7 MAPK-motifs (Tab. 3.5), of which only two are conserved in all type B kinases. The peptide for the first conserved motif (T402) was included in the sequence coverage by our MS-analysis of AtPIP5K6 and not found to be phosphorylated. The second motif (S420) is situated between arginine and lysine residue and upon cleavage with trypsin a seven amino acid peptide is created which is too small for detection. Still, although specific amino acid sequences can be identified as protein kinase motifs, the single presence of such motifs is no proof for their phosphorylation or physiological relevance.

Figure 4.1: AtPIP5K6 is the only pollen specific PI4P 5-kinase with two MAP-kinase recognition motifs in the catalytic domain. A local alignment of an excerpt of the catalytic domain of all nine type B PI4P 5-kinases. Black areas show identical amino acids. Grey areas show similar amino acids. Open arrowheads indicate the two MAP-kinase motifs of AtPIP5K6, dashed line indicates pollen PI4P 5-kinase specific region.

The kinase assay as well as the mass spectrometric verification of the AtPIP5K6 variants supports the notion, that AtPIP5K6 is a substrate of MPK6 and becomes dually phosphorylated at positions T590 and T597, which are assumed MAPK-motifs. T402, one of the two conserved MAPK-motifs identified in the sequence of AtPIP5K6, was identified as a non-phosphorylated peptide with mass spectrometric analysis. The residual phosphorylation determined in the MPK6 kinase assay with phosphor ablation variants of AtPIP5K6 argue against a third phosphorylation site. It can be concluded that T402 and S420 are inactive MAPK-motifs. The phosphorylation sites identified in this thesis enable the assignment of T590 and T597 as MAPK-motifs and identify MPK6 as the responsible protein kinase *in vitro*. Interestingly, the

determination of T590 and T597 as phosphorylation sites in AtPIP5K6 from Arabidopsis pollen (Mayank *et al.* 2012) suggests that MPK6 may also be responsible for AtPIP5K6 phosphorylation *in vivo*. Thus, it can be concluded that MPK6 is the (or one of several) protein kinase(s) responsible for the phosphorylation of AtPIP5K6 that has previously been reported. Still it cannot be excluded that AtPIP5K6 is a target for other MAPK, for instance MPK3, which also recognizes S/T-residues adjacent to proline.

It can be speculated, if AtPIP5K3 and AtPIP5K5 were also phosphorylated by MPK6 (Fig. 3.8). For AtPIP5K5, the corresponding phosphor image shows a weak signal, compared to the phosphorylation intensity of AtPIP5K6 (Fig. 3.8). This difference might be explained by the presence of only one of the target phosphorylation motifs of MPK6 in AtPIP5K5 (Fig. 4.1). The signal for the root hair specific PI4P 5-kinase AtPIP5K3 was somewhat stronger and, interestingly, MPK6 also plays a role in root hair development (Lopez-Bucio *et al.* 2014). AtPIP5K3 lacks these pollen-specific motifs (Fig. 4.1), but contains additional motifs in the N-terminus of the protein. In future studies the impact of MPK6 on AtPIP5K3 should be further investigated.

4.4.1 Phosphorylation of AtPIP5K6 by MPK6 controls activity

It was shown in this work that AtPIP5K6 is a substrate for MPK6 protein kinase activity and becomes dually phosphorylated at threonine residues within the catalytic domain of AtPIP5K6. The data so far indicate that AtPIP5K6 is phosphorylated by MPK6 and that this phosphorylation also takes place *in vivo*. An *in vitro* activity test determined that MPK6 activity after a 30 min treatment with recombinantly expressed and activated AtPIP5K6 showed ~55 % reduction of activity compared to a control without MPK6 treatment (Fig. 3.10). This effect was not observed when the phosphoablation variant AtPIP5K6 T590A T597A was treated with MPK6 (Fig. 3.11). Together with the data from the MS-analysis, this finding provides evidence that MPK6 inhibits AtPIP5K6 activity by phosphorylation. The concomitant finding that the activity of a variant AtPIP5K6 lacking the relevant phosphorylation sites T590 and T597A was no longer modulated by MPK6, links phosphorylation with the functional effect. This observation fits to the working hypothesis that the introduction of a negative charge, for example phosphorylation, lowers the affinity of a PI4P 5-kinase towards the negatively charged PM by electrostatic interaction and thus substrate conversion is inhibited.

However, this concept is not supported by the presumed orientation of T590 and T597 in the AtPIP5K6 protein (Fig. 4.2). Information about the spatial positioning of the residues T590 and T597 can be gained by a calculated model (Fig. 4.2) based on the on the x-ray crystallography data from HsPIPKIIβ (PDB: 1BO1, Rao *et al.* 1998).

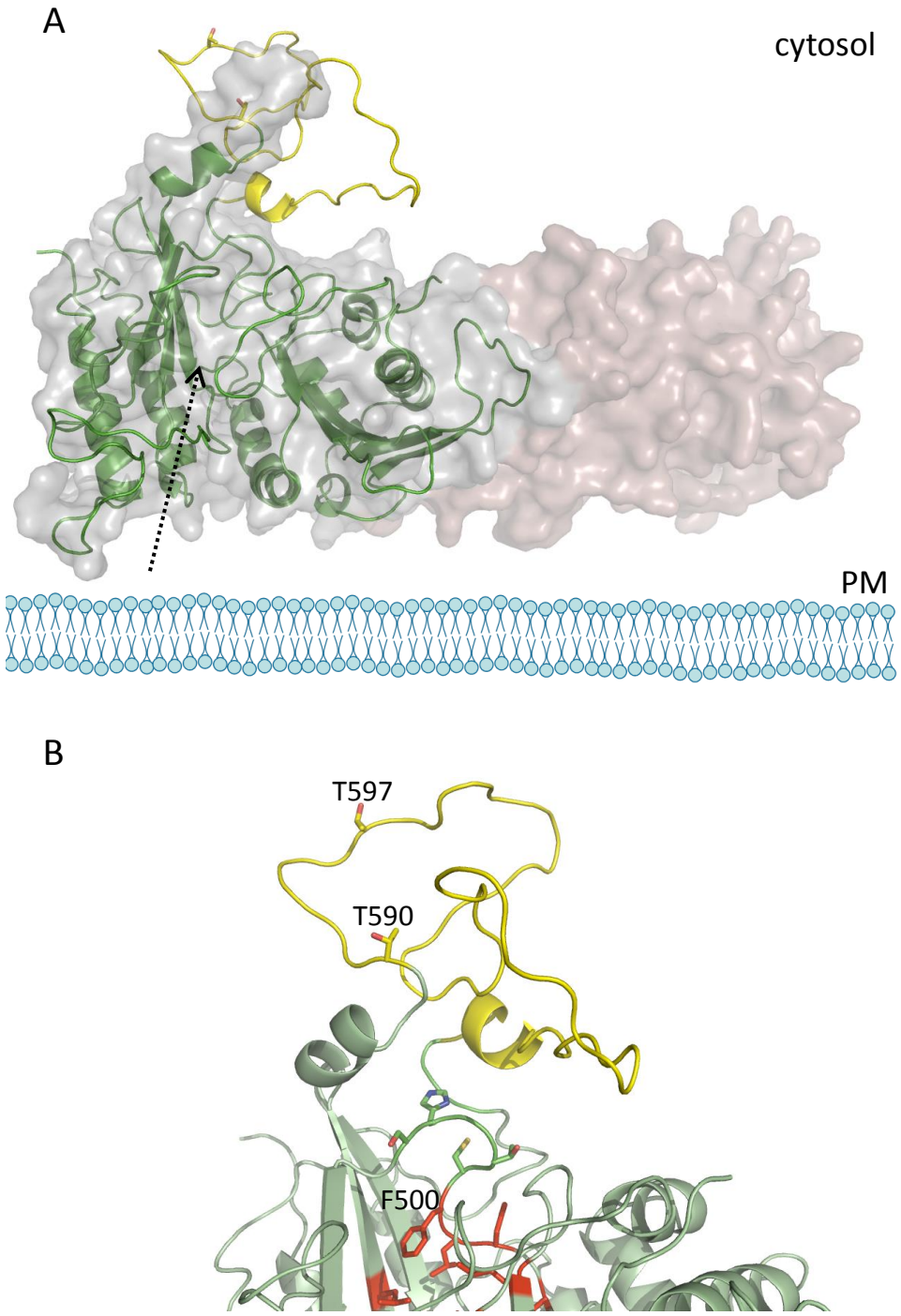

Figure 4.2: Positions T590 and T598 are located on the membrane-averted side of AtPIP5K6. A model of AtPIP5K6 was calculated by PD. Dr. Iris Thondorf (Department of Molecular Modelling, MLU Halle-Wittenberg) based on the x-ray crystallography data from HsPIPKIIβ (1BO1, Rao et. al., 1998). The model was calculated with Lomets (Zhang Labs) server, minimized with Amber12.0 in vacuum with 5000 steps. A, Overview of the surface of dimeric HsPIPKIIβ and the calculated, monomeric model of AtPIP5K6 in a cartoon display. AtPIP5K6 (green) possesses a flexible loop (yellow) within the catalytic domain. This structure of loop is energy minimized, but was not present in the x-ray crystallography data from HsPIPKIIβ. The dashed arrow indicates the active center where ATP, Mg^{2+} and PtdIns4P enter the enzyme. B, Close up of the flexible loop (yellow). The MPK6-phosphorylation sites, residues T590 and T597, are located within a flexible loop on the surface of the membrane-averted side of AtPIP5K6. Residues of the ATP-binding site are indicated in red. Images were prepared with PyMol.

The quality of the model was tested by the overlay of residues important for catalytic activity of the template HsPIPKIIβ (PDB 1BO1) and the calculated model of AtPIP5K6 (Fig. 7.7). Residues are well-aligned and support the validity of the model. The structural information about HsPIPKIIβ suggests that the enzyme possesses a flattened, basic membrane interaction domain that facilitates electrostatic interaction between the protein and the negatively charged PM (Rao *et al.* 1998). According to the calculated model, the residues T590 and T597 are located within a flexible loop on the surface of the membrane-averted side of AtPIP5K6 (Fig. 4.2 A). This loop is not present in the protein sequence of HsPIPKIIβ, but the structural information of the loop (Fig. 4.2 B, yellow) was energy minimized, based on the primary structure of AtPIP5K6 protein sequence. However, it can be assumed that decreased *in vitro* PI4P 5-kinase activity of AtPIP5K6 might not be caused by electrostatic interference with membrane association. In contrast to the hypothesis of the electrostatic switch model (Fairn *et al.* 2009; Rao *et al.* 1998), our data indicate that the regulation of AtPIP5K6 by MPK6 takes place on the membrane-averted side of the protein. When AtPIP5K6 is associated with the PM, the identified phosphorylation sites could be accessible by cytosolic MPK6, supporting that MPK6 might inhibits AtPIP5K6 at its site of action. It can be speculated that phosphorylation within the flexible loop induces a conformational change and thereby affecting the orientation of F500 (Fig. 4.2 B, center), which is an important residue for ATP-binding. According to this hypothesis, reduced AtPIP5K6 activity could be explained the prevention of the ATP-binding in the catalytic center of the enzyme. To elucidate this assumption, it would be possible to measure the affinity of pure, recombinant AtPIP5K6 for ATP with a fluorescence-labeled ATP in isothermal titration calorimetry (ITC) or thermophoresis.

The creation of the phosphoablation and -mimicry variants AtPIP5K6 T590A/D, AtPIP5K6 T597A/D and AtPIP5K6 T590A/D T597A/D did not turn out to be a helpful tool to elucidate the influence of the single phosphorylation sites on PI4P5-kinase activity of AtPIP5K6 (Fig. 7.4). A possible explanation is that these residues are important and the modification of these positions influences ATPIP5K6 activity sustainably.

Phosphomimicry has at least two shortcomings as a tool to study phosphorylation: i) the amino acid sequence flanking the phosphorylation site often serves as recognition motif for the protein kinase responsible and furthermore ii) the biophysical properties of aspartate do not match those of a phosphate group (Dephoure *et al.* 2013). Phosphoablation and -mimicry can lead to loss and gain of function mutations and the experiments with such modifications have to be generally interpreted with caution. An example for a gain of function mutation of an MPK6 substrate protein is ACS6 which is phosphorylated by MPK6 at three positions (see section 1.5.1). Upon phosphorylation, ACS6 is activated to produce ethylene (Liu and Zhang

2004). Arabidopsis plants expressing the variant ACS6 S480D S483D S488D triple mutant in an *acs6* background are constitutive active ethylene producers, while ethylene production in the triple alanine variant cannot be triggered anymore (Liu and Zhang 2004). Although there are studies available where a negatively charged residues can mimic a phosphorylation site, examples for phosphor-site substitutions in the plant field that match the theoretical requirements for phosphoregulation are rare (Dissmeyer and Schnittger 2011).

In addition to the *in vitro* studies, *in vivo* experiments with the double variants AtPIP5K6 T590A/D T597A/D in tobacco pollen tubes showed a similar incidence of phenotypes as observed for wild type AtPIP5K6 (Fig. 7.3). This implies that the variant enzymes retained key functions of PI4P 5-kinase activity. Phosphoablation and -mimicry experiments have to be generally interpreted with caution and for the activity of the phoshomimetic variants of AtPIP5K6 no conclusions can be drawn.

Taken together, the results of the study of variant AtPIP5K6 cannot be used to answer the question about the influence of the single phosphorylation sites. However the identification of T590 and T597 by independent *in vivo* studies (Mayank *et al.* 2012), by phosphorylation with pollen tube extract (only T590) and by *in vitro* kinase assays determines that these sites are important. The observation that a T590A T597A variant of AtPIP5K6 is no longer phosphorylated and also no longer inactivated by MPK6 provides conclusive evidence for the functional regulation of AtPIP5K6 through MPK6-mediated phosphorylation.

4.5 Functional connection of AtPIP5K6 and MPK6 *in vivo*

The *in vitro* characterization of the interconnection of AtPIP5K6 and MPK6 is supported *by in vivo* data. The transient co-transformation of MPK6 and AtPIP5K6 in tobacco pollen tubes revealed that MPK6 not only reduced *in vitro* PI4P 5-kinase activity, but also modulated *in vivo* functionality of the enzyme. Shifting the incidence of stunted pollen tubes to a statistically significant higher number of branched pollen tubes is a clear indication for reduced functionality of AtPIP5K6 (Fig. 3.12), as has previously been described (Ischebeck *et al.* 2010b). A similar, but even stronger effect was observed for the homologous tobacco enzymes NtPIP5K6 and NtSIPK (Fig. 3.17). Upon co-expression of these enzymes, the incidence of stunted pollen tubes was reduced with statistical significance and simultaneously the number of normal growing pollen tubes was doubled (Fig. 3.17). The less pronounced effects observed for the heterologous expression of AtPIP5K6 and MPK6 in tobacco pollen tubes might be explained by the better integration of the overexpressed homologous proteins in the regulatory machinery of the tobacco cell, possibly via specific scaffolding proteins. For yeast

and mammals, scaffolding proteins have been identified that facilitate the interaction of MAPKs and their substrates (Morrison and Davis 2003; Widmann *et al.* 1999). So far no such proteins were identified for plants, but the presence of scaffolding proteins cannot be ruled out. The results of the *in vivo* experiments with tobacco enzymes show similar effects as the observations made for Arabidopsis AtPIP5K6 and MPK6, supporting that the identification of MPK6 from tobacco pollen extract is valid. Taken together, NtSIPK from tobacco pollen tube extract as well as recombinantly expressed and activated MPK6 phosphorylate AtPIP5K6 and NtPIP5K6 *in vitro* and affect enzyme functionality *in vivo*.

This notion is further supported by another experiment in which tobacco RNAi lines containing antisense mRNA for two tobacco MAPKs of high sequence identity (*WIPK/SIPK*; Seo *et al.* 2007) were used (Fig. 3.18). In these lines with reduced levels of endogenous NtSIPK, NtPIP5K6 functionality was significantly increased demonstrating a reciprocal effect to the observations upon NtSIPK overexpression. A further experiment to test for altered NtPIPK6 activity *in vivo* could be the measurement of endogenous PI4P 5-kinase activity in extracts prepared from pollen of tobacco plants with reduced *WIPK/SIPK* RNAi background. These results support the assumptions from the prior section that selected PI4P 5-kinases are indeed functionally regulated *in vivo* by the presence of a MAPK.

4.6 The interplay of MPK6 and AtPIP5K6 in pollen tube growth

The larger picture of biologically relevant processes controlled by the interplay of MPK6 and AtPIP5K6 can be assessed based on known functions of these enzymes. Pollen tube growth within the female organ is guided by the sporophyte and the gametophyte (Dresselhaus and Franklin-Tong 2013). The mechanism of how external cues are integrated into the behavior of pollen tubes during sperm cell delivery is not completely elucidated to today. MPK6 was shown to be involved in funicular guidance of pollen tubes, but its exact role remained unclear so far (Guan *et al.* 2014). It is known from other contexts that MAPK-signaling cascades are linked with the elicitation of cell surface receptors, such as FLS2 or CERK1 (Gomez-Gomez and Boller 2000; Meng and Zhang 2013; Miya *et al.* 2007). These receptors mediate recognition of pathogen-associated molecular patterns (PAMPs) to activate MAPK signaling. In pollen tubes, the presence of FLS2 or CERK1 has not been reported, and, based on their biological function; the cells have no strict need for pathogen defense. Nonetheless, it is possible that MAPKs, including MPK6, are also linked to cell surface receptors in pollen tubes, and that these receptors have a role in the perception of extracellular guidance signals from the female ovules. A possible explanation how funicular guidance cues are transformed into an MPK6-

signal could, thus, be the perception of such cues by pollen tube-specific surface receptors, activating MAPKKK and starting the MAPK-cascade (Fig. 4.3).

In consequence, AtPIP5K6 becomes phosphorylated and hence inhibited by MPK6, resulting in reduced PtdIns(4,5)P_2-levels and effects on growth. A local inhibition of PtdIns(4,5)P_2 dependent vesicle trafficking could lead to a directional impulse for pollen tube growth or more generally to the deceleration of pollen tube elongation. It is also possible that a localized, asymmetric inhibition of AtPIP5K6 would result in pollen tube bending and, thus, directional growth as required for funicular guidance.

The phosphorylation of AtPIP5K3 by MPK6 observed in an *in vitro* kinase assay (Fig. 3.8) supports the assumption that MAPK and PI signaling are involved in processes of polar growth. Besides, AtPIP5K3 is a root hair specific PI4P 5-kinase and involved in the establishment and maintenance of root hair polarity (Kusano *et al.* 2008; Stenzel *et al.* 2008). The interconnection of AtPIP5K3 and MPK6 could be a subject of future research to understand the role of MAPK and PI signaling outside the specialized pollen tube system.

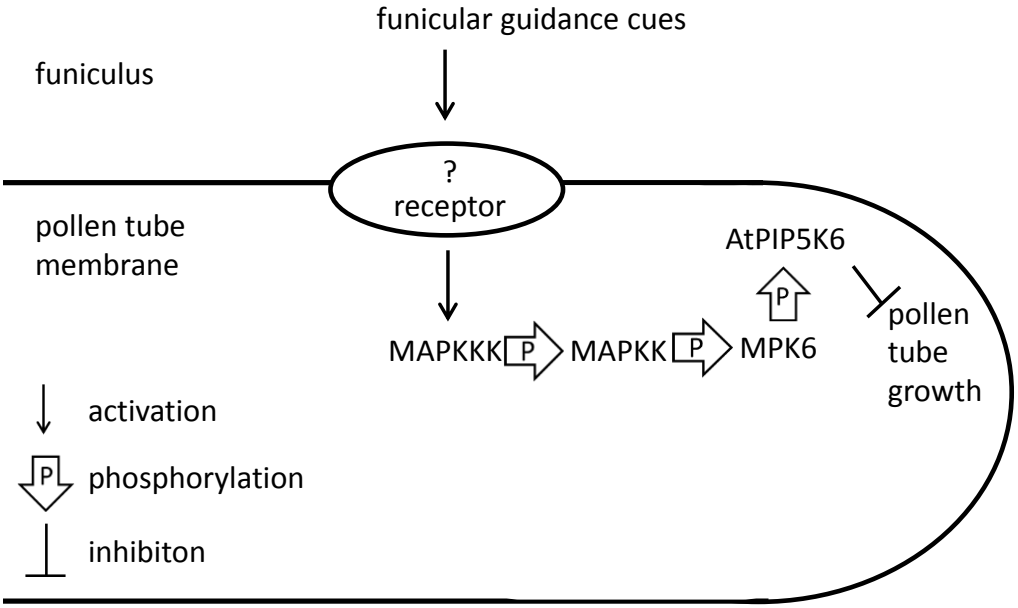

Figure 4.3: Proposed model of MPK6/AtPIP5K6 mediated signaling in growing pollen tubes. MAPK-signaling might be activated in growing pollen tubes by funicular guidance cues, which are received by a receptor in the pollen tube membrane. By initiating the MAPK-cascade AtPIP5K6 is phosphorylated and inactivated by MPK6 and pollen tube growth machinery is inhibited.

Another aspect of the MPK6/AtPIP5K6 interplay is suggested by the fact that AtPIP5K6 is a pollen-expressed type B kinase which also shows expression in Arabidopsis stem and leaf veins (promotor-GUS studies, Dr. Irene Stenzel, MLU Halle-Wittenberg; unpublished data). A systemic role of AtPIP5K6 and MPK6 interaction that functions similar to the proposed model cannot be ruled out and is subject of future studies. Additionally, besides the characterization of the MPK6/AtPIP5K6 interaction, another interesting protein kinase was identified as a

candidate to regulate AtPIP5K6 in the IGKA. This candidate is the calcium-dependent protein kinase CPK11.

4.7 Verification of CPK11 and AtPIP5K6 protein-protein interaction

CPK11 activity is modulated by calcium, which is a key regulator of pollen tube growth and, like PtdIns(4,5)P_2, involved in vesicle trafficking processes and the maintenance of polarity within the apex of pollen tubes. This is important, because AtPIP5K6 also plays an important role in membrane trafficking and delivery of vesicles loaded with cell wall material in growing pollen tubes. After the undirected identification of CPK11 as a potential upstream kinase of AtPIP5K6, connections between AtPIP5K6 and CPK11 were illuminated in this work. While many CPKs have myristoylation motifs to recruit to the PM, CPK11 is soluble and apparently not associated to the PM (Boudsocq *et al.* 2012). Nuclear localization of CPK11 was observed in mesophyll protoplasts (Rodriguez Milla *et al.* 2006; Zhao *et al.* 2013); however this was not observed in pollen ((Gutermuth *et al.* 2013) and this study). AtPIP5K6 is localized to the apical PM, with residual distribution in the cytosol ((Stenzel *et al.* 2012) and this thesis). The subcellular localization of both proteins in the growing pollen tube showed that expression of AtPIP5K6 and CPK11 overlaps in the cytosol. Protein-protein interaction studies in yeast showed that AtPIP5K6 and MPK6 physically interact. The interaction of AtPIP5K6 and CPK11 in the SUS was strong, in comparison to the signal observed for the interaction of MPK6 and AtPIP5K6. The explanation for the better detection might be that CPK11 is a cytosolic protein and the encounter with AtPIP5K6 is not reduced by the accumulation in a certain compartment. The formation of a complex between AtPIP5K6 and CPK11 was confirmed in *in vivo* BiFC-studies in growing pollen tubes. This revealed that AtPIP5K6 and CPK11 interaction takes place at the apical PM. This was also observed for the *in vivo* interaction of AtPIP5K6 and MPK6. It can only be hypothesized if the interaction takes place at the interface of PM and cytosol, or if AtPIP5K6 actively recruits CPK11 to the PM.

4.8 Phosphorylation of AtPIP5K6 by CPK11

The phosphorylation motifs proposed for CDPKs in the literature are described as a serine or threonine +/-2 amino acids in distance from a basic amino acid (basic-X-X-S/T or S/T-X-X-basic) or variations of this motif (basic-X-S/T) (Harper and Harmon 2005). These motifs are not very diagnostic. AtPIP5K6 alone possesses 29 residues that fit the motifs basic-X-X-S/T and S/T-X-X-basic. The kinase assay performed with selected Arabidopsis PI4P 5-kinases and CPK11 from *E. coli* crude extract showed that all PI4P 5-kinases tested were phosphorylated by CPK11. It was

also noticeable that not only full-length MBP-PIP5K protein but fusion-protein bands of smaller sizes ranging from 70 kDa to 40 kDa were phosphorylated, whereas sole MBP-protein was not phosphorylated (Fig. 3.22). These observations could account for an unspecific phosphorylation of PI4P 5-kinases by CPK11. A calculation of the distribution of the basic-X-X-S or S/T-X-X-basic motifs across all tested Arabidopsis PI4P5-kinases sequences revealed that the enzymes contained 3.5-5 CPK-motifs per 100 amino acids. Uno and coworkers observed in a study from 2009, validating interaction partners of CPK11 from a yeast-two-hybrid screen, that CPK11 did not phosphorylate all proteins presented in an *in vitro* kinase-assay. In that study, all proteins containing more than three CPK11-motifs per 100 amino acids were phosphorylated by CPK11 (Uno *et al.* 2009), but sufficient data to confirm this observation is not available. Arabidopsis PI4P 5-kinases possess high sequence identity and possibly share CPK-recognition motifs. Although CPK11 might not differentiate between the different PI4P 5-kinases, control experiments showed that phosphorylation of AtPIP5K6 is calcium-dependent and the inactive variant CPK11 D150A has no residual kinase activity, excluding protein kinase activity from *E. coli* extract (Fig. 3.23).

The investigation of phosphorylation sites introduced by CPK11 was not accessible as straightforward as it was achieved for MPK6 (Fig. 3.22), and MS-analysis did not reveal phosphorylated peptides with high probability values. Assuming that relevant peptides, generated with trypsin digestion might be too small or unfavorable for ionization, protein digestion was performed in further experiments with the alternative endopeptidase Lys-C (data not shown). By cleaving only C-terminal of lysine residues, the peptide pattern was changed compared to trypsin digestion. Unfortunately, this approach did not lead to the identification of further phosphorylation sites in AtPIP5K6. The sites T604 and S607 of AtPIP5K6 were suggested to be phosphorylated by CPK11 with low probability after trypsin digestion. Although these sites are not part of a CPK-motif, the threonine residues were mutagenized to the corresponding alanine variants AtPIP5K6 T604A and AtPIP5K6 S607A. A previous study also described the identification of a phosphothreonine residue outside of a CPK-motif which was then experimentally validated (Rodriguez Milla *et al.* 2006). A kinase assay performed with the phosphoablation variants for the positions T604 and S607 did not confirm these as phosphorylation sites (Fig. 7.5). Based on our data, it can be assumed that AtPIP5K6 is phosphorylated by CPK11, but the exact phosphorylation site(s) could not be identified. One reason could be an insufficient phosphorylation of the samples for MS analysis. The success of unlabeled transphosphorylation of AtPIP5K6 by CPK11 can be monitored by selective staining of phosphoproteins by ProQ Diamond stain in acrylamide gels, but this approach proved not to be a feasible method for the monitoring of Arabidopsis PI4P 5-kinases

(data not shown). Since it cannot be excluded that AtPIP5K6 was not sufficiently phosphorylated, the conditions for unlabeled *in vitro* phosphorylation might have to be additionally considered. An alternative approach could include the use of a constitutively active CPK11 variant which would probably enhance the kinase activity of CPK11.

4.9 CPK11 negatively influences AtPIP5K6 activity *in vitro*

The *in vitro* activity test performed, revealed that CPK11 has indeed an obvious inhibitory effect on AtPIP5K6 PI4P 5-kinase activity (Fig. 3.23). A similar effect was observed for the incubation of AtPIP5K6 and MPK6, where phosphorylation was positively determined. A further complication in the characterization of the CPK11/AtPIP5K6 interaction was that calcium interferes with the lipid kinase assay, potentially by depolarizing substrate micelles containing negatively charged PtdIns4P (Fig. 7.6). To avoid this problem, AtPIP5K6 was immobilized on beads to remove calcium, crucial for CPK11 activity, after pre-incubation. As a control, AtPIP5K6 was incubated with CPK11, calcium and chelating EGTA to monitor the effect of non-activated CPK11. The catalytic inactive variant CPK11 D150A was not used in this experiment, because it was aimed to observe a calcium-dependent effect on *in vitro* activity. Obviously, it is difficult to create a calcium-free environment for the enzyme, so it cannot be excluded that CPK11, used in the control preparation, was completely inactive. When EGTA was omitted, the PI4P 5-kinase activity of AtPIP5K6 was reduced by ~50 % compared to the control (Fig. 3.24). This activity reduction can be correlated directly with active CPK11 and together with the results from the protein-protein interaction studies support a functional connection of AtPIP5K6 and CPK11. The *in vitro* data are supported by *in vivo* experiments. Transient co-transformation of CPK11 with AtPIP5K6 negatively influenced *in vivo* functionality of AtPIP5K6, similar to the observations made in the *in vitro* activity test of AtPIP5K6 pre-incubated with CPK11. Upon AtPIP5K6 expression, the incidence of pollen tubes with a stunted growth phenotype was drastically reduced when CPK11 was co-expressed, indicating an inhibitory effect of CPK11 on AtPIP5K6 *in vivo*. Taken together, it can be assumed that AtPIP5K6 interacts with CPK11 at the apical PM of growing pollen tubes. Furthermore, the *in vitro* data suggests that the PI4P 5-kinase activity of AtPIP5K6 might be regulated by calcium-dependent phosphorylation by CPK11. At this point, the identification of the residues phosphorylated by CPK11 remains open.

4.10 The interplay of CPK11 and AtPIP5K6 in pollen tube growth

Co-expression of CPK11 and AtPIP5K6 in tobacco pollen tube and the quantification of AtPIP5K6 pollen tube phenotypes showed that CPK11 negatively influences AtPIP5K6 functionality *in vivo* (Fig. 3.24). In pollen, the overexpression of calcium-binding CPK11 in the cell could perturb the tightly regulated calcium gradient established and might interfere with polar growth. To investigate altered calcium levels within the pollen tube it would be interesting to co-transform AtPIP5K6 and the catalytic inactive variant of AtPIP5K6 with CPK11 and a calcium sensor probe, for example a cameleon variant (Nagai *et al.* 2004). This experiment would give information about the influence of the interplay between AtPIP5K6 and CPK11 on the calcium distribution in growing pollen tubes, and might elucidate an influence of PtdIns(4,5)P_2 in this context. When *cpk11* pollen from an Arabidopsis T-DNA insertion line was germinated in the presence of high calcium concentration, pollen tube length was enhanced by nearly 30 % compared to wild type (Zhao *et al.* 2013), suggesting that *CPK11* is a negative regulator of pollen tube elongation. The reports of Zhao *et al.* from 2010 showed that pollen of Arabidopsis, stably transformed with a vector encoding for mRNA interfering with *AtPIP5K6*, had a growth rate reduced by 50 %. Thus, indicating that AtPIP5K6 is a positive regulator of pollen tube elongation.

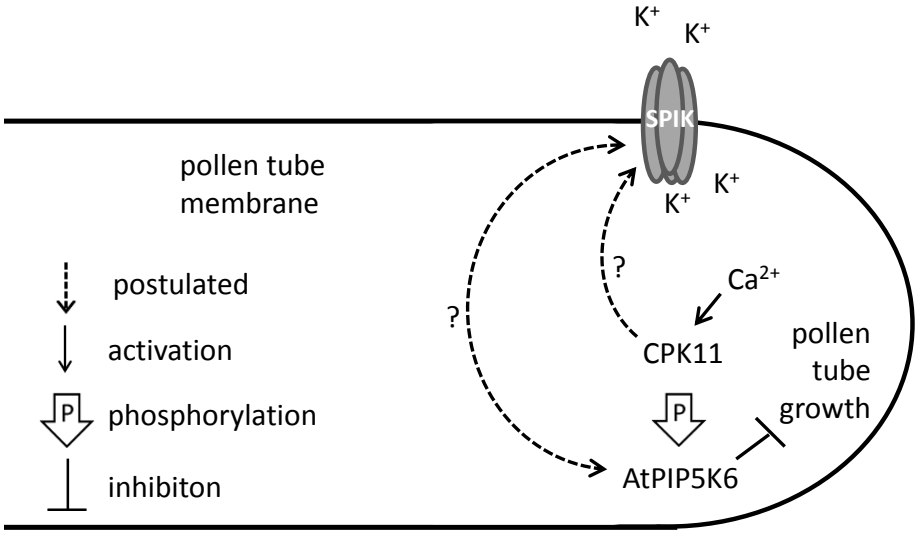

Figure 4.4: Proposed model of CPK11/AtPIP5K6 mediated signaling in growing pollen tubes. CPK11 becomes activated by calcium present in higher concentrations the apical tip of the growing pollen tube. CPK11 together with CPK24 (not shown in this model) mediate the activity of shaker pollen inward K+ channel protein (SPIK) (Zhao *et al.* 2013). Upon calcium activation CPK11 phosphorylates AtPIP5K6, leading to reduced levels of PtdIns(4,5)P_2 and the inhibition of PtdIns(4,5)P_2-related mechanisms involved in pollen tube growth. PtdIns(4,5)P_2 produced by AtPIP5K6 could be assumed to be involved in the mediation of SPIK by binding/modulating channel activity like it was shown for inward-rectifying K^+-channels AtKAT1 and tomato LK1 (Liu *et al.* 2005).

Taken together, it can be hypothesized that the increased growth of *cpk11* pollen on medium with high concentration of calcium could be mediated by enhanced PI4P 5-kinase activity,

lacking its physiological antagonist. One explanation could be a possible connection between PtdIns(4,5)P_2 and the modulation of ion channels. Several reports from the literature correlate CPK activity with the control of ion channels (Gutermuth *et al.* 2013). For pollen tubes CPK11 was shown to indirectly modulate the activity of the K^+-channel SPIK (shaker pollen inward K^+ channel) together with CPK24 by so far unknown mechanisms (Zhao *et al.* 2013). Interestingly, SPIK is a shaker-type K^+-channel, and this group of channels has been demonstrated to be regulated by PtdIns(4,5)P_2. For instance, PtdIns(4,5)P_2 it is accepted to bind and modulate ion channels in mammals (Hilgemann and Ball 1996; Hilgemann *et al.* 2001; Hille *et al.* 2015; Suh and Hille 2005). For plants it was shown that PtdIns(4,5)P_2 modulates the activity of Arabidopsis KAT1 and tomato LK1, both inward-rectifying K^+-channels (Liu *et al.* 2005). It can be hypothesized that CDPK11 regulate PtdIns(4,5)P_2 production by inhibiting PI4P 5-kinase activity, resulting in the modulation of SPIK and controlling ion currents. By the inhibition of PI4P 5-kinases by CPK11, less PtdIns(4,5)P_2 is available in the PM which could affect the stability of a certain state of an ion channel or other porous transmembrane proteins by a so far unknown mechanism. A proposed role for AtPIP5K6 and PtdIns(4,5)P_2 as the missing link in CPK11/CPK24 mediated SPIK modulation is not complete, because the information about the involvement of CPK24 remains to be elucidated. The regulation of pollen tube elongation employs complex biochemical mechanisms and is dependent on many signaling processes. One broader explanation for the physiological effects of pollen tube phenotypes upon co-expression of AtPIP5K6 and CPK11 could be a generally negative effect on secretion. Nonetheless, the experiments presented in this work support that CPK11 phosphorylates and regulates AtPIP5K6 and, furthermore, point to the interconnection of calcium signaling and PI-signaling which has not been described in detail before.

4.11 Interconnection of the regulation of AtPIP5K6 by MPK6 and CPK11

The outcome of this thesis provides the first evidence about the regulation of PI4P 5-kinases by phosphorylation and illuminates responsible protein kinases as well as corresponding phosphorylation sites. A clearly novel finding is that two conserved signaling pathways, MAPK-signaling and calcium-signaling are interconnected with PI-signaling. This notion will influence the view of plant PI-signaling in the long run.

A review from Wurzinger and coworkers suggeted a link between MAPK and calcium signaling (Wurzinger *et al.* 2011). Experimental evidence for this concept arises from a study where a CPK phosphorylated and activated a MAPK in rice, indicating that calcium-dependent protein kinases and MAPK-signaling are interconnected (Xie *et al.* 2014). Furthermore, it can be

hypothesized that AtPIP5K6 becomes concomitantly phosphorylated by both protein kinases. This hypothesis has not yet been tested. Additionally, it can be assumed that the phosphorylation of AtPIP5K6 by one kinase favors or antagonizes its phosphorylation by the second kinase. The reduction of AtPIP5K6 activity observed upon phosphorylation by either kinase did not account for 100 %, and maybe full inhibition will only be achieved by the combined action of several protein kinases on AtPIP5K6. To support these assumptions, experiments could be performed where tobacco pollen is transiently transformed with AtPIP5K6 in the presence of both MPK6 and CPK11. If there is functional cooperativity in the regulation of AtPIP5K6 by MAPK and calcium signaling, AtPIP5K6 activity was further reduced in those pollen tubes.

While a substantial volume of new data has been obtained and these data can be interpreted in a meaningful concept, it is a great result to have new questions and experimental plans that will advance the field of plant signal transduction and indicate new ways how important signaling pathways are interconnected, including MAPKs, calcium, protein phosphorylation and PIs.

5 Summary

The regulatory phospholipid phosphatidylinositiol-4,5-bisphosphate (PtdIns(4,5)P_2) is synthesized in plants by PI4P 5-kinases and is involved in the regulation of various cellular processes in eukaryotic cells, for instance in the orchestration of vesicle trafficking in polar tip growth of pollen tubes. The activity of PI4P 5-kinases of different eukaryotic organisms can be modulated by phosphorylation. The aim of the present dissertation was to investigate whether plant PI4P 5-kinases are also regulated by phosphorylation, to identify upstream protein kinases, and to characterize biochemical and physiological effects of the phosphorylation *in vitro* and *in vivo*. It was found that AtPIP5K6 was phosphorylated by kinase activity from a protein extract prepared from tobacco pollen tubes. Protein kinases involved in the phosphorylation of AtPIP5K6 were identified by an in-gel kinase-assay. The identification was approached by data-independent acquisition with MS^E and yielded several candidate protein kinases. Based on interaction with AtPIP5K6 in split-ubiquitin membrane-based protein-protein interaction studies and on published functional links, the candidate protein kinases, mitogen-activated protein kinase 6 (MPK6) and calcium-dependent protein kinase 11 (CPK11), from Arabidopsis were chosen for more detailed characterization. Interaction of AtPIP5K6 with MPK6 and CPK11 was shown by *in vivo* bimolecular fluorescence complementation to take place at the apical PM of growing tobacco pollen tubes, indicating that the interaction might be of functional relevance for pollen tube growth control. Purified recombinant AtPIP5K6 was dually phosphorylated *in vitro* by activated recombinant MPK6 at positions T590 and T597. These sites are located in the catalytic domain of AtPIP5K6 and their phosphorylation inhibited the catalytic activity of the enzyme. The effect on AtPIP5K6 activity was not observed for a double substitution variant AtPIP5K6 T590A T597A, suggesting that the inhibitory effect of AtPIP5K6 by MPK6 was a result of phosphoregulation. The *in vitro* findings were corroborated by *in vivo* experiments demonstrating an attenuation of AtPIP5K6 effects on pollen tube growth upon co-expression of MPK6. The key findings for the Arabidopsis enzymes were confirmed for their homologous counterparts from tobacco, furthermore indicating that NtPIP5K6, a close homolog of AtPIP5K6, is increased in functionality in pollen with reduced MAPK activity.

Experiments performed with CPK11 revealed that AtPIP5K6 was phosphorylated by CPK11 in a calcium-dependent way, and that CPK11 had a calcium-dependent inhibitory effect on AtPIP5K6 *in vitro* activity. However, phosphorylation sites could not be determined with certainty to date. The *in vitro* results are also corroborated by *in vivo* experiments

demonstrating an attenuation of AtPIP5K6 effects on pollen tube growth upon co-expression of CPK11. Taken together, the data presented in this thesis establish a new link between PI metabolism and upstream protein kinases in the context of the control of polar tip growth in plants. The reported link may have profound ramifications for the function of PI-dependent processes and signaling cascades involving MAPK6 and CPK11 also in vegetative tissues.

6 Literature

Audhya A, Emr SD (2003) Regulation of PI4,5P2 synthesis by nuclear-cytoplasmic shuttling of the Mss4 lipid kinase. EMBO J. 22: 4223-4236

Balla T (2006) Phosphoinositide-derived messengers in endocrine signaling. J. Endocrinol. 188: 135-153

Biondi RM, Nebreda AR (2003) Signalling specificity of Ser/Thr protein kinases through docking-site-mediated interactions. Biochem J. 372: 1-13

Bosch M, Cheung AY, Hepler PK (2005) Pectin methylesterase, a regulator of pollen tube growth. Plant Physiol. 138: 1334-1346

Bosch M, Hepler PK (2005) Pectin methylesterases and pectin dynamics in pollen tubes. Plant Cell 17: 3219-3226

Boudsocq M, Droillard MJ, Regad L, Lauriere C (2012) Characterization of Arabidopsis calcium-dependent protein kinases: activated or not by calcium? Biochem J. 447: 291-299

Boudsocq M, Sheen J (2013) CDPKs in immune and stress signaling. Trends Plant Sci. 18: 30-40

Bradford MM (1976) A rapid and sensitive method for the quantitation of microgram quantities of protein utilizing the principle of protein-dye binding. Anal. Biochem. 72: 248-254

Brown MD, Sacks DB (2009) Protein scaffolds in MAP kinase signalling. Cell Signal 21: 462-469

Burden LM, Rao VD, Murray D, Ghirlando R, Doughman SD, Anderson RA, Hurley JH (1999) The flattened face of type II beta phosphatidylinositol phosphate kinase binds acidic phospholipid membranes. Biochemistry 38: 15141-15149

Cardenas L, Lovy-Wheeler A, Kunkel JG, Hepler PK (2008) Pollen tube growth oscillations and intracellular calcium levels are reversibly modulated by actin polymerization. Plant Physiol. 146: 1611-1621

Chang L, Karin M (2001) Mammalian MAP kinase signalling cascades. Nature 410: 37-40

Chen CY, Wong EI, Vidali L, Estavillo A, Hepler PK, Wu HM, Cheung AY (2002) The regulation of actin organization by actin-depolymerizing factor in elongating pollen tubes. Plant Cell 14: 2175-2190

Cho MH, Chen Q, Okpodu CM, Boss WF (1992) Separation and quantification of of [^{3}H]inositol phospholipids using thin-layer-chromatography and a computerized ^{3}H imaging scanner. LC-GC 10: 464-468

Chomczynski P, Mackey K (1995) Short technical reports. Modification of the TRI reagent procedure for isolation of RNA from polysaccharide- and proteoglycan-rich sources. Biotechniques 19: 942-945

Clark G, Cantero-Garcia A, Butterfield T, Dauwalder M, Roux SJ (2005) Secretion as a key component of gravitropic growth: implications for annexin involvement in differential growth. Gravit Space Biol Bull 18: 113-114

Dahan J, Pichereaux C, Rossignol M, Blanc S, Wendehenne D, Pugin A, Bourque S (2009) Activation of a nuclear-localized SIPK in tobacco cells challenged by cryptogein, an elicitor of plant defence reactions. Biochem J. 418: 191-200

Dephoure N, Gould KL, Gygi SP, Kellogg DR (2013) Mapping and analysis of phosphorylation sites: a quick guide for cell biologists. Mol Biol Cell 24: 535-542

Dissmeyer N, Schnittger A (2011) The age of protein kinases. Methods Mo.l Biol. 779: 7-52

Doczi R, Okresz L, Romero AE, Paccanaro A, Bogre L (2012) Exploring the evolutionary path of plant MAPK networks. Trends Plant Sci. 17: 518-525

Dresselhaus T, Franklin-Tong N (2013) Male-female crosstalk during pollen germination, tube growth and guidance, and double fertilization. Mol. Plant 6: 1018-10136

Fairn GD, Ogata K, Botelho RJ, Stahl PD, Anderson RA, De Camilli P, Meyer T, Wodak S, Grinstein S (2009) An electrostatic switch displaces phosphatidylinositol phosphate kinases from the membrane during phagocytosis. J. Cell. Biol. 187: 701-714

Feijo JA, Sainhas J, Hackett GR, Kunkel JG, Hepler PK (1999) Growing pollen tubes possess a constitutive alkaline band in the clear zone and a growth-dependent acidic tip. J. Cell. Biol. 144: 483-496

Feijo JA, Sainhas J, Holdaway-Clarke T, Cordeiro MS, Kunkel JG, Hepler PK (2001) Cellular oscillations and the regulation of growth: the pollen tube paradigm. Bioessays 23: 86-94

Fischer R, Zekert N, Takeshita N (2008) Polarized growth in fungi--interplay between the cytoskeleton, positional markers and membrane domains. Mol. Microbiol. 68: 813-826

Franklin-Tong VE (1999) Signaling and the modulation of pollen tube growth. Plant Cell 11: 727-738

Fu Y (2010) The actin cytoskeleton and signaling network during pollen tube tip growth. Journal of integrative plant biology 52: 131-137

Galvao RM, Kota U, Soderblom EJ, Goshe MB, Boss WF (2008) Characterization of a new family of protein kinases from *Arabidopsis* containing phosphoinositide 3/4-kinase and ubiquitin-like domains. Biochem J. 409: 117-127

Gomez-Gomez L, Boller T (2000) FLS2: an LRR receptor-like kinase involved in the perception of the bacterial elicitor flagellin in Arabidopsis. Mol. Cell 5: 1003-1011

Guan Y, Lu J, Xu J, McClure B, Zhang S (2014) Two Mitogen-Activated Protein Kinases, MPK3 and MPK6, Are Required for Funicular Guidance of Pollen Tubes in Arabidopsis. Plant Physiol. 165: 528-533

Gungabissoon RA, Jiang C-J, Drobak BK, Maciver SK, Hussey PJ (1998) Interaction of maize actin-depolymerising factor with actin and phosphoinositides and its inhibition of plant phospholipase C. Plant J. 16: 689-696

Gutermuth T, Lassig R, Portes MT, Maierhofer T, Romeis T, Borst JW, Hedrich R, Feijo JA, Konrad KR (2013) Pollen tube growth regulation by free anions depends on the interaction between the anion channel SLAH3 and calcium-dependent protein kinases CPK2 and CPK20. Plant Cell 25: 4525-4543

Harper JF, Harmon A (2005) Plants, symbiosis and parasites: a calcium signalling connection. Nature reviews. Molecular cell biology 6: 555-566

Heazlewood JL, Durek P, Hummel J, Selbig J, Weckwerth W, Walther D, Schulze WX (2008) PhosPhAt: a database of phosphorylation sites in Arabidopsis thaliana and a plant-specific phosphorylation site predictor. Nucleic Acids Res. 36: D1015-1021

Heilmann I (2015) Information processing and survival strategies. In: Nies DH, Krauss G-J (eds) Ecological biochemistry. Wiley-VCH, Weinheim, pp 125-152

Heilmann M, Heilmann I (2015) Plant phosphoinositides-complex networks controlling growth and adaptation. Biochim. Biophys. Acta 1851: 759-769

Helm S, Dobritzsch D, Rodiger A, Agne B, Baginsky S (2014) Protein identification and quantification by data-independent acquisition and multi-parallel collision-induced dissociation mass spectrometry (MS(E)) in the chloroplast stroma proteome. Journal of proteomics 98: 79-89

Hepler PK, Kunkel JG, Rounds CM, Winship LJ (2012) Calcium entry into pollen tubes. Trends Plant Sci. 17: 32-38

Hepler PK, Vidali L, Cheung AY (2001) Polarized cell growth in higher plants. Annu Rev Cell Dev Biol 17: 159-187

Hepler PK, Winship LJ (2015) The pollen tube clear zone: clues to the mechanism of polarized growth. Journal of integrative plant biology 57: 79-92

Hilgemann DW, Ball R (1996) Regulation of cardiac Na+,Ca2+ exchange and KATP potassium channels by PIP2. Science 273: 956-959

Hilgemann DW, Feng S, Nasuhoglu C (2001) The complex and intriguing lives of PIP2 with ion channels and transporters. Sci STKE 2001: RE19

Hille B, Dickson EJ, Kruse M, Vivas O, Suh BC (2015) Phosphoinositides regulate ion channels. Biochim. Biophys. Acta 1851: 844-856

Hinchliffe KA, Irvine RF (2006) Regulation of type II PIP kinase by PKD phosphorylation. Cell Signal 18: 1906-1913

Holdaway-Clarke TL, Feijo JA, Hackett GR, Kunkel JG, Hepler PK (1997) Pollen Tube Growth and the Intracellular Cytosolic Calcium Gradient Oscillate in Phase while Extracellular Calcium Influx Is Delayed. Plant Cell 9: 1999-2010

Holdaway-Clarke TL, Weddle NM, Kim S, Robi A, Parris C, Kunkel JG, Hepler PK (2003) Effect of extracellular calcium, pH and borate on growth oscillations in Lilium formosanum pollen tubes. J. Exp. Bot. 54: 65-72

Hood EE, Gelvin SB, Melchers LS, Hoekema A (1993) New Agrobacterium helper plasmids for gene transfer to plants. Transgenic Res 2: 208-218

Horton HR, Moran LA, Scrimgeour KG, Perry MD, Rawn JD (2006) Lipids and membranes. In: Carlson G (ed) Principles of Biochemistry. Pearson Prentice Hall, Upper Saddle River, New Jersey, pp 253-292

Hoser R, Zurczak M, Lichocka M, Zuzga S, Dadlez M, Samuel MA, Ellis BE, Stuttmann J, Parker JE, Hennig J, Krzymowska M (2013) Nucleocytoplasmic partitioning of tobacco N receptor is modulated by SGT1. New Phytol. 200: 158-171

Hrabak EM, Chan CW, Gribskov M, Harper JF, Choi JH, Halford N, Kudla J, Luan S, Nimmo HG, Sussman MR, Thomas M, Walker-Simmons K, Zhu JK, Harmon AC (2003) The Arabidopsis CDPK-SnRK superfamily of protein kinases. Plant Physiol. 132: 666-680

Hunter T (1996) Tyrosine phosphorylation: past, present and future. Biochem Soc Trans 24: 307-327

Hurley JH, Grobler JA (1997) Protein kinase C and phospholipase C: bilayer interactions and regulation. Curr Opin Struct Biol 7: 557-565

Ischebeck T (2008) Distinct roles of PI4P 5-kinases in polar growth of pollen tubes. Department of Plant Biochemistry. Georg-August-University Göttingen, Göttingen, p 139

Ischebeck T, Heilmann I (2010) PIP-kinases as key regulators of plant function. In: Munnik T (ed) Lipid Signaling in Plants. Springer, Berlin, Germany, pp 79-93

Ischebeck T, Seiler S, Heilmann I (2010a) At the poles across kingdoms: phosphoinositides and polar tip growth. Protoplasma 240: 13-31

Ischebeck T, Stenzel I, Heilmann I (2008) Type B phosphatidylinositol-4-phosphate 5-kinases mediate pollen tube growth in *Nicotiana tabacum* and *Arabidopsis* by regulating apical pectin secretion. Plant Cell 20: 3312-3330

Ischebeck T, Stenzel I, Hempel F, Jin X, Mosblech A, Heilmann I (2011) Phosphatidylinositol-4,5-bisphosphate influences Nt-Rac5-mediated cell expansion in pollen tubes of Nicotiana tabacum. Plant J. 65: 453-468

Ischebeck T, Vu LH, Jin X, Stenzel I, Löfke C, Heilmann I (2010b) Functional cooperativity of enzymes of phosphoinositide conversion according to synergistic effects on pectin secretion in tobacco pollen tubes. Mol. Plant 3: 870-881

Ischebeck T, Werner S, Krishnamoorthy P, Lerche J, Meijon M, Stenzel I, Löfke C, Wiessner T, Im YJ, Perera IY, Iven T, Feussner I, Busch W, Boss WF, Teichmann T, Hause B, Persson S, Heilmann I (2013) Phosphatidylinositol 4,5-bisphosphate influences PIN polarization by controlling clathrin-mediated membrane trafficking in Arabidopsis. Plant Cell 25: 4894-4911

Ito H, Fukuda Y, Murata K, Kimura A (1983) Transformation of intact yeast cells treated with alkali cations. J Bacteriol 153: 163-168

Johnson SA, Hunter T (2005) Kinomics: methods for deciphering the kinome. Nat Methods 2: 17-25

Johnsson N, Varshavsky A (1994) Split ubiquitin as a sensor of protein interactions in vivo. Proc. Natl. Acad. Sci. U S A 91: 10340-10344

Kang S, Yang F, Li L, Chen H, Chen S, Zhang J (2015) The Arabidopsis transcription factor BRASSINOSTEROID INSENSITIVE1-ETHYL METHANESULFONATE-SUPPRESSOR1 is a direct substrate of MITOGEN-ACTIVATED PROTEIN KINASE6 and regulates immunity. Plant Physiol. 167: 1076-1086

Kawashima T, Berger F (2011) Green love talks; cell-cell communication during double fertilization in flowering plants. AoB plants 2011: plr015

Klahre U, Becker C, Schmitt AC, Kost B (2006) Nt-RhoGDI2 regulates Rac/Rop signaling and polar cell growth in tobacco pollen tubes. Plant J. 46: 1018-1031

Klein TM, Harper EC, Svab Z, Sanford JC, Fromm ME, Maliga P (1988) Stable genetic transformation of intact Nicotiana cells by the particle bombardment process. Proc. Natl. Acad. Sci. U S A 85: 8502-8505

Klein TM, Kornstein L, Sanford JC, Fromm ME (1989) Genetic Transformation of Maize Cells by Particle Bombardment. Plant Physiol. 91: 440-444

Kolukisaoglu U, Weinl S, Blazevic D, Batistic O, Kudla J (2004) Calcium sensors and their interacting protein kinases: genomics of the Arabidopsis and rice CBL-CIPK signaling networks. Plant Physiol. 134: 43-58

Komis G, Illes P, Beck M, Samaj J (2011) Microtubules and mitogen-activated protein kinase signalling. Curr. Opin. Plant Biol. 14: 650-657

König S, Ischebeck T, Lerche J, Stenzel I, Heilmann I (2008) Salt stress-induced association of phosphatidylinositol-4,5-bisphosphate with clathrin-coated vesicles in plants. Biochem J. 415: 387-399

Kost B, Lemichez E, Spielhofer P, Hong Y, Tolias K, Carpenter C, Chua NH (1999) Rac homologs and compartmentalized phosphatidylinositol 4, 5-bisphosphate act in a common pathway to regulate polar pollen tube growth. J. Cell. Biol. 145: 317-330

Krichevsky A, Kozlovsky SV, Tian GW, Chen MH, Zaltsman A, Citovsky V (2007) How pollen tubes grow. Dev Biol 303: 405-420

Krinke O, Novotna Z, Valentova O, Martinec J (2007) Inositol trisphosphate receptor in higher plants: is it real? J. Exp. Bot. 58: 361-376

Kudla J, Xu Q, Harter K, Gruissem W, Luan S (1999) Genes for calcineurin B-like proteins in Arabidopsis are differentially regulated by stress signals. Proc. Natl. Acad. Sci. U S A 96: 4718-4723

Kusano H, Testerink C, Vermeer JEM, Tsuge T, Shimada H, Oka A, Munnik T, Aoyama T (2008) The *Arabidopsis* phosphatidylinositol phosphate 5-kinase PIP5K3 is a key regulator of root hair tip growth. Plant Cell 20: 367-380

Lassing I, Lindberg U (1985) Specific interaction between phosphatidylinositol 4,5-bisphosphate and profilactin. Nature 314: 472-474

Lin W, Li B, Lu D, Chen S, Zhu N, He P, Shan L (2014) Tyrosine phosphorylation of protein kinase complex BAK1/BIK1 mediates Arabidopsis innate immunity. Proc. Natl. Acad. Sci. U S A 111: 3632-3637

Liu K, Li L, Luan S (2005) An essential function of phosphatidylinositol phosphates in activation of plant shaker-type K^+ channels. Plant J. 42: 433-443

Liu Y, Zhang S (2004) Phosphorylation of 1-aminocyclopropane-1-carboxylic acid synthase by MPK6, a stress-responsive mitogen-activated protein kinase, induces ethylene biosynthesis in Arabidopsis. Plant Cell 16: 3386-3399

Lopez-Bucio JS, Dubrovsky JG, Raya-Gonzalez J, Ugartechea-Chirino Y, Lopez-Bucio J, de Luna-Valdez LA, Ramos-Vega M, Leon P, Guevara-Garcia AA (2014) Arabidopsis thaliana mitogen-activated protein kinase 6 is involved in seed formation and modulation of primary and lateral root development. J. Exp. Bot. 65: 169-183

Luan S, Kudla J, Rodriguez-Concepcion M, Yalovsky S, Gruissem W (2002) Calmodulins and calcineurin B-like proteins: calcium sensors for specific signal response coupling in plants. Plant Cell 14 Suppl: S389-400

Majovsky P, Naumann C, Lee CW, Lassowskat I, Trujillo M, Dissmeyer N, Hoehenwarter W (2014) Targeted proteomics analysis of protein degradation in plant signaling on an LTQ-Orbitrap mass spectrometer. J Proteome Res 13: 4246-4258

Mao G, Meng X, Liu Y, Zheng Z, Chen Z, Zhang S (2011) Phosphorylation of a WRKY transcription factor by two pathogen-responsive MAPKs drives phytoalexin biosynthesis in Arabidopsis. Plant Cell 23: 1639-1653

Mayank P, Grossman J, Wuest S, Boisson-Dernier A, Roschitzki B, Nanni P, Nuhse T, Grossniklaus U (2012) Characterization of the phosphoproteome of mature Arabidopsis pollen. Plant J. 72: 89-101

Mei Y, Jia WJ, Chu YJ, Xue HW (2012) Arabidopsis phosphatidylinositol monophosphate 5-kinase 2 is involved in root gravitropism through regulation of polar auxin transport by affecting the cycling of PIN proteins. Cell Res. 22: 581-597

Meng X, Xu J, He Y, Yang KY, Mordorski B, Liu Y, Zhang S (2013) Phosphorylation of an ERF transcription factor by Arabidopsis MPK3/MPK6 regulates plant defense gene induction and fungal resistance. Plant Cell 25: 1126-1142

Meng X, Zhang S (2013) MAPK cascades in plant disease resistance signaling. Annu Rev Phytopathol 51: 245-266

Miya A, Albert P, Shinya T, Desaki Y, Ichimura K, Shirasu K, Narusaka Y, Kawakami N, Kaku H, Shibuya N (2007) CERK1, a LysM receptor kinase, is essential for chitin elicitor signaling in Arabidopsis. Proc. Natl. Acad. Sci. U S A 104: 19613-19618

Morrison DK, Davis RJ (2003) Regulation of MAP kinase signaling modules by scaffold proteins in mammals. Annu Rev Cell Dev Biol 19: 91-118

Moscatelli A, Ciampolini F, Rodighiero S, Onelli E, Cresti M, Santo N, Idilli A (2007) Distinct endocytic pathways identified in tobacco pollen tubes using charged nanogold. J. Cell Sci. 120: 3804-3819

Moscatelli A, Idilli AI (2009) Pollen tube growth: a delicate equilibrium between secretory and endocytic pathways. Journal of integrative plant biology 51: 727-739

Mueller-Roeber B, Pical C (2002) Inositol phospholipid metabolism in *Arabidopsis*. Characterized and putative isoforms of inositol phospholipid kinase and phosphoinositide-specific phospholipase C. Plant Physiol. 130: 22-46

Myers C, Romanowsky SM, Barron YD, Garg S, Azuse CL, Curran A, Davis RM, Hatton J, Harmon AC, Harper JF (2009) Calcium-dependent protein kinases regulate polarized tip growth in pollen tubes. Plant J. 59: 528-539

Nagai T, Yamada S, Tominaga T, Ichikawa M, Miyawaki A (2004) Expanded dynamic range of fluorescent indicators for Ca(2+) by circularly permuted yellow fluorescent proteins. Proc. Natl. Acad. Sci. U S A 101: 10554-10559

Nakagami H, Sugiyama N, Mochida K, Daudi A, Yoshida Y, Toyoda T, Tomita M, Ishihama Y, Shirasu K (2010) Large-scale comparative phosphoproteomics identifies conserved phosphorylation sites in plants. Plant Physiol. 153: 1161-1174

Nito K, Wong CC, Yates JR, 3rd, Chory J (2013) Tyrosine phosphorylation regulates the activity of phytochrome photoreceptors. Cell reports 3: 1970-1979

Obermeyer G, Weisenseel MH (1991) Calcium channel blocker and calmodulin antagonists affect the gradient of free calcium ions in lily pollen tubes. Eur J Cell Biol 56: 319-327

Oh MH, Wu X, Kim HS, Harper JF, Zielinski RE, Clouse SD, Huber SC (2012) CDPKs are dual-specificity protein kinases and tyrosine autophosphorylation attenuates kinase activity. FEBS Lett. 586: 4070-4075

Olsen JV, Blagoev B, Gnad F, Macek B, Kumar C, Mortensen P, Mann M (2006) Global, in vivo, and site-specific phosphorylation dynamics in signaling networks. Cell 127: 635-648

Palin R, Geitmann A (2012) The role of pectin in plant morphogenesis. Bio Systems 109: 397-402

Park SJ, Itoh T, Takenawa T (2001) Phosphatidylinositol 4-phosphate 5-kinase type I is regulated through phosphorylation response by extracellular stimuli. J. Biol. Chem. 276: 4781-4787

Parre E, Geitmann A (2005) Pectin and the role of the physical properties of the cell wall in pollen tube growth of Solanum chacoense. Planta 220: 582-592

Pawson T, Scott JD (2005) Protein phosphorylation in signaling--50 years and counting. Trends Biochem. Sci. 30: 286-290

Pecher P, Eschen-Lippold L, Herklotz S, Kuhle K, Naumann K, Bethke G, Uhrig J, Weyhe M, Scheel D, Lee J (2014) The Arabidopsis thaliana mitogen-activated protein kinases MPK3

and MPK6 target a subclass of 'VQ-motif'-containing proteins to regulate immune responses. New Phytol. 203: 592-606

Perera IY, Davis AJ, Galanopoulou D, Im YJ, Boss WF (2005) Characterization and comparative analysis of Arabidopsis phosphatidylinositol phosphate 5-kinase 10 reveals differences in Arabidopsis and human phosphatidylinositol phosphate kinases. FEBS Lett. 579: 3427-3432

Perez-Salamo I, Papdi C, Rigo G, Zsigmond L, Vilela B, Lumbreras V, Nagy I, Horvath B, Domoki M, Darula Z, Medzihradszky K, Bogre L, Koncz C, Szabados L (2014) The heat shock factor A4A confers salt tolerance and is regulated by oxidative stress and the mitogen-activated protein kinases MPK3 and MPK6. Plant Physiol. 165: 319-334

Picton JM, Steer MW (1983) Membrane recycling and the control of secretory activity in pollen tubes. J. Cell Sci. 63: 303-310

Pierson ES, Miller DD, Callaham DA, Shipley AM, Rivers BA, Cresti M, Hepler PK (1994) Pollen tube growth is coupled to the extracellular calcium ion flux and the intracellular calcium gradient: effect of BAPTA-type buffers and hypertonic media. Plant Cell 6: 1815-1828

Pierson ES, Miller DD, Callaham DA, van Aken J, Hackett G, Hepler PK (1996) Tip-localized calcium entry fluctuates during pollen tube growth. Dev Biol 174: 160-173

Pietzsch J (2004) Mind the membrane. Horizon Symposia: A living frontier – exploring the dynamics of the cell membrane. Nature Publishing Group, Houndmills, Basingstoke, Hampshire, UK, pp 1-4

Pitzschke A, Schikora A, Hirt H (2009) MAPK cascade signalling networks in plant defence. Curr. Opin. Plant Biol. 12: 421-426

Pokotylo I, Kolesnikov Y, Kravets V, Zachowski A, Ruelland E (2014) Plant phosphoinositide-dependent phospholipases C: variations around a canonical theme. Biochimie 96: 144-157

Proust J, Houlne G, Schantz ML, Shen WH, Schantz R (1999) Regulation of biosynthesis and cellular localization of Sp32 annexins in tobacco BY2 cells. Plant Mol. Biol. 39: 361-372

Rao VD, Misra S, Boronenkov IV, Anderson RA, Hurley JH (1998) Structure of type IIbeta phosphatidylinositol phosphate kinase: a protein kinase fold flattened for interfacial phosphorylation. Cell 94: 829-839

Rodriguez-Boulan E, Powell SK (1992) Polarity of epithelial and neuronal cells. Annu Rev Cell Biol 8: 395-427

Rodriguez MC, Petersen M, Mundy J (2010) Mitogen-activated protein kinase signaling in plants. Annu. Rev. Plant Biol. 61: 621-649

Rodriguez Milla MA, Uno Y, Chang IF, Townsend J, Maher EA, Quilici D, Cushman JC (2006) A novel yeast two-hybrid approach to identify CDPK substrates: characterization of the interaction between AtCPK11 and AtDi19, a nuclear zinc finger protein. FEBS Lett. 580: 904-911

Rounds CM, Bezanilla M (2013) Growth mechanisms in tip-growing plant cells. Annu. Rev. Plant Biol. 64: 243-265

Rozengurt E, Rey O, Waldron RT (2005) Protein kinase D signaling. J. Biol. Chem. 280: 13205-13208

Ryan E, Steer M, Dolan L (2001) Cell biology and genetics of root hair formation in Arabidopsis thaliana. Protoplasma 215: 140-149

Samaj J, Baluska F, Menzel D (2004) New signalling molecules regulating root hair tip growth. Trends Plant Sci. 9: 217-220

Samaj J, Muller J, Beck M, Bohm N, Menzel D (2006) Vesicular trafficking, cytoskeleton and signalling in root hairs and pollen tubes. Trends Plant Sci. 11: 594-600

Sanders D, Pelloux J, Brownlee C, Harper JF (2002) Calcium at the crossroads of signaling. Plant Cell 14 Suppl: S401-417

Schulz P, Herde M, Romeis T (2013) Calcium-dependent protein kinases: hubs in plant stress signaling and development. Plant Physiol. 163: 523-530

Schweighofer A, Kazanaviciute V, Scheikl E, Teige M, Doczi R, Hirt H, Schwanninger M, Kant M, Schuurink R, Mauch F, Buchala A, Cardinale F, Meskiene I (2007) The PP2C-type phosphatase AP2C1, which negatively regulates MPK4 and MPK6, modulates innate immunity, jasmonic acid, and ethylene levels in Arabidopsis. Plant Cell 19: 2213-2224

Seo S, Katou S, Seto H, Gomi K, Ohashi Y (2007) The mitogen-activated protein kinases WIPK and SIPK regulate the levels of jasmonic and salicylic acids in wounded tobacco plants. Plant J. 49: 899-909

Shevchenko A, Wilm M, Vorm O, Mann M (1996) Mass spectrometric sequencing of proteins silver-stained polyacrylamide gels. Analytical chemistry 68: 850-858

Shi J, Kim KN, Ritz O, Albrecht V, Gupta R, Harter K, Luan S, Kudla J (1999) Novel protein kinases associated with calcineurin B-like calcium sensors in Arabidopsis. Plant Cell 11: 2393-2405

Singer SJ, Nicholson GL (1972) The fluid mosaic model of the structure of cell membranes. Science 175

Sousa E, Kost B, Malho R (2008) *Arabidopsis* Phosphatidylinositol-4-Monophosphate 5-Kinase 4 Regulates Pollen Tube Growth and Polarity by Modulating Membrane Recycling. Plant Cell 20: 3050-3064

Stagljar I, Korostensky C, Johnsson N, te Heesen S (1998) A genetic system based on split-ubiquitin for the analysis of interactions between membrane proteins in vivo. Proc. Natl. Acad. Sci. U S A 95: 5187-5192

Steinhorst L, Kudla J (2013) Calcium - a central regulator of pollen germination and tube growth. Biochim. Biophys. Acta 1833: 1573-1581

Steinhorst L, Kudla J (2014) Signaling in cells and organisms - calcium holds the line. Curr. Opin. Plant Biol. 22: 14-21

Stenzel I, Ischebeck T, König S, Holubowska A, Sporysz M, Hause B, Heilmann I (2008) The type B phosphatidylinositol-4-phosphate 5-kinase 3 is essential for root hair formation in *Arabidopsis thaliana*. Plant Cell 20: 124-141

Stenzel I, Ischebeck T, Quint M, Heilmann I (2012) Variable regions of PI4P 5-kinases direct PtdIns(4,5)P2 toward alternative regulatory functions in tobacco pollen tubes. Front. Plant Sci. 2: 1-14

Stevenson JM, Perera IY, Boss WF (1998) A phosphatidylinositol 4-kinase pleckstrin homology domain that binds phosphatidylinositol 4-monophosphate. J. Biol. Chem. 273: 22761-22767

Stevenson JM, Perera IY, Heilmann I, Persson S, Boss WF (2000) Inositol signaling and plant growth. Trends Plant Sci. 5: 252-258

Suarez-Rodriguez MC, Adams-Phillips L, Liu Y, Wang H, Su SH, Jester PJ, Zhang S, Bent AF, Krysan PJ (2007) MEKK1 is required for flg22-induced MPK4 activation in Arabidopsis plants. Plant Physiol. 143: 661-669

Suh BC, Hille B (2005) Regulation of ion channels by phosphatidylinositol 4,5-bisphosphate. Curr Opin Neurobiol 15: 370-378

Tanoue T, Nishida E (2003) Molecular recognitions in the MAP kinase cascades. Cell Signal 15: 455-462

Tejos R, Sauer M, Vanneste S, Palacios-Gomez M, Li H, Heilmann M, van Wijk R, Vermeer JE, Heilmann I, Munnik T, Friml J (2014) Bipolar PM Distribution of Phosphoinositides and Their Requirement for Auxin-Mediated Cell Polarity and Patterning in Arabidopsis. Plant Cell 5: 2114-2128

Tena G, Boudsocq M, Sheen J (2011) Protein kinase signaling networks in plant innate immunity. Curr. Opin. Plant Biol. 14: 519-529

Thole JM, Nielsen E (2008) Phosphoinositides in plants: novel functions in membrane trafficking. Curr. Opin. Plant Biol. 11: 620-631

Uno Y, Rodriguez Milla MA, Maher E, Cushman JC (2009) Identification of proteins that interact with catalytically active calcium-dependent protein kinases from Arabidopsis. Molecular genetics and genomics : MGG 281: 375-390

Vancurova I, Choi JH, Lin H, Kuret J, Vancura A (1999) Regulation of phosphatidylinositol 4-phosphate 5-kinase from Schizosaccharomyces pombe by casein kinase I. J. Biol. Chem. 274: 1147-1155

Vidal D, Gil MT, Alvarez-Florez F, Moysset L, Simon E (2007) Protein kinase activity in Cucumis sativus cotyledons: effect of calcium and light. Phytochemistry 68: 438-445

Wang F, Shang Y, Fan B, Yu JQ, Chen Z (2014) Arabidopsis LIP5, a positive regulator of multivesicular body biogenesis, is a critical target of pathogen-responsive MAPK cascade in plant basal defense. PLoS pathogens 10: e1004243

Westergren T, Dove SK, Sommarin M, Pical C (2001) AtPIP5K1, an *Arabidopsis thaliana* phosphatidylinositol phosphate kinase, synthesizes PtdIns(3,4)P(2) and PtdIns(4,5)P(2) in vitro and is inhibited by phosphorylation. Biochem J. 359: 583-589

Widmann C, Gibson S, Jarpe MB, Johnson GL (1999) Mitogen-activated protein kinase: conservation of a three-kinase module from yeast to human. Physiol. Rev. 79: 143-180

Willats WG, McCartney L, Mackie W, Knox JP (2001) Pectin: cell biology and prospects for functional analysis. Plant Mol. Biol. 47: 9-27

Winter D, Vinegar B, Nahal H, Ammar R, Wilson GV, Provart NJ (2007) An "Electronic Fluorescent Pictograph" browser for exploring and analyzing large-scale biological data sets. PLoS One 2: e718

Wolf S, Greiner S (2012) Growth control by cell wall pectins. Protoplasma 249 Suppl 2: S169-S175

Wurzinger B, Mair A, Pfister B, Teige M (2011) Cross-talk of calcium-dependent protein kinase and MAP kinase signaling. Plant Signal. Behav. 6: 8-12

Xie K, Chen J, Wang Q, Yang Y (2014) Direct phosphorylation and activation of a mitogen-activated protein kinase by a calcium-dependent protein kinase in rice. Plant Cell 26: 3077-3089

Yang HC, Pon LA (2002) Actin cable dynamics in budding yeast. Proc. Natl. Acad. Sci. U S A 99: 751-756

Yin HL, Janmey PA (2003) Phosphoinositide regulation of the actin cytoskeleton. Annu Rev Physiol 65: 761-789

Zhang S, Klessig DF (1997) Salicylic acid activates a 48-kD MAP kinase in tobacco. Plant Cell 9: 809-824

Zhang S, Klessig DF (1998) The tobacco wounding-activated mitogen-activated protein kinase is encoded by SIPK. Proc. Natl. Acad. Sci. U S A 95: 7225-7230

Zhang X, Cheng T, Wang G, Yan Y, Xia Q (2013) Cloning and evolutionary analysis of tobacco MAPK gene family. Molecular biology reports 40: 1407-1415

Zhao LN, Shen LK, Zhang WZ, Zhang W, Wang Y, Wu WH (2013) Ca2+-dependent protein kinase11 and 24 modulate the activity of the inward rectifying K+ channels in Arabidopsis pollen tubes. Plant Cell 25: 649-661

Zhao Y, Yan A, Feijo JA, Furutani M, Takenawa T, Hwang I, Fu Y, Yang Z (2010) Phosphoinositides regulate clathrin-dependent endocytosis at the tip of pollen tubes in Arabidopsis and tobacco. Plant Cell 22: 4031-4044

Zhu J, Wu X, Yuan S, Qian D, Nan Q, An L, Xiang Y (2014) Annexin5 plays a vital role in Arabidopsis pollen development via Ca2+-dependent membrane trafficking. PLoS One 9: e102407

Zonia L, Munnik T (2008) Vesicle trafficking dynamics and visualization of zones of exocytosis and endocytosis in tobacco pollen tubes. J. Exp. Bot. 59: 861-873

7 Appendix

7.1 List of abbreviations

ABP	actin binding protein
ACN	acetonitrile
ACS	1-aminocyclopropan-1-carboxylic acid synthase
ADF	actin depolymerisation factor
ADP	adenosine diphosphate
Amp^R	ampicilin resistance
AP	alkaline phosphatase
APS	ammonium persulfate
At	*Arabidopsis thaliana*
ATP	adenosine triphosphate
BCIP	5-bromo-4-chloro-3-indolyl phosphate
BiFC	bimolecular fluorescence complementation
BSA	bovine serum albumin
$CaCl_2$	calcium chloride
CAM	calmodulin
CAMK	calmodulin-dependent protein kinase
Cat	catalytic domain
CBL	calcineurin B-like protein
cDNA	complementary deoxyribonucleic acid
CDPK	calcium-dependent protein kinase
CIPK	CBL-interacting protein kinase
CKI	casein kinase I
CPK	calcium-dependent protein kinase
$CuSO_4$	copper sulfate
DAG	diacyl glycerol
DDA	data-dependent aquisition
ddH_20	double distilled water
DIA	data-independent aquisition
Dim	dimerization domain

DMF	dimethyl formamide
DMSO	dimethyl sulfoxide
DN	dominant negative
DNA	deoxyribonucleic acid
dNTPs	desoxynucleotides
DTT	dithiotreitol
E. coli	*Escherichia coli*
EDTA	ethylene diamine tetraacetic acid
EGTA	ethylene glycol tetraacetic acid
ER	endoplasmic reticulum
ERF	ethylene response factor
EYFP	enhanced yellow fluorescent protein
FA	formic acid
H_3BO_3	boric acid
HCl	hydrochloric acid
HR/AM MS	high-resolution accurate mass spectrometry
IGKA	in-gel kinase assay
IPTG	isopropyl β-D-1-thiogalactopyranoside
KanR	kanamycin resistance
KCl	potassium chloride
KOH	potassium hydroxide
LC-MS	liquid-chromatography coupled to mass-spectrometry
Lin	linker domain
LiOAc	lithium acetate
m/z	mass-to-charge ratio
MAPK	mitogen-activated protein kinase
MBP	maltose binding protein
MCS	multiple cloning site
MES	2-(N-morpholino)ethanesulfonic acid
$MgCl_2$	magnesium chloride
$MnCl_2$	manganese chloride
MORN	membrane occupation and recognition nexus domain
Na_2MoO_4	sodium molybdate
NA_3VO_4	sodium orthovanadate
NaCl	sodium chloride

NaF	sodium fluoride
NBT	nitro blue tetrazolium chloride
NH_4CO_3	ammonium carbonate
NH_4OH	ammonium hydroxide
NT	N-terminal domain
Nt	*Nicotiana tabacum*
NtSIPK	*Nicotiana tabacum* salicylic acid-induced protein kinase
NtWIPK	*Nicotiana tabacum* wound-induced protein kinase
ONPG	*ortho*-nitrophenyl-β-D-galactopyranoside
PCR	polymerase chain reaction
PDB	protein data base
PI	phosphoinositide
PI4P5K	phosphatidylinositol 4,5-bisphosphate kinase
PIPK	phosphatidylinositol-bisphosphate kinase
PI-PLC	PI-specific phospholipase C
PKA	protein kinase A
PKD	protein kinase D
PLC	phospholipase C
PM	plasma membrane
PMSF	phenylmethanesulfonyl fluoride
PP1	serine/threonine protein phosphatase 1
PSM	peptide spectral matches
PtdIns	phosphatidylinositol
PtdIns(4,5)P_2	phosphatidylinositol 4,5-bisphosphate
PtdIns4P	phosphatidylinositol 4-phosphate
RNA	ribonucleic acid
RNAi	interference RNA
SDS	sodium lauryl sulfate
SPIK	shaker pollen inward K+ channel protein
SUS	split-ubiquitin membrane-based yeast two-hybrid system
TCA	trichloroacetic acid
TEMED	tetramethylethylenediamine
TFA	trifluoroacetic acid
TRIS	2-Amino-2-hydroxymethyl-propane-1,3-diol
Ub	ubiquitin

Table 7.1. List of the oligonucleotides used in this thesis

No.	Oligonucleotide sequence	Purpose
P1	5‘-gccatgccatatgatgtcggtagcacacgcagatga-3‘	AtPIP5K6 NdeI for
P2	5’-gccatgcgtcgactcagtggtggtggtggtggtgagcgtcttca acgaagaccc-3‘	AtPIP5K6 His6 SalI rev
P3	5‘-atgcggccattacggccggatggacggtggttcaggtca-3‘	MPK6 SfiI for
P4	5‘-atgcggccgaggcggccctattgctgatattctggat-3‘	MPK6 Sfi rev
P5	5’-atgcggccattacggccatggagacgaagccaaaccc -3’	CPK11 Sfi for
P6	5’-atgcggccgaggcggcctcagtcatcagatttttcac -3’	CPK11 SfiI rev
P7	5’-atgcggccattacggccatggcgaacaaaccaagaac -3’	CLPK9 SfiI for
P8	5’-atgcggccgaggcggcctcagacattcatagactcat -3’	CLPK9 SfiI rev
P9	5’-atgcggccattacggccatgcttcctccttcacgccg -3	SNRK 2.5 SfiI for
P10	5’-atgcggccgaggcggccttaagctttgggaggctctt-3’	SNRK 2.5 SfiI for
P 11	5’-atgcgtcgacatggagacgaagccaaaccc-3’	CPK11 SalI for
P 12	5’-atgcgcggccgcgtcatcagatttttcaccat -3’	CPK11 NotI rev
P 13	5’- atgcggcgcgccatgtcggtagcacacgcaga -3’	AtPIP5K6 AscI for
P 14	5’- atgcctcgagagcgtcttcaacgaagaccc -3’	AtPIP5K6 XhoI rev
P 15	5’-ctgctatcaaggactctgccgctcctacttccggcgctcgaac-3‘	QuickChange site-directed mutagenesis, PIPK6 T590A for
P 16	5’-gttcgagcgccggaagtaggagcggcagagtccttgatagcag-3’	QuickChange site-directed mutagenesis, PIPK6 T590A rev
P17	5’-ctgctatcaaggactctgccgatcctacttccggcgctcgaac-3‘	QuickChange site-directed mutagenesis, PIPK6 T590D for
P 18	5’-gttcgagcgccggaagtaggatcggcagagtccttgatagcag-3’	QuickChange site-directed mutagenesis, PIPK6 T590D rev
P 19	5’-ctacttccggcgctcgagcccctaccggaaattcaga-3’	QuickChange site-directed mutagenesis, PIPK6 T597A for
P 20	5’-tctgaatttccggtaggggctcgagcgccggaagtag-3’	QuickChange site-directed mutagenesis, PIPK6 T597A rev
P 21	5’-ctacttccggcgctcgagaccctaccggaaattcaga-3’	QuickChange site-directed mutagenesis, PIPK6 T597D for
P 22	5’-tctgaatttccggtagggtctcgagcgccggaagtag-3’	QuickChange site-directed mutagenesis, PIPK6 T597D rev
P 23	5’-atgcgtcgacatggacggtggttcaggtca-3’	MPK6 SalI for
P 24	5’-atgctctagattgctgatattctggattga-3’	MPK6 XbaI rev
P 25	5’-atgcaggcgcgccttgctgatattctggattga-3’	MPK6 SgsI rev
P 26	5’-atgcggccattacggcccatgtcggtagcacacgcaga-3’	AtPIP5K6 + 1b SfiI for

Table 7.1. List of the oligonucleotides used in this thesis (continued)

P 27	5’-atgcggccgcctcggccgcagcgtcttcaacgaagaccc-3’	AtPIP5K6 SfiI rev
P 28	5’-atgcggccattacggcccatgagcaaagaatttagtgg-3’	NtPIP5K6 + 1b SfiI for
P 29	5’-atgcggccgcctcggccgcagtgtcttctgcaaaaactt-3’	NtPIP5K6 SfiI rev
P 30	5’-atgcggccattacggccggatggatggttctggtcag-3’	NtSIPK SfiI for
P 31	5’-atgcggccgaggcggcctcacatatgctggtattcag-3’	NtSIPK SfiI rev
P 32	5’-atgcggcgcgccatgagcaaagaatttagtgg-3’	NtPIP5K6 AscI for
P 33	5’-atgcctcgagagtgtcttctgcaaaaactt-3’	NtPIP5K6 XhoI rev
P 34	5’-atgcggcgcgccatggatggttctggtcagca-3’	NtSIPK AscI for
P 35	5’-atgcctcgagcatatgctggtattcaggat-3’	NtSIPK XhoI rev
P 36	5’-atgcggcgcgccatggagacgaagccaaaccc-3’	CPK11 AscI for
P 37	5’-atgcctcgaggtcatcagatttttcaccat-3’	CPK11 XhoI rev
P 38	5’-ggtgttatgcatagagctctcaaacctgag-3’	QuickChange site-directed mutagenesis,CPK11 D150A
P 39	5’- gcttaaggctaccgcttttggtttgtctg -3’	QuickChange site-directed mutagenesis,CPK11 D150A

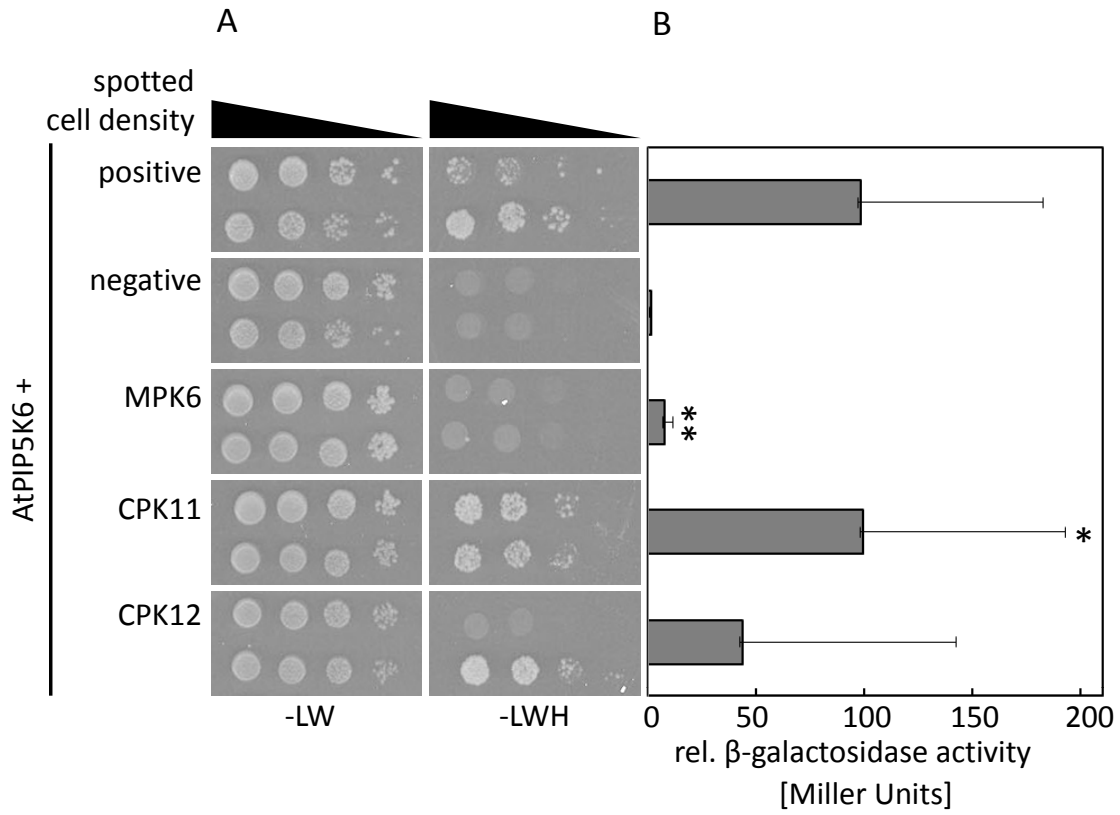

Fig. 7.1: Verification of interaction of putative protein kinases identified by IGKA and AtPIP5K6 in a SUS. Yeast strain NMY51 was transformed with pBT3C-OST4-PIP5K6 as bait and pAI-Alg5 pDL2-Alg5, pPR3N-CPK11, pPR3N-MPK6 as prey-plasmids. The pBT3C-OST4-PIP5K6 and pPR3N plasmids each bear an auxotrophy selection gene for L and W respectively to control for transformation efficiency and success. Clones were diluted from OD_{600} 1, 0.1, 0.01 and 0.001 from left to right. Dilutions were plated on SD plates lacking L and W to control for transformation of bait and prey plasmids (left part, SD-LW). The interaction of the clones was tested on selection for the histidine auxotrophy marker (right part, SD-LWH). B, ONPG-test of relative ß-galactosidase-activity in Miller Units. Error bars resemble the standard deviation, which was calculated based on the entire value population. 5-10 individual clones were tested. For statistical analysis a two-tailed t-test was performed. Significance levels are $\rho < 0.05$ (*), $\rho < 0.01$ (**), and $\rho < 0.001$ (***).

```
  1 MSVAHADDAD DYSRPTGESY HAEKALPSGD FYTGQWRDNL PHGHGKYLWT
 51 DGCMYVGDWH RGKTMGKGRF SWPSGATYEG DFKNGYMDGK GTYIDSSGDL
101 YRGSWVMNLR HGQGTKSYVN GDCYDGEWRR GLQDGHGRYQ WKNENHYIGQ
151 WKNGLMNGNG TMIWSNGNRY DGSWEDGAPK GNGTFRWSDG SFYVGVWSKD
201 PKEQNGTYYP STSSGNFDWQ PQQVFYVDLS ECVVCTCQRI PVLPSQKMPV
251 WYGASEQSSS GNRTKNSERP RRRSVDGRVS NGEMELRSNG SGYLQVDDNA
301 ESTRSSLGPL RIQPAKKQGQ TISKGHKNYE LMLNLQLGIR HSVGRPAPAT
351 SLDLKASAFD PKEKLWTKFP SEGSKYTPPH QSCEFKWKDY CPVVFRTLRK
401 LFSVDAADYM LSICGNDALR ELSSPGKSGS FFYLTNDDRY MIKTMKKAET
451 KVLIRMLPAY YNHVRACENT LVTKFFGLHC VKLTGTAQKK VRFVIMGNLF
501 CTGHSIHRRF DLKGSSHGRL TTKPESEIDP NTTLKDLDLN FAFRLQKNWF
551 QEFCRQVDRD CEFLEQERIM DYSLLVGLHF REAAIKDSAT PTSGARTPTG
601 NSETRLSRAE MDRFLLDASK LASIKLGINM PARVERTARR SDCENQLVGD
651 PTGEFYDVIV YFGIIDILQD YDISKKLEHA YKSMQYDPTS ISAVDPKQYS
701 RRFRDFIFRV FVEDA
```

Fig. 7.2.: Sequence coverage of AtPIP5K6 for MS-analysis of trypsin digested peptides. Recombinant MBP-AtPIP5K6 protein was phosphorylated with recombinant MPK6 *in vitro*. Proteins were separated by SDS-PAGE and an in-gel trypsin digest was performed. The resulting peptides were analysed by MS. Bold black, measured peptides from the protein sequence of AtPIP5K6. Grey, peptides not accessible to MS. Underlined, identified phosphorylation sites.

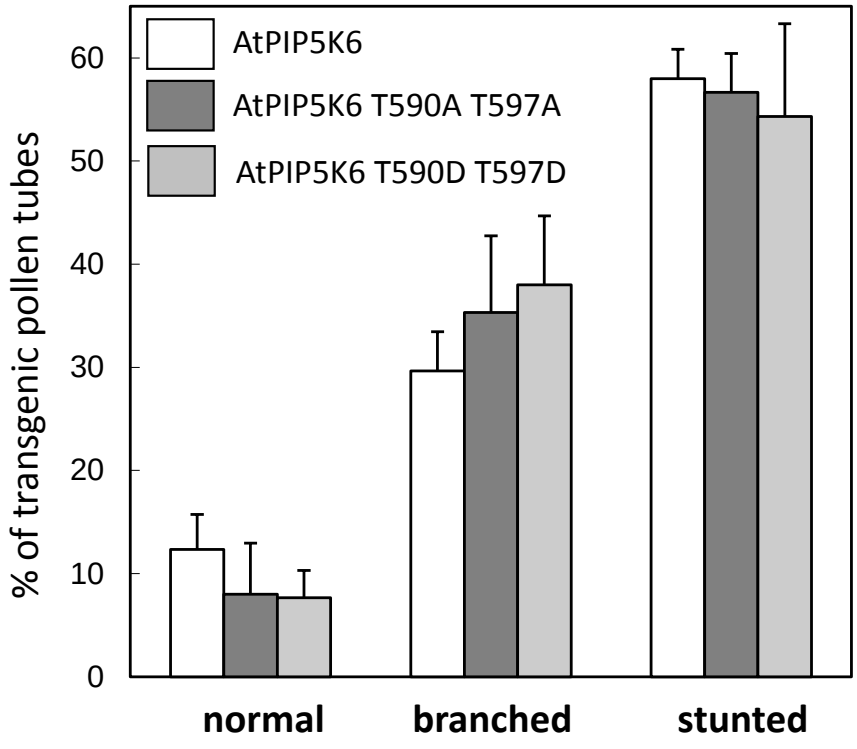

Fig. 7.3.: Analysis of phenotype distribution upon coo-expexpression of AtPIP5K6 and variant AtPIP5K6. The values show the distribution of phenotypes upon transient overexpression lat52:AtPIP5K6-EYFP (white), lat52:AtPIP5K6 T590A T597A-EYFP (dark grey) and lat52:AtPIP5K6 T590D T597D-EYFP (light grey) expressed as percentage, in tobacco pollen tubes. Pollen was germinated for 6-8h. The data is the result of three individual experiments. For each experiment 100 pollen tubes were scored. Error bars resemble the standard deviation, which was calculated based on the entire value population.

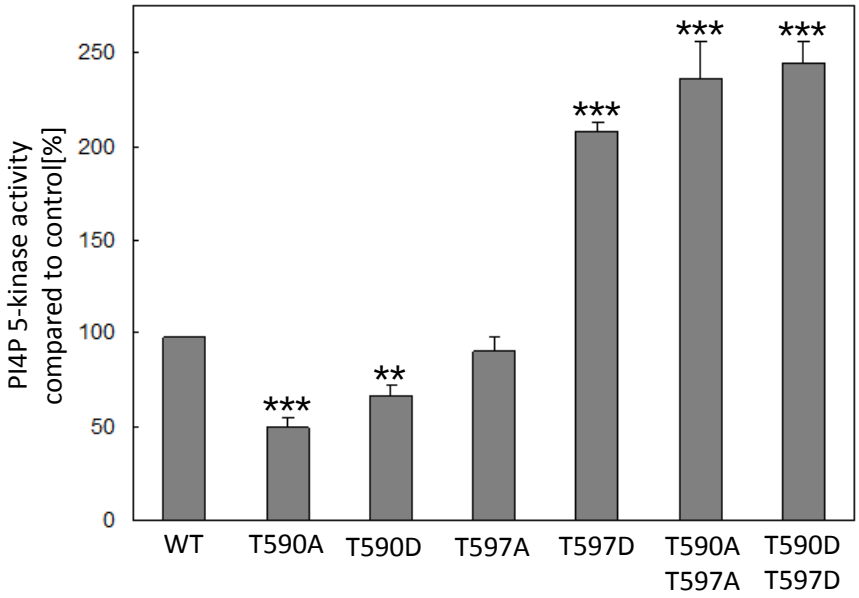

Fig. 7.4: *In vitro* activity of AtPIP5K6 variants. Recombinant MBP-AtPIP5K6 and MBP-AtPIP5K6 variants were mixed with PtdIns4P,10 µCi γ-[^{33}P]-ATP and 1 mM cold ATP for 1h to examine residual PI4P 5-kinase activity. Synthesized PtdIns(4,5)P_2 was isolated by acidic lipid extraction and separated with thin layer chromatography. ^{33}P-incorporation was detected with phosphor image technology and calculated with TINA-software. Activity is presented as percentage of control to the PI4P 5-kinase activity of AtPIP5K6 wild type enzyme. The experiment was performed three times with comparable results. Error bars resemble the standard deviation, which was calculated based on the entire value population. For statistical analysis a two-tailed t-test was performed. Significance levels are ρ <0.05 (*), ρ <0.01 (**), and ρ <0.001 (***) and were compared to wild type AtPIP5K6

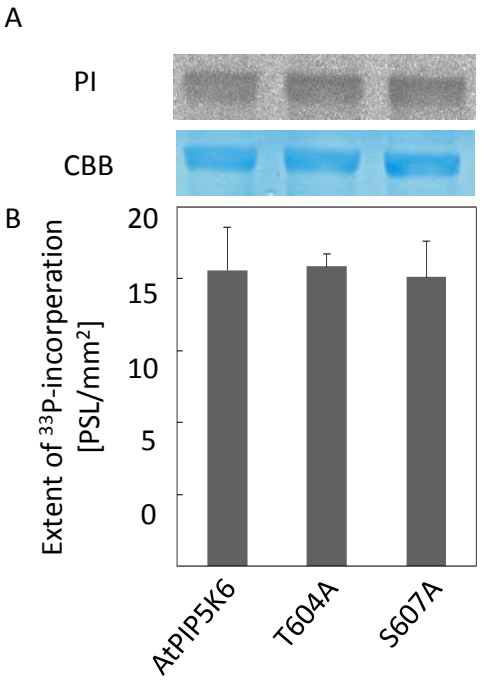

Figure 7.5: *In vitro* phosphorylation of MPB-AtPIP5K6 T604A and MBP-PIP5K6 S607A. MBP-AtPIP5K6 T604A and MBP-AtPIP5K6 S607A were tested for phosphorylation by recombinant CPK11 from *E. coli* crude extract and γ-[^{33}P]-ATP. Proteins were separated by SDS-PAGE and the incorporation of ^{33}P was visualized by phosphor image technology. A, section of a phosphorimage (PI, top) and the corresponding Coomassie-stained gel (CBB, bottom). B, level of ^{33}P-incorporation. The bars resemble the mean values of a triplicate measurement. Error bars resemble the standard deviation, which was calculated based on the entire value population. The experiment was performed three times with similar results.

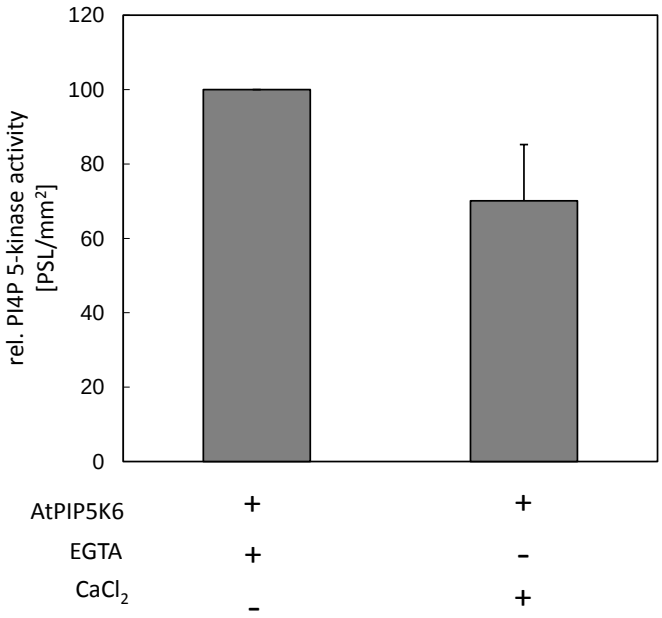

Figure 7.6: In vitro activity of AtPIP5K6 variants. Recombinant MBP-AtPIP5K6 was mixed with PI4P and 10 µCi γ-[^{33}P]-ATP and 1 mM EGTA or 0.55 mM $CaCl_2$ for 1h to examine residual PI4P 5-kinase activity. Synthesized PtdIns(4,5)P_2 was isolated by acidic lipid extraction and separated with thin layer chromatography. ^{33}P-incorporation was detected with phosphor image technology and calculated with TINA-software. Activity is presented as percentage of control to the PI4P 5-kinase activity of AtPIP5K6 wild type enzyme. The experiment was performed three times with comparable results. Error bars resemble the standard deviation, which was calculated based on the entire value population.

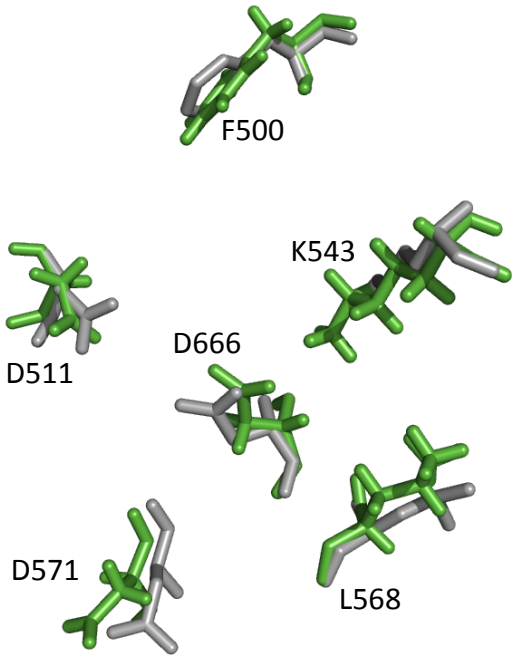

Figure 7.7: Residues of the active site of HsPIPKIIβ and modeled AtPIP5K6 are well-aligned. Catalytically important residues of HsPIPKIIβ (grey; 1BO1, Rao *et. al.* 1998) and the model of AtPIP5K6 (green), calculated on the x-ray crystallography data from HsPIPKIIβ. The model was calculated with Lomets (Zhang Labs) server, minimized with Amber12.0 in vacuum with 5000 steps by PD Dr. Iris Thondorf, Department of Molecular Modelling, MLU Halle-Wittenberg. Residues are well-aligned and reflect the quality of the model. Amino acid labels apply for AtPIP5K6 only. Images were prepared with PyMol.

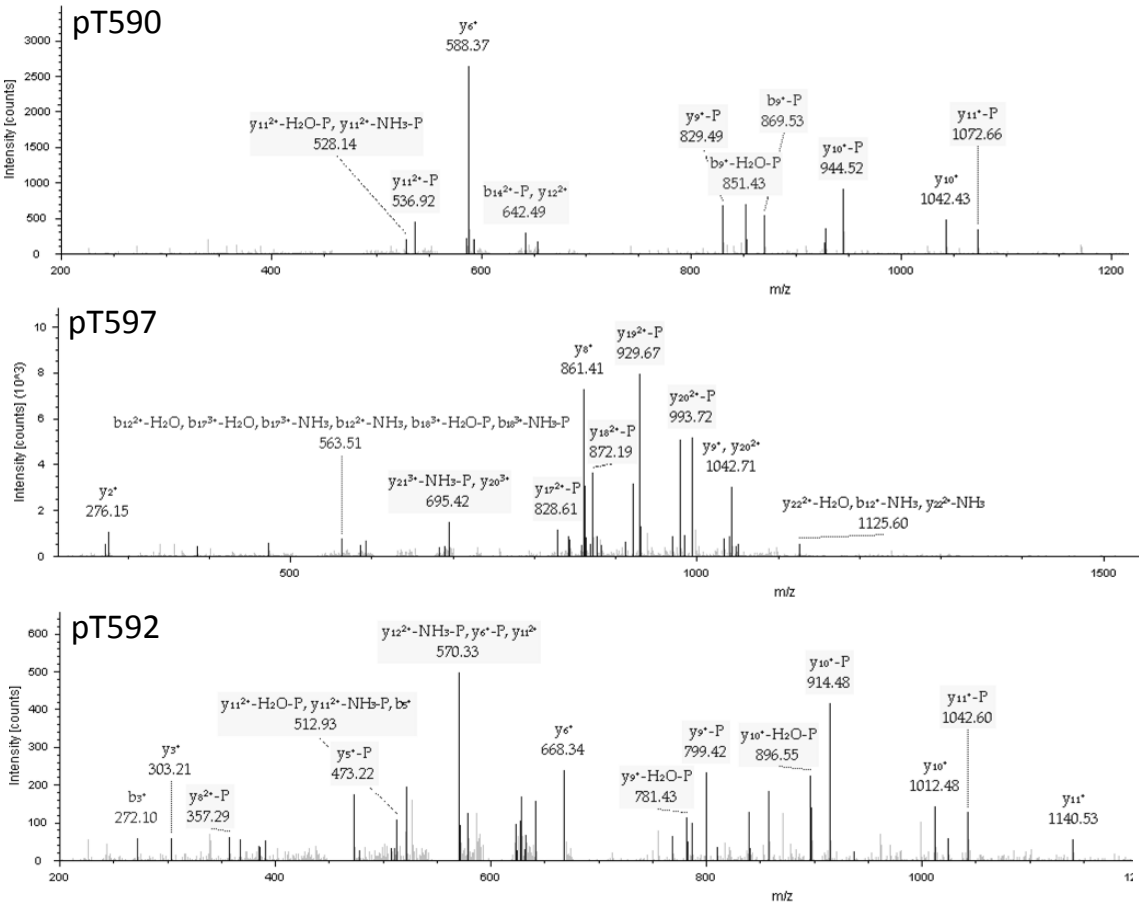

Fig. 7.8: Spectra of phosphorylated peptides identified with MS-analysis. Recombinant AtPIP5K6 and its variants were phosphorylated with recombinant and activated MPK6 *in vitro*. The proteins were digested with trypsin and analysed by HR/AM LC-MS by Dr. Wolfgang Hoehenwarter (Proteome Analytics, IPB, Halle (Saale).

Table 7.2: List of phosphopeptides identified by analysis of MPK6-treated AtPIP5K6. Proteins were digested with trypsin and measured with HR/AM LC-MS. m/z, mass-to-charge ration; RT, retention time; #PMS peptide spectral matches. The phosphorylation site in the column P-Site has the highest phosphorylation probability of all possible phosphorylation sites in the peptide sequence based on interpretation of the MS/MS fragment ion pattern by the phosphoRS software. The probabilities as opposed to the other possible sites are given in the column Probability. § T11 is the site with the second highest probability as opposed to S16 which was considered the most probable site by the software.

Protein Substrate	Sequence	Charge	m/z [Da]	RT [min]	Exp Value	Mascot IonScore	#PSMs	P-Site	Probability
PIPK6	EAAIKDSAtPTSGAR	2	777.861	9.95	8.20E-05	54	108	T9	95.00%
PIPK6	DSATPTSGARtPTGNSETR	3	662.621	9.06	3.70E-04	49	321	T11	11.50%
PIPK6_T590A	DSAAPTSGARtPTGNSETR	3	652.618	11.8	1.80E-03	41	113	T11	99.00%
PIPK6_T590A	EAAIKDSAAPTSGARtPTGNSETR	3	823.382	14.62	1.20E-01	25	18	T16	78.80%
PIPK6_T597A	EAAIKDSAtPTSGAR	2	777.860	10.15	1.10E-06	72	148	T9	95.60%
PIPK6_T590A _T597A	EAAIKDSAAPtSGAR	2	762.855	9.92	2.00E-03	39	17	T11	88.20%
Pollen extract	EAAIKDSAtPTSGAR	2	777.861	9.76	9.10E-04	43	15	T9	99.80%
Pollen extract	DSATPTSGARTPTGNsETR	3	662.622	9.1	4.00E-03	38	229	T11	14.60% §

8 Publications

Publications in peer-reviewed journals:

Mähs A., Ischebeck T., Heilig Y., Stenzel I., Hempel F., Seiler S., Heilmann I. (2012) The essential phosphoinositide kinase MSS-4 is required for polar hyphal morphogenesis, localizing to sites of growth and cell fusion in Neurospora crassa. 2012;7(12):e51454.

Ischebeck T., Stenzel I., Hempel F., Jin X., Mosblech A., Heilmann I. (2011) Phosphatidylinositol-4,5-bisphosphate influences Nt-Rac5-mediated cell expansion in pollen tubes of Nicotiana tabacum. Plant J. 2011 Feb;65(3):453-68.

Onnis V., Congiu C., Björklund E., Hempel F., Söderström E., Fowler CJ. (2010) Synthesis and evaluation of paracetamol esters as novel fatty acid amide hydrolase inhibitors. J Med Chem. 2010 Mar 11;53(5):2286-98.

Oral presentations:

Phosphorylation of *Arabidopsis* PI4P 5-kinases involved in polar growth. *Fall Meeting GRK1026, Naumburg 2012*

Phosphorylation of *Arabidopsis* PI4P 5-kinases involved in polar growth. *Fall Meeting GRK1026, Meißen 2012*

Phosphorylation of *Arabidopsis* PI4P 5-kinases involved in polar growth. 9th Plant Science Students Conference (*PSSC), Halle (Saale) 2013*

Unraveling the role of PI4P 5-kinase phosphorylation in the control of polar growth. 12. *Mitteldeutsche Pflanzenphysiologie-Tagung, Dresden 2014*

A Ca^{2+}-dependent protein kinase that phosphorylates PI4P 5-kinases involved in pollen tube growth. 27. Tagung Molekularbiologie der Pflanze, Dabringhausen 2014

A Ca^{2+}-dependent protein kinase that phosphorylates PI4P 5-kinases involved in pollen tube growth. Plant Calcium Signaling (PCS), Münster 2014

Poster presentations:

Franziska Hempel, Jennifer Lerche, Irene Stenzel and Ingo Heilmann. Phosphorylation of *Arabidopsis* PI4P 5-kinases involved in polar growth. *International Conference of Arabidopsis Research (ICAR), Vienna (Austria) 2012*

Franziska Hempel, Jennifer Lerche, Irene Stenzel and Ingo Heilmann. Phosphorylation of *Arabidopsis* PI4P 5-kinases involved in polar growth. *26. Tagung Molekularbiologie der Pflanze, Dabringhausen 2013*

Franziska Hempel, Jennifer Lerche, Stefan Helm, Wolfgang Hoehenwarter and Ingo Heilmann. Phosphorylation of *Arabidopsis* PI4P 5-kinases involved in polar growth. *Deutsche Botanikertagung, Tübingen 2013*

Franziska Hempel, Jennifer Lerche, Stefan Helm, Wolfgang Hoehenwarter and Ingo Heilmann. Phosphorylation of *Arabidopsis* PI4P 5-kinases involved in polar growth. *3rd International Meeting „Conformational transitions in macromolecular interactions" GRK1026, Halle (Saale) 2013*

9 Acknowledgements – Danksagung

Ich möchte allen danken, die zum Entstehen der vorliegenden Arbeit beigetragen haben.

Mein besonderer Dank gilt dabei meinem Doktorvater Herrn Prof. Dr. Ingo Heilmann. Ich bedanke mich für das spannende Thema, die Diskussion und die einzigartige Betreuung, besonders beim Abfassen dieser Arbeit. Mit Freude habe ich dieses interessante Projekt bearbeitet und die Zeit als Mitglied der AG Heilmann wird mir immer in sehr guter Erinnerung bleiben.

Dem GRK1026 möchte ich danken für finanzielle Unterstützung zu verschiedenen internationalen Tagungen fahren zu können, sowie der Möglichkeit meine Ergebnisse bei GRK-internen Tagungen zu präsentieren und interdisziplinär zu diskutieren.

Ganz besonders möchte ich mich bei Herrn Dr. Wolfgang Hoehenwarter und Frau Petra Majovsky der Proteomeanalytik des IPBs (Halle(Saale) für die Vorbereitung und Messung meiner MS-Proben und dem geduldigen Beantworten meiner vielfältigen Fragen bedanken.

Auch der Arbeitsgruppe von Herrn Prof. Dr. Sacha Baginsky (Abteilung Pflanzenbiochemie, MLU Halle-Wittenberg) möchte ich mich für die Messung von Proben bedanken. Ein besonders Dankeschön geht dabei an Herrn Stefan Helm und Herrn Dr. Dirk Dobritzsch für Messung der MS-Proben und die lehrreichen Fragestunden zur Massenspektrometrie bedanken.

Für die Zurverfügungstellung gereinigter und aktivierter MPK6 bedanke ich mich bei Herrn Pascal Pecher und Herrn Dr. Lennart Eschen-Lippold (Abteilung Zelluläre Signaltransduktion, IPB Halle(Saale)). Außerdem möchte ich mich in diesem Zusammenhang für die Diskussion meiner Ergebnisse mit Dr. Justin Lee und Prof. Dr. Dierk Scheel bedanken.

Ein großes Dankeschön geht an PD Dr. Magret Köck und Karin Klar für die Nutzung des Isotopenlabors, die Hilfsbereitschaft und das Beseitigen der von mir produzierten Abfälle.

Frau PD Dr. Iris Thondorf (Abteilung *Molecular Modeling*, MLU Halle-Wittenberg) möchte ich für das berechnete Model der AtPIP5K6 danken, dass mir eine große Hilfe bei der Interpretation meiner Ergebnisse war.

Für hilfreiche Diskussionen und das Interesse am CPK-Projekt bedanke ich mich bei Prof. Dr. Jörg Kudla aus Münster (Universität Münster, Abteilung Molekulare Entwicklungsbiologie der Pflanzen).

Ich danke Herrn Dr. Shigemi Seo und Herrn Dr. Shinpei Katou vom National Institute of Agrobiological Sciences, Tsukuba, Ibaraki, Japan für die Zurverfügungstellung der Tabak *WIPK/SIPK* RNAi-Linien.

Dem Institut für Biologie der MLU Halle-Wittenberg danke ich für die Möglichkeit zur Nutzung des konfokalen Mikroskops.

Ich danke Marion Sonntag für die zuverlässige und hochwertige Versorgung mit Puffern und Medien aller Art. Das hat mir sehr viel Arbeit abgenommen. Dankeschön.

Meinen beiden Bachelorstudentinnen Sarah Bönisch und Janette Gleiche sei für ihre Mitarbeit und das Interesse an diesem Projekt gedankt.

Frau Dr. Mareike Heilmann möchte ich für die Zurverfügungstellung der Vektoren für die BiFC-Experimente und die modifizierten Hefevektoren, sowie der Bereitstellung von unzähligen Tool, Tipps und Ratschlägen danken. Außerdem danke ich ihr für die stete intellektuelle, emotionale und modische Unterstützung und die vielen Hilfestellungen, auf die ich mich in den vergangenen Jahren immer verlassen konnte. Das ist überhaupt nicht selbstverständlich und dafür ein großes DANKE.

Bei Frau Dr. Irene Stenzel möchte ich mich besonders für die liebevolle Versorgung der Tabakpflanzen bedanken. Außerdem für danke ich ihr für die gute Zusammenarbeit in Labor 160 und dafür, dass sie immer eine Konstante für mich war.

Herrn Dr. Danilo Meyer möchte ich für die intensive Einführung in die Expression, Reinigung und Charakterisierung von Proteinen sowie die Vielzahl von anregenden Diskussionen über enzymologische und proteinchemische Themen danken. Außerdem bedanke ich mich für die Hilfe mit PyMol und vielen anderen Kleinigkeiten.

Meiner ehemaligen Kollegin und Lieblingskommilitonin Frau Dr. Jennifer Lerche danke ich für die täglichen Diskussionen während unserer gemeinsamen Arbeitszeit, der Teamarbeit und unsere Freundschaft, die uns hoffentlich noch sehr lange verbinden wird.

An dieser Stelle möchte ich mich auch bei allen ehemaligen und neuen Mitgliedern der AG Heilmann für die gute Zusammenarbeit und den Spaß, während und außerhalb der Arbeitszeit, bedanken. Ganz besonderer Dank gilt dabei der Katha, Mareike, Steffie und Willi.

Ein großes Dankeschön gilt meiner Mutter Sigrid, die mich auf allen von mir gewählten Wegen stets unterstützt hat. Auch Norbert und meiner Tante Carla sei an dieser Stelle für den Zuspruch gedankt.
Abschließend möchte ich mich von Herzen bei Danilo bedanken, für die Motivation, die Aufmunterung, das Verständnis sowie das stoische Rezitieren des Satzes: „Alles wird gut. Alles ist gut!“.

Lebenslauf

Persönliche Daten

Name	Franziska Hempel
Arbeit	Abteilung Zelluläre Biochemie Institut für Biochemie und Biotechnologie Martin-Luther-Universität Halle Wittenberg Kurt-Mothes Straße 3, 06120 Halle (Saale), Germany
Privat	Fritz-Reuter-Str. 15, 06114 Halle (Saale)
Email	franziska.hempel@biochemtech.uni-halle.de

Staatsangehörigkeit	Deutsch
Familienstand	ledig, keine Kinder
Geburtsdatum und -ort	02. April 1985 in Göttingen

Bildungsweg

02.2011-05.2015	Promotion im Fachbereich Biochemie und Biotechnologie an der Martin-Luther-Universität Halle-Wittenberg in der Arbeitsgruppe von Prof. Dr. Ingo Heilmann Titel der Arbeit: New links for old pathways: Protein kinases that target PI4P 5-kinases with roles in polar tip growth in plants
11.2008-09.2009	Diplomarbeit im Fachbereich Pflanzenbiochemie an der Georg-August-Universität Göttingen Titel der Arbeit: Regulation von PI4P 5-Kinasen durch Phosphorylierung Note: sehr gut (1,0)
10.2004-09.2009	Biologiestudium an der Georg-August-Universität Göttingen Hauptfach: Biochemie Nebenfächer: organische Chemie, Mikrobiologie Abschluss: Diplom, Note: sehr gut (1,2)
2001-2004	Unescoprojektschule Hainberg-Gymnasium Göttingen Abschluss: allgemeine Hochschulreife

Eidesstattliche Erklärung

Sehr geehrte Damen und Herren,

hiermit erkläre ich, dass ich die beigefügte Dissertation selbstständig verfasst und keine anderen als die angegebenen Hilfsmittel genutzt habe. Alle wörtlich oder inhaltlich übernommenen Stellen habe ich als solche gekennzeichnet.

Ich versichere außerdem, dass ich die beigefügte Dissertation nur in diesem und keinem anderen Promotionsverfahren eingereicht habe und, dass diesem Promotionsverfahren keine endgültig gescheiterten Promotionsverfahren vorausgegangen sind.

Halle (Saale), _____ _____

Ort, Datum Unterschrift